School of Doctoral Studies in Biological Sciences
University of South Bohemia in České Budějovice
Faculty of Science

Regulation of photosynthesis and primary production of phytoplankton under nutrient and light stress

Ph.D. Thesis

Mgr. Kristina Felcmanová

Supervisor: prof. RNDr. Ondřej Prášil, Ph.D.
Institute of Microbiology CAS

České Budějovice 2018

This thesis should be cited as:

Felcmanová K., 2018: Regulation of photosynthesis and primary production of phytoplankton under nutrient and light stress, Ph.D. Thesis Series, No. 6. University of South Bohemia, Faculty of Science, School of Doctoral Studies in Biological Sciences, České Budějovice, Czech Republic, 141 pp.

❁ Annotation

Regulation of photosynthesis and primary production in globally important cyanobacterium *Prochlorococcus marinus* under nitrogen and light stress were examined. The study investigated the model describing relationship between photosynthetic activity and primary production. The photosynthetic energy budget and the efficiency of converting the photosynthetic energy into biomass were described. Molecular and physiological approaches were applied to analyse the utilization of photosynthetic energy and regulation of metabolism to investigate the influence of streamlined oxygen-evolving cluster on the photosynthetic activities.

❁ Declaration [in Czech]

This thesis originated from a partnership of Faculty of Science, University of South Bohemia, and Institute of Microbiology of the CAS (centre ALGATECH in Třeboň), supporting doctoral studies in the Physiology and Developmental Biology study programme.

❀ **List of papers and author's contribution**

The thesis is based on the following papers:

I. Felcmanová K., Lukeš M., Kotabová E., Lawrenz E., Halsey K. H., Prášil O. (2017) Carbon use efficiencies and allocation strategies in *Prochlorococcus marinus* strain PCC 9511 during nitrogen-limited growth. Photosynthesis Research 134 (1), 71-82. (IF = 3.864)
K. Felcmanová participated in laboratory experiments, data evaluation and manuscript writing.

II. Partensky F., Mella-Flores D., Six C., Garczarek L., Czjzek M., Marie D., Kotabová E., Felcmanová K. and Prášil O. Comparison of photosynthetic performances of marine picocyanobacteria with different configurations of the oxygen-evolving complex. Photosynthesis Research (first online 25 June 2018), https://doi.org/10.1007/s11120-018-0539-3. (IF = 3.864)
K. Felcmanová participated in data evaluation and manuscript writing.

III. Felcmanová K., Lukeš M., Kotabová E., Halsey K. H., Prášil O. Carbon metabolism differs in low-light and high-light ecotypes of *Prochlorococcus marinus*. (Manuscript in preparation)
K. Felcmanová participated in laboratory experiments, data evaluation and manuscript writing.

✤   **Content**

1. General introduction
1.1 Background

The origin of the first oxygenic photosynthetic cyanobacteria, which have evolved from anoxygenic bacteria 2.5-3 billion years ago, was a key step for the creation of oxygenic atmosphere on the Earth. Then later the evolution of photosynthetic eukaryotic algae, simple plants and their inhabiting of land enabled the development of life, as we know it. Oxygenic photosynthesis is one of the most important biological processes of the world changing the solar energy into reductants and chemically bound energy. The reductants are used for CO_2 fixation primarily and thus enable conversion of inorganic carbon form to its organic form, which is stored as a biomass. The photosynthetically assimilated carbon is also called as primary production and its quantification is much debated and intensively studied field.

The global net primary production of Earth's biosphere is estimated to be approx. 105 petagrams of carbon per year (Field et al. 1998). On the base of these integrated estimates obtained from global models based on satellite measurements it was found, that aquatic environments contribute almost 50% to the net primary production. Despite the fact that the aquatic primary producers represent only 0.2% of the photosynthetically active carbon biomass (Field et al. 1998), quantitative estimates of their primary production range from 45 to 57 Pg C y^{-1} (Falkowski et al. 2003). Interestingly, small picocyanobacteria living in oligotrophic regions of oceans (Fig. 1), which were considered ocean deserts for a long time, contribute to the net primary production approx. 25% (Price et al. 2011).

One of the most important cyanobacteria living in these regions is *Prochlorococcus marinus*. Although with the size 0.6 µm in diameter it is the smallest known unicellular phototroph, with cell density reaching up to 10^5 cells ml^{-1} (Partensky et al. 1999), *Prochlorococcus* is considered the most abundant oxygen-evolving photosynthetic organism. It was shown that it accounts for 50% of the total chlorophyll in the oligotrophic areas (Partensky and Garczarek 2010). Such a high cell density makes it

the major contributor to the primary production and essential key element of the global carbon cycle. It is estimated that *Prochlorococcus* contributes an estimated 30-50% of the total aquatic primary productivity in the oligotrophic regions (Goericke and Welschmeyer 1993, Zubkov et al. 2003) which means that it produces approx. 4 gigatons of fixed carbon per year. Interestingly, this is comparable to the primary productivity of global croplands (Biller et al. 2015).
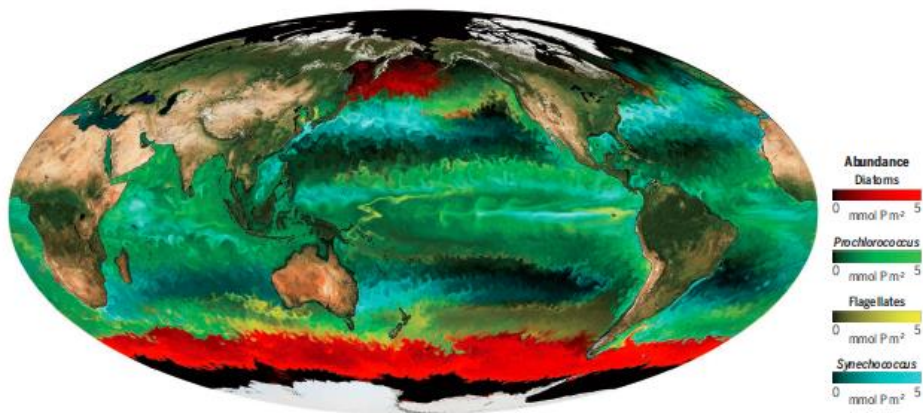
Fig. 1: Model showing the most dominant types of phytoplankton in the world's oceans (Pennisi 2017). Cyanobacterium *Prochlorococcus* is dominant in the nutrient poor tropical and subtropical regions (marked green).

Thus, for its significance, *Prochlorococcus marinus* is intensively studied phototroph. Many studies focused on its cultivation and photo-physiology (Moore and Chisholm 1999, Rippka et al. 2000, Moore et al. 2007), genome content (Rocap et al. 2003, Dufresne et al. 2005, Ting et al. 2009, Malstrom et al. 2013) and also geographic distribution (Moore et al. 1998, Johnson et al. 2006, Flombaum et al. 2013).

During the last decades, the quantitative determination of the gross and net primary production (GPP and NPP, respectively) of oceanic ecosystems became essential. Current estimates of oceanic NPP are based

on data obtained from satellites. However, to calculate the global NPP, mathematical models depend on input variables such as nutrients, light intensity and temperature in order to obtain correct results (Laws et al. 2002). To improve these estimations, and to find how nutrient availability and irradiance influence energetic metabolism of phytoplankton, many laboratory and field studies focused on production measurements using ^{14}C incorporation measurements, oxygen measurements and fluorescence-based measurements (Falkowski et al. 2003, Bruyant and Babin et al. 2005, Jakob et al. 2007, Pei and Laws 2013, Halsey and Jones 2015, Fisher and Halsey 2016).

However, most of these studies were performed on model eukaryotic algae. Therefore, this work tried to elucidate efficiency of energetic metabolism and carbon cycling in the most abundant cyanobacterium *Prochlorococcus marinus* in order to better understand its ecological role.

1.2 *Prochlorococcus marinus* discovery

Due to its small size (0.6 μm in average), *P. marinus* was for a long time invisible by classic light microscope, thus remained hidden for marine scientist using traditional microscopic techniques. The first observations of small "chroococoid" cyanobacteria were during the 1970's using the electron microscopy. The first published record of *Prochlorococcus* called as "Type II" cells obtained from marine samples was reported in a paper by Johnson and Sieburth in 1979. However, it was mistakenly identified as another marine cyanobacterium *Synechococcus*, which was discovered around that time (Guillard et al. 1985). The second published record came indirectly in early 1980's from the discovery of unknown red-shifted chlorophyll *a* derivative (Gieskes and Kraay 1983). *Prochlorococcus* was identified and visualized only when flow cytometry and HPLC techniques were developed several years later (Chisholm et al. 1988, Chisholm et al. 1992). The first *Prochlorococcus* strain was

isolated by Brian Palenik from a depth of 120 m in the Sargasso Sea in May 1988 (Chisholm et al 1992). The findings that these photosynthetic cells lacked phycobilisomes and possessed an unusual divinyl derivative of Chl *a* and *b* and their distinctive prokaryotic structure suggested that they belong to the free-living relative of *Prochloron*. The announcement of the discovery of new photosynthetic picoplankton *Prochlorococcus* was made by Chisholm et al. 1988. The first axenic strain was derived from the SARG strain in 1995 and designated as PCC 9511 (Rippka et al. 2000).

Since this time, many strains have been found, isolated and described worldwide in the euphotic zone in subtropical and tropical oligotrophic waters (Veldhuis and Kraay 1990, Goericke and Welschmeyer 1993, Vaulot et al. 1995, Partensky et al. 1999) and have been the object for many studies. Last decade, many studies focused on *Prochlorococcus* genome, its sequencing, comparative genomics, and meta- and pangenomics (Dufresne et al. 2003, Rocap et al. 2003, Coleman et al. 2006, Malstrom et al. 2013, Delmont and Eren 2018).

1.3 Cyanobacterium *Prochlorococcus marinus*

As *Prochlorococcus* is prokaryote containing divinyl chlorophyll *a* and *b* pigments (DV-Chl *a/b*) and lacking phycobilisomes, it was assigned to the Prochlorophyta suggesting that it is closely related to the freshwater *Prochlorotrix* and symbiotic *Prochloron* (Chisholm et al. 1988). However, according to the 16S rRNA and RNA polymerase gene sequencing, *Prochlorococcus* belongs to the cyanobacterial radiation and create branch, which is different from Prochlorophyta. Moreover, closer relation between *Prochlorococcus* and *Synechococcus* was revealed (Palenik and Haselkorn 1992, Urbach et al. 1992). Although *P. marinus* belongs to the cyanobacteria and forms a sister clade with *Synechococcus* (Ting et al. 2002), its antenna complex is different from that found in

most cyanobacteria including *Synechococcus* (Fig. 2). First, in the light-harvesting antennae, the DV-Chl *a* is bound to the membrane-intrinsic-light-harvesting proteins (Pcb) instead of the well-known chlorophyll *a* (Chl *a*), which is unique trait among photosynthetic organisms. The DV-Chl *a* absorbs maximally in the blue part of the visible spectrum. Interestingly, the absorption spectrum of DV-Chl *a* is red-shifted and therefore the red peak of DV-Chl *a* is shifted approx. 7 nm towards the blue region (i.e. to longer wavelengths) in comparison to classic Chl *a* giving to the *P. marinus* the advantage when living in deep waters enriched with blue light (Partensky et al. 1999, Ting et al. 2002). Second, *P. marinus* lacks phycobilisomes, extrinsic antennas associated with Photosystem II (PSII) in cyanobacteria and red algae, which are in *P. marinus* replaced by transmembrane Pcb proteins (Wiethaus et al. 2010). Third, the oxygen-evolving complex (OEC) associated with PSII at the luminal side of thylakoid membrane is modified among *P. marinus* strains. Standard cyanobacterial OEC consists of five extrinsic proteins (PsbO, PsbU, PsbV, PsbP and PsbQ) which constitute Mn_4Ca-cluster that catalyzes the production of oxygen by water-splitting (Ting et al. 2009). However, all *P. marinus* strains lack PsbQ protein and moreover, most of strains also lack PsbU and PsbV proteins which were shown to play a role in the shielding of the Mn_4Ca-cluster from reductants (Kamiya and Shen 2003, Ferreira et al. 2004, Partensky et al. 2018).
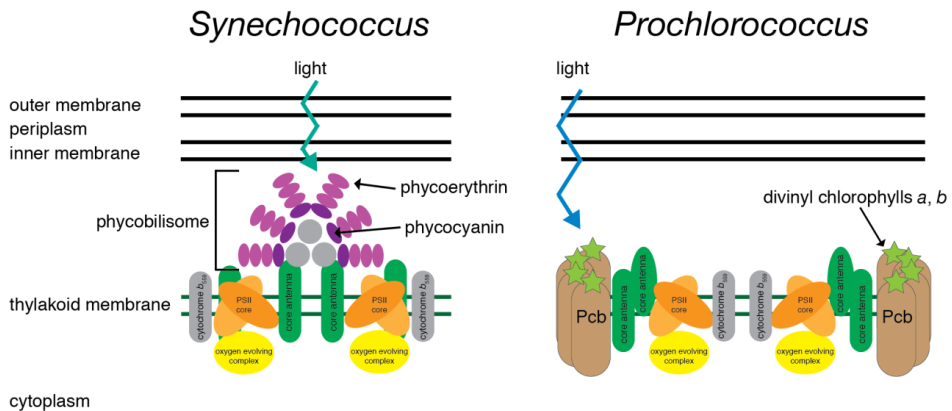
Fig. 2: The differences in the structure of the light-harvesting antenna and pigment composition of closely related marine cyanobacteria *Synechococcus* and *Prochlorococcus* (Biller et al. 2015).

1.4 Ecotypic differentiation

Members of the *Prochlorococcus* genus belong to the most diverse group of phytoplankton on the Earth. They live throughout the illuminated (euphotic) water column from the surface of ocean to the bottom of the euphotic zone mostly in stratified oligotrophic regions (Partensky and Garczarek 2010). In this environment, strains have to cope with changing conditions such as irradiance, temperature optima or nutrient availability. These factors have driven the diversification of *Prochlorococcus* genus and led to the niche partitioning by genetic adaptation (West and Scanlan 1999, Johnson et al. 2006, Zinser et al. 2007). Originally, the *Prochlorococcus* genus was simply divided into two physiologically and genetically distinct groups termed as low- and high-light adapted (hereafter LL and HL, respectively) ecotypes according to their light acclimation responses (Moore et al. 1998, Moore and Chisholm 1999). It was assumed that LL strains are restricted to the deep euphotic zone, with relatively high nutrient conditions but with irradiances reaching only 0.1% of irradiance at the surface of the ocean. This group is characterized

by high DV-Chl *b/ a* ratio and relatively larger cell size and genome. By contrast, HL strains were supposed to predominate in more irradiated surface waters with lower nutrient concentrations and possess low DV-Chl *b/ a* ratio, smaller size of their cells and of genomes (Rocap et al. 2003, Ting et al. 2009, Partensky and Garczarek 2010). Nevertheless, this division is an oversimplification. According to the new studies, based on the sequences of 16S-23S rRNA internal transcribed spacer (ITS), HL strains evolved into 6 clades (HLI-HLVI) and LL strains are separated into seven clades (LLI-LLVII) (Fig. 3) (Johnson et al. 2006, Huang et al. 2012, Malstrom et al. 2013, Biller et al. 2015). Within these clades, there are physiologically and ecologically distinct ecotypes, which show seasonal, depth and geographical patterns (Moore et al. 1998, Johnson et al. 2006, Zinser et al. 2007). However, each clade hides a huge amount of further genotypic and phenotypic diversity. This diversity is not randomly distributed, but is connected to the abiotic and biotic factors. *Prochlorococcus* lives at various sites, e.g. in the Pacific Ocean, Atlantic Ocean, Sargasso Sea, and Mediterranean Sea which have different biogeochemical regimes. By genome sequencing, it was found that these populations display fundamental genomic differences (Kettler et al. 2007, Kent et al. 2016, Biller et al. 2014, Kashtan et al. 2014, 2017).
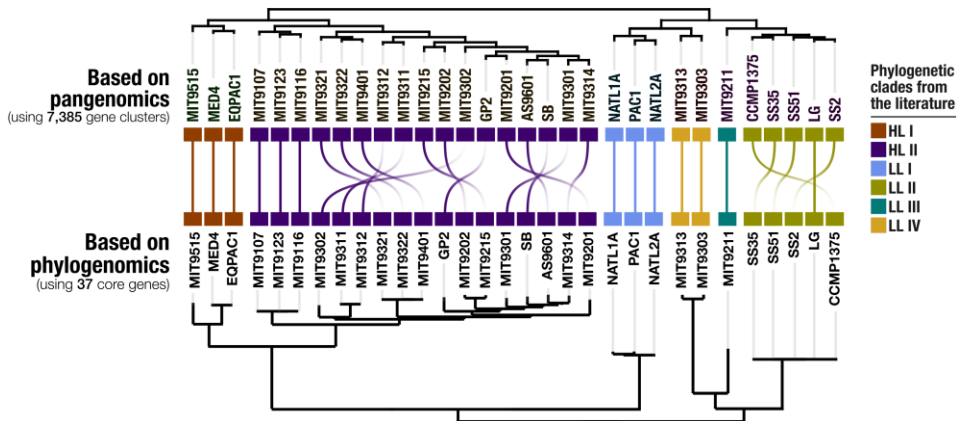
Fig. 3: Organization of *Prochlorococcccus* genomes based on pangenomics (shared gene clusters) in comparison to phylogenomics with colour affiliations to the clades commonly used in the literature (Delmont and Eren 2018).

To study *Prochlorococcus* global ocean distribution and its genome diversity, the metagenomics and pangenomics are recently widely used. These approaches allow identifying core and accessory genes and their function, and can characterize gene gain and loss, which is probable driving force of evolution (Coleman and Chisholm 2010, Berube et al. 2015, Kent et al. 2016). Investigation of gene clusters of individual strains is crucial for understanding of their potential role in the fitness, ecology and selection pressure, which resulted in niche partitioning (Kashtan et al. 2017). The metapangenomic study by Delmont and Eren 2018 revealed differences within the members of specific clades and also revealed closely related isolates with different levels of fitness (Fig. 4).
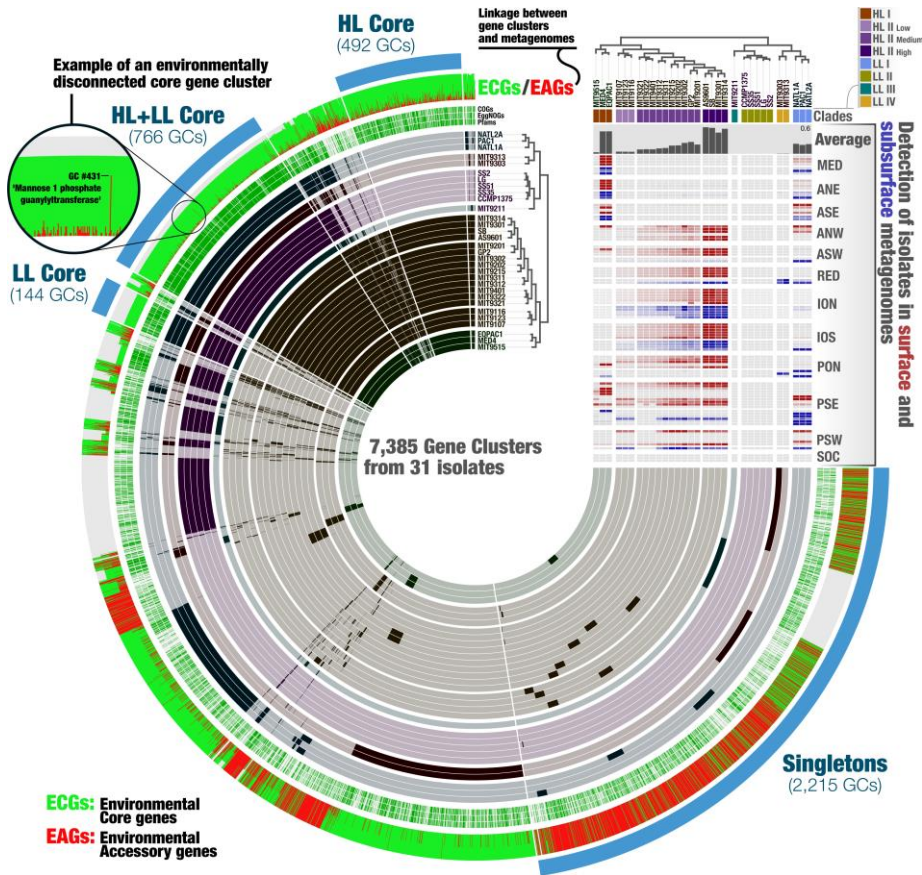
Fig. 4: The metapangenome of *Prochlorococcus*. An overview of the distribution of core and accessory genes obtained from 31 isolates (Delmont and Eren 2018).

1.5 Light-harvesting complex and associated pigments

Prochlorococcus strains possess a unique Pcb light-harvesting antenna, which binds the major light-harvesting pigments DV-Chl *a* and also DV-Chl *b,* if this is present. *Prochlorococcus* is one of few oxygenic phototrophs that do not possess Chl *a* as the major light-harvesting pigment. Interestingly, when mutants of cyanobacterium *Synechocystis* accumulated DV-Chl *a* instead of Chl *a* they were not able to survive

under medium and high-light as a consequence of photodamage. It is suggested that the chlorophyll-binding proteins Pcb evolved during the *Prochlorococcus* evolution to fit to DV-Chl *a* (Goericke and Repeta 1992, Ito et al. 2011). Pcb are integral membrane proteins with six transmembrane helices. These proteins are members of family that includes the Chl *a* binding proteins CP43 and CP47, which form the PSII core antenna in all oxygenic photosynthetic organisms, and IsiA, a Chl *a* binding protein induced by iron starvation in freshwater cyanobacteria (La Roche et al. 1996). It is suggested that *pcb* genes evolved from an ancestral gene similar to *psbC* encoding CP43 (Ting et al. 2009).

According to the comparative genomic analyses, at least eight *pcb* genes (*pcbA - pcbH*) exist in *Prochlorococcus* genus, however different strains exhibit different number of these genes (Ting et al. 2009). Interestingly, it was shown that most of *pcb* genes encoding PSII antenna proteins are constitutively expressed, however in LL strains some *pcb* genes encoding PSI antenna are iron-stress-induced only (Bibby et al. 2003). Generally, LL strains possess from two to eight *pcb* genes, by contrast with HL strains which have only one *pcb* gene - *pcbA* (Bibby et al. 2003, Ting et al. 2009). The higher amount of *pcb* genes in LL strains is caused by multiplication of genes probably (Garczarek et al. 2000). Together with the red shifted absorption maximum, and higher DV-Chl *b/a* ratio, the presence of multiple *pcb* genes in LL strains could be another crucial feature in acclimation to low-light levels.

Structural studies of Photosystem II revealed that Pcb subunits associate with PSII. The amount of associated Pcb per PSII is variable among strains ranging from four to seven subunits. This association to the PSII reaction center (RCII) dimer forms Pcb-PSII supercomplex to increase the light-harvesting capacity of PSII (Bibby et al. 2003, Ting et al. 2009). By contrast, studies of Photosystem I indicate that PSI complexes have trimeric organization and Pcb proteins and associated pigments can form a ring around the PSI reaction center (RCI) (Garczarek et al. 1998, Ting et al. 2002). It was found that in LL strain SS120 the PSI forms a large supercomplex, where the RCI is surrounded by light-harvesting antenna

ring composed of 18 Pcb units. Interestingly, this supercomplex is similar to that which is described in freshwater cyanobacteria deprived of iron. On the other hand, studies on LL strain MIT9313 did not reveal the presence of this supercomplex, but only trimeric organization of PSI complexes (Ting et al. 2002, Bibby et al. 2003).

Additional pigments of *Prochlorococcus* include Chl *b*, zeaxanthin, α-carotene, small amount of Chl *c*-like pigment (Mg 3,8 divinyl phaeoporphyrin a_5), unknown carotenoid and small amounts of phycoerythrin (Goericke and Repeta 1992, Morel et al 1993).

The presence of phycoerythrin (PE) in *Prochlorococcus* strains is much debated. In other cyanobacteria, PE is situated at the periphery of phycobilisomes, which are located at thylakoid membrane, and serves for harvesting light energy and its transmission to other types of phycobiliproteins and eventually to reaction centers. PE also serves as nitrogen storage. Although *Prochlorococcus* lacks phycobilisomes, some strains possess genes *cpeA* and *cpeB* for encoding PE *α* and *β* subunits similar to PE from cyanobacterium *Synechococcus*. PE in *Prochlorococcus* has several structural differences, which led to designation of new PE type called as Type-III (Hess et al. 1996). The PE-III was found first in LL ecotypes of *Prochlorococcus* (i.e. SS120, MIT9313), which live at the bottom of the euphotic zone, where low levels of blue light were detected (Hess et al. 1996, Ting et al. 2001). Using electron microscopy and immuno-labeling with gold particles, Hess et al. 1999 proved that PE-III is predominantly localized within the thylakoid membranes. This result concurrently with the result of study by Lokstein et al. 1999 support its light-harvesting function, although contribution to the total light-harvesting capacity is very low (Steglich et al. 2003). PE was also detected in HL adapted strain MED4, though this strain lost PE α subunit during the evolution probably and the β subunit occurs in degenerated form only (Ting et al. 2001). Because it was found that strain MED4 has 100 times less of PE than strain SS120, it is hypothesized that functional coupling of PE to the DV-chl antenna is very unlikely and perhaps it serves as a photoreceptor (Steglich et al. 2005).

1.6 Physiology and photosynthesis - what is known

1.6.1 Nitrogen assimilation

It is well known that the areas, where *Prochlorococcus marinus* can thrive are restricted to the subtropical and tropical oceans known for their oligotrophic conditions. Due to the physical constrains the water near the surface is stratified. As a result, nitrogen (N) forms are reduced and N concentration can be extremely low in comparison to the deeper layer, where mostly nitrates are present (Partensky et al. 1999).

Prochlorococcus strains are able to use N in various forms e.g. ammonium, nitrate, nitrite, urea, cyanate and amino acids but they are not able to fix dinitrogen. Mainly reduced N sources are preferred for assimilation even if several different N sources are available. Cyanobacteria possess a regulatory system for detection of reduced forms of nitrogen. This system involved the global nitrogen regulator NtcA, the signal transduction P_{II} and PipX that are involved in carbon and nitrogen metabolism and in the control of nitrogen gene expression (Domínguez-Martín et al. 2017). Moreover, NtcA is involved in the response of the cell to changing N conditions. This protein regulates the expression of its own gene and other genes required for the utilization of nitrite and nitrate (Lindell et al. 2002). Nevertheless, the role of these proteins in *Prochlorococcus* is not clear so far and seems to work differently in comparison to other cyanobacteria (Domínguez-Martín et al. 2017).

All *Prochlorococcus* strains can use and prefer ammonium (NH_4^+) as N source. Ammonium is obtained due to the high-affinity amonium transporter, which is encoded by *amt1* gene (Lindell et al. 2002). Nitrogen in this form provides to a cell a big energetic advantage because it is directly incorporated by glutamine synthetase into glutamine and further by glutamate synthase to glutamic acid. This metabolic pathway is common for all *Prochlorococcus* strains (Fig. 5). For the reduction of NH_4^+ to glutamate, only one ATP and two electrons are necessary (García-Fernández et al. 2004). Thus, the reducing power is very low in

comparison to reduction process of nitrate to glutamate (10 electrons needed) or nitrite to glutamate (8 electrons needed) giving the cell the ability to use the saved energy in other metabolic requirements. In the presence of ammonium, genes encoding nitrate reductase, nitrite reductase, glutamine synthase and the transporters of nitrate, nitrite and ammonium as well as of ntcA itself are downregulated. Only if ammonium is depleted, pathways for utilization of different N sources become activated (García-Fernández et al. 2004).
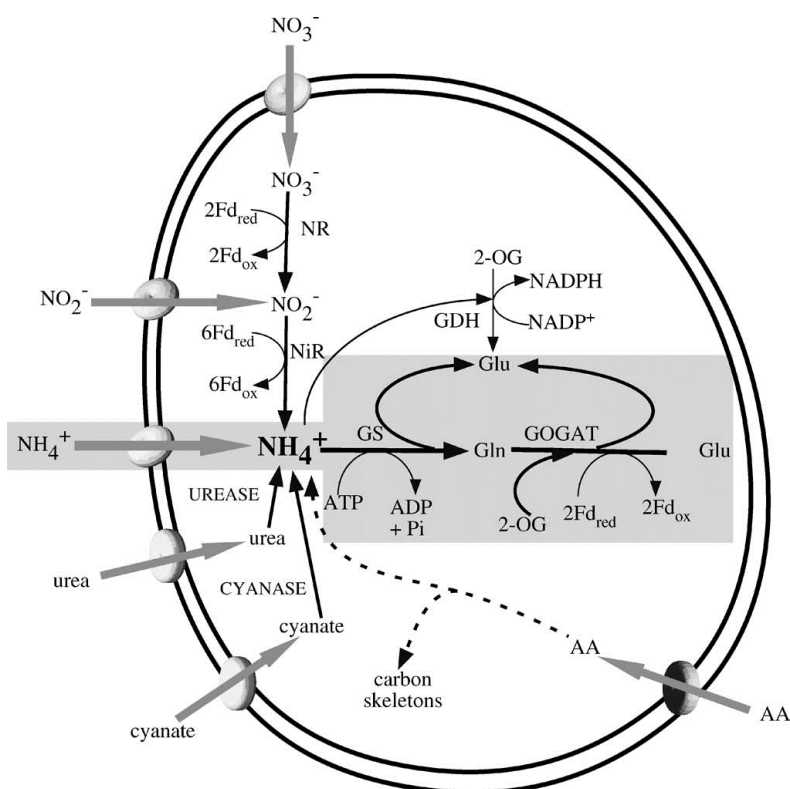
Fig. 5: Nitrogen assimilation routes observed in *Prochlorococcus*. The central pathway for ammonium transport and assimilation is common to all *Prochlorococcus* strains. The utilization of alternative nitrogen sources is strain-specific (García-Fernández et al. 2004).

Assimilation of amino acids such as arginine, glutamine or methionine was also reported (Flores and Herrero 1994, Zubkov et al. 2003). Although, amino acids were not used as a sole N source for *Prochlorococcus* growth, Zubkov et al. 2003 proved that amino acids can fulfil up to 10% of the *Prochlorococcus* requirements for nitrogen. However, not all strains are capable of usage of amino acids although it provides to the cell an important energetic advantage. Two studies revealed that PCC 9511 strain is not able to utilize any of amino acids (Rippka et al. 2000, García-Fernández et al. 2004). Interestingly, study by Yelton et al. 2016 showed that assimilation of organic nutrients is not such an exceptional phenomenon as was suggested. By analysing of genomic and metagenomics data it was revealed that different *Prochlorococcus* isolates possess various amounts and types of transporters to take up amino acids and polypeptides.

Another studies revealed presence of genes responsible for nitrite and cyanate uptake in the *Prochlorococcus* genome and moreover, these compounds such as nitrite, urea or cyanate were positively tested as a sole N source for growth of different *Prochlorococcus* strains (Rippka et al. 2000, Moore et al. 2002, García-Fernández et al. 2004, Martiny et al. 2009, Kamennaya et al. 2011).

It was supposed for a long time, that *Prochlorococcus* is not able to use nitrate as N source, because nearly all known isolates lack the genes needed for its utilization. Moreover, this N form requires high energetic expense for its reduction to molecules that can be assimilated. However, recent study of Berube et al. (2015) proved the existence of genes for nitrate assimilation in strains belonging to both HL and LL ecotypes. Three *Prochlorococcus* strains (HL – SB, MIT0604; LL – PAC1) possess nitrate reductase gene essential for NO_3^- utilization that enables them to growth on NO_3^- as a sole source of nitrogen. Interestingly, the growth of two HL strains on nitrate was approx. 17% slower in comparison to their growth in the presence of ammonium.

Nitrogen metabolism of *Prochlorococcus* is different from that known in classic cyanobacteria. It was found that genes involved in C/N regulation

(namely *ntcA*, *gln B* and *pipX*) and encoding NtcA, P_{II} proteins and PipX do not operate in *Prochlorococus* in the same way as was described in cyanobacteria (Lindell et al. 2002, Palinska et al. 2002). Moreover, the activity and expression of gluthamine synthetase did not change significantly under N starvation or in darkness (El Alaoui et al. 2001, 2003). It was revealed that nitrogen assimilatory pathways vary among strains. The central ammonium assimilation route was retained, however N-related pathways were modified and optimized according to available N sources at the depth where specific strain lives (Moore et al. 2002, Rocap et al 2003, García-Fernández et al. 2004). In addition, recent studies focused on regulation of key enzymes and metabolites involved in N assimilation in different *Prochlorococcus* strains revealed the variety in C/N balance regulation. According to these results, the control of the C/N balance seems to be streamlined probably due to the evolution (Gómez-Baena et al. 2015, Domínguez-Martín et al. 2017, 2018).

1.6.2 Glucose uptake

Prochlorococcus was considered for a long time to be the only photoautotrophic cyanobacterium incapable to use glucose. Initial studies on *Prochlorococcus* strain PCC 9511 revealed no evidence for beneficial effect of glucose on its growth (Rippka et al. 2000). First speculations about possibility of partial heterotrophy came with sequencing of *Prochlorococcus* genome. Genes for sugar transporters were found in strain MIT9313 (Rocap et al. 2003) and gene *pro1404* encoding Na^+/galactoside symporter MelB was discovered in strain SS120 (Dufresne et al. 2003). The first results proving glucose uptake by *Prochlorococcus* were reported in Gómez-Baena et al. 2008 by radioactively labelled ^{14}C-glucose. In addition, it was found that glucose addition in medium leads to the enhanced expression of several glucose-related genes. By further studying the gene *pro1404* encoding the sugar transporter, the multiphasic (biphasic) kinetic behaviour reflecting low- and high-affinity capacity mode in dependence on sugar concentration

was revealed (Munoz-Marín et al. 2013). The biphasic kinetic of the glucose transporter was confirmed by recent study of Munoz-Marín et al. (2017) where five *Prochlorococcus* strains from different clades were tested. Interestingly, only one strain TAK9803-2 lacks this kinetic. The maximum glucose uptake rate was the highest in strain SS120. It is worth noting that both mentioned studies reported about evidence of glucose uptake in natural *Prochlorococcus* populations in the central Atlantic Ocean.

It is suggested that glucose uptake mechanism is a primary transporter. Once glucose is assimilated, it could be fully oxidized providing either twelve molecules of NADPH or two molecules of ATP. Thus, the energetic cost of glucose transport is lower than glucose biosynthesis. Therefore, this might provide an advantage to strains which thrive under low metabolic rates in depths around 200 m, where the energy input from sunlight is very low (Gómez-Baena et al. 2008).

By analysing genomic and metagenomic data it was shown that gene for glucose transporter *melB* (recently known as *glcH* having high affinity for glucose than for other sugars) is highly conserved among *Prochlorococcus* strains. Moreover, these data indicate that mixotrophy is globally distributed in picocyanobacteria, as reported in Yelton et al. (2016). By analysing *Prochlorococcus* and *Synechococcus* genome isolates, various numbers and types of transporters for uptake of organic compounds were revealed. Interestingly, the number of these transporters among *Prochlorococcus* isolates exhibited decreasing pattern from deeply branched LL strains to recently evolved HL strains (Fig. 6).
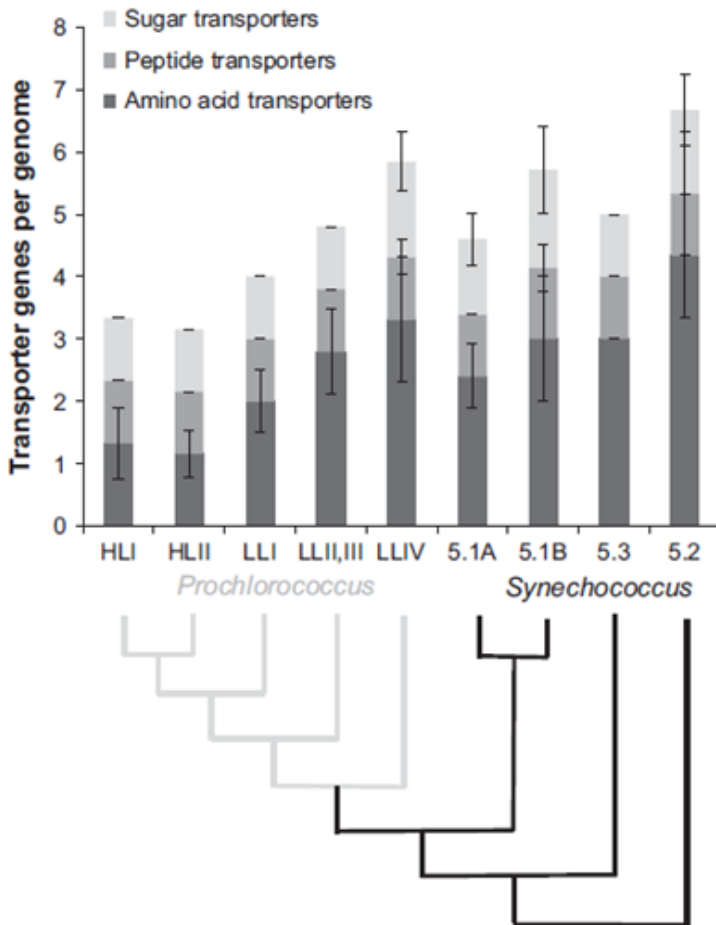
Fig. 6: The number of genes for transporters of organic compounds in genomes of *Prochlorococcus* and *Synechococcus* isolates (Yelton et al. 2016).

Although mixotrophy was confirmed in *Prochlorococcus* strains, they still perform photosynthesis continuously, using glucose as an additional source of carbon and energy when available (Munoz-Marín et al. 2017).

1.6.3 Carbon concentrating mechanism

The carbon concentrating mechanism (CCM) is a system evolved in cyanobacteria to effectively concentrate CO_2 near ribulose-1,5 bis-fosfate

carboxylase oxygenase (Rubisco) for enhancing photosynthetic CO_2 fixation reactions. The CCM ensures active uptake, accumulation, and conversion of inorganic carbon (Ci) into CO_2. This conversion takes place in carboxyzomes - a microcompartment where the Rubisco and carbonic anhydrase (CA) are located. The key element of this mechanism is specific CA, an enzyme that co-localizes with Rubisco and catalyzes the conversion of bicarbonate to CO_2. Most of CAs are fast enzymes catalysing about one million conversions per second. It was revealed that CAs can be divided into five classes (α, β, γ, δ, ζ), which evolved independently (Kupriyanova et al 2013).

To achieve suitable rate of CO_2 fixation, cyanobacteria have to accumulate Ci actively. Five distinct transport systems for active Ci were identified including three HCO_3^- transporters (high-affinity bicarbonate BCT1, high-affinity sodium/ bicarbonate symporter SbtA, low-affinity sodium/ bicarbonate symporter BicA) and two CO_2 uptake systems based on modified NADPH dehydrogenase complexes (NDH-I_4, NDH-I_3). These transport systems differ in maximum flux rates and affinity for substrate (Price 2011, Kupriyanova et al. 2013).

Carboxyzome is polyhedral particle with proteinaceous shell with thickness 3-6 nm around the enzymatic core. This shell is selectively permeable; HCO_3^- can diffuse into the carboxyzome and concurrently the shell works as a barrier, which restricts CO_2 to escape and allows for its significant accumulation inside (Espie and Kimber 2011, Ting et al. 2014). Through the evolution, cyanobacteria have developed two types of carboxyzomes, which differ in their protein composition; α-carboxyzome is typical for oceanic cyanobacteria and β-carboxyzome is found in those living in freshwater (Badger et al. 2006, Price 2008). According to the types of carboxyzome, the cyanobacteria were divided to two groups termed as α- and β-cyanobacteria (Badger et al. 2002). It was found that these two cyanobacteria groups possess different types of Rubisco and vary in possessing of HCO_3^- transport systems in the plasma membrane (Giordano et al. 2005). However, the ecological significance of the

differences in CCMs between α- and β-cyanobacteria still remains enigmatic (Badger et al. 2002).

Rubisco have competitive carboxylase and oxygenase functions. Thus, it is hypothesized that CCMs have evolved due to the sharp increase of oxygen in the atmosphere to avoid oxygenase reaction of Rubisco and to ensure effective CO_2 fixation (Kupriyanova et al. 2013). Although, cyanobacterial Rubisco has lower CO_2 affinity in comparison to other algae, this system allows it to work near its enzymatic maximum (Price 2008). The cyanobacterial CCM is probably the most efficient of any photosynthetic organisms, concentrating CO_2 up to 1000-fold in the close vicinity of Rubisco (Badger and Price 2003). There are four known types of Rubisco among microorganisms: forms IA-D, II, III and IV that are structurally unique and vary in kinetic parameters (Tabita et al. 1999, Scott et al. 2007, Tabita et al. 2008). Cyanobacteria possess either Rubisco form IA in α-carboxyzome (α-cyanobacteria) or form IB in β-carboxyzome (β-cyanobacteria) (Ting et al. 2014).

Prochlorococcus genus belongs to the α-cyanobacteria having the α-carboxyzome and Rubisco type Form IA. The mechanism of inorganic carbon (Ci) transportation through the plasma membrane is still not clear in this genus. According to the studies (Price 2011, Kupriyanova et al. 2013), Ci can enter to the cell either in the form of CO_2 by diffusion or in the form of bicarbonate by two Na^+/HCO_3^- symporters that are energized by inwardly directed Na^+ gradient which is formed by Na^+/H^+ antiporter. The constitutive low-affinity symporter BicA and the inducible high-affinity symporter SbtA, respectively. According to comparative genomic analyses, it was revealed that *Prochlorococcus* lacks genes encoding BCT1 and both CO_2 uptake systems (Giordano et al. 2005, Ting et al. 2014). The bicarbonate is transported through cytoplasm to the carboxyzomes by diffusion. It was shown that carboxyzomes in *Prochlororococcus* tend to cluster probably for better utilization of CO_2 and reduction of its loss by leakage (Ting et al. 2002). Interestingly, study Ting et al. 2007 reported that carboxyzome size vary among *Prochlorococcus* strains. Moreover, deeply branched strains (e.g.

MIT9313) possess carboxyzome gene (*csoS1E*) encoding additional shell protein in comparison to those strains which have recently evolved (e.g. MED4). The bicarbonate can diffuse into the carboxyzomes where it is transformed to CO_2 by CA belonging to the novel ε-class. As was recently shown by structural studies, this class is a subclass of β-CA (Ting et al. 2014). Remarkably, LL strain SS120 does not encode any known CA. Thus, it is suggested that its function might be taken over by an unidentified protein (Dufresne et al. 2003). Fundamental components of CCM within *Prochlorococcu*s lineage are shared and highly conserved (Fig. 7). However, some specific elements have diversified between strains probably due to the optimizing of CCM functions.
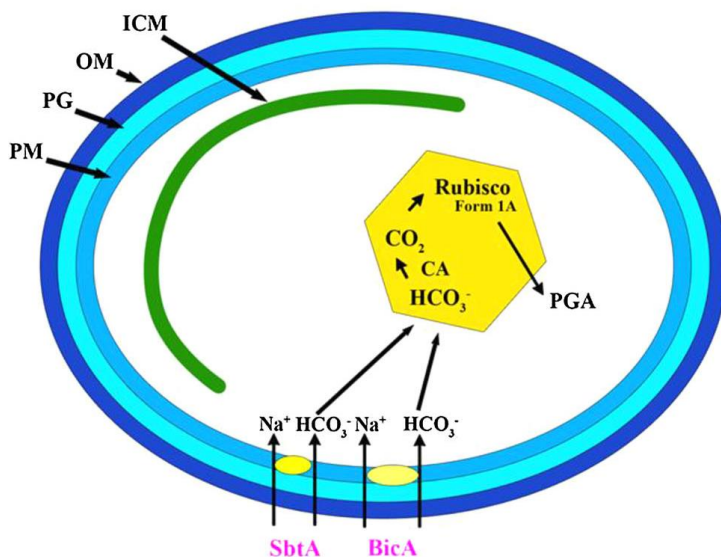
Fig. 7: A schema of CCM model in *Prochlorococcus* with Na^+/HCO_3^- symporters and carboxyzome-associated reactions. PM plasma membrane, PG peptidoglycan, OM outer membrane, ICM intracytoplasmic lamellae, PGA phosphoglyceric acid, CA carbonic anhydrase (Ting et al. 2014).

1.6.4 Oxygen evolution

Photosynthetic water oxidation is catalyzed by oxygen-evolving complex (OEC) associated with PSII at the luminal side of thylakoid membrane and leads to the production of protons and molecular oxygen. The catalytical center of this reaction is Mn_4Ca-cluster containing four Mn atoms and one Ca atom, which exists in five oxidation states from S_0 to S_4 (Veerman et al. 2005, Kawakami et al. 2011). The water-splitting undergoes a cyclic process when four electrons and four protons are extracted from two molecules of water, and one molecule of oxygen is evolved (Umena et al. 2011). According to the crystal structure of PSII of *Thermosynechococcus elongatus* and *T. vulcanus*, cyanobacterial OEC is composed of three extrinsic proteins PsbO, PsbU and PsbV that together form a large protein cap that shields Mn_4Ca-cluster from the aqueous phase (Kamiya and Shen 2003, Ferreira et al. 2004, Guskov et al. 2009). Nevertheless, it was shown that some cyanobacteria also possess PsbQ and PsbP proteins, which are anchored to the thylakoid membrane (De Las Rivas et al. 2004, Thornton et al. 2004).

PsbO, the larger subunit, is common to all photosynthetic organisms and plays an important role in maintaining stability and activity of the Mn_4Ca-cluster (Balint et al. 2006, Enami et al. 2008). PsbP unit is associated with the thylakoid membrane and it was suggested that it has a regulatory role in association of calcium and chloride to the domain, which is responsible for oxygen evolution. Together with PsbQ are required for optimal oxygen evolution activity, and they are involved in modulating the $CaCl_2$ requirement for PSII activity. Moreover, it was shown, that this protein has a key role in water-splitting when PsbU and PsbV are not present (Thornton et al. 2004). PsbU unit is important in stabilization and protection of OEC and protects it against heat. Together with PsbV it protect PSII against dark inactivation and photodamage (Nishiyama et al. 1997, Dufresne et al. 2003, Kimura et al. 2002, Inoue-Kashino et al. 2005).

The oxygen-evolving complex in *Prochlorococcus* genus exhibited important differences not only in comparison to the OEC of classic cyanobacteria but also among *Prochlorococcus* strains (Fig. 8). OEC in most of *Prochlorococcus* strains is minimalist, composed of only two proteins, i.e. PsbO and PsbP that create a specific environment of the Mn_4Ca-cluster where the water-splitting takes place (Ting et al. 2009). Thus, most of strains lack essential units PsbU and PsbV. Such a huge reduction of OEC was caused by gene loss through evolution to streamline the *Prochlorococcus* genome. Interestingly, it was shown that deletion of *psbU* and *psbV* genes in cyanobacterium *Synechocystis* sp. PCC 6803 severely limited its photo-physiology. Mutants exhibited decreased growth, significantly lower oxygen evolution and destabilization of PSII complex (Shen et al. 1995, 1997, Inoue-Kashino et al. 2005). Remarkably, comparative genomic analyses revealed, that in two LL strains (MIT9313 and MIT9303, according to the phylogeny both of them were found at the base of *Prochlorococcus* radiation), OEC is still made up of four proteins. These two strains possess extra genes encoding PsbU and PsbV units (Ting et al. 2009).
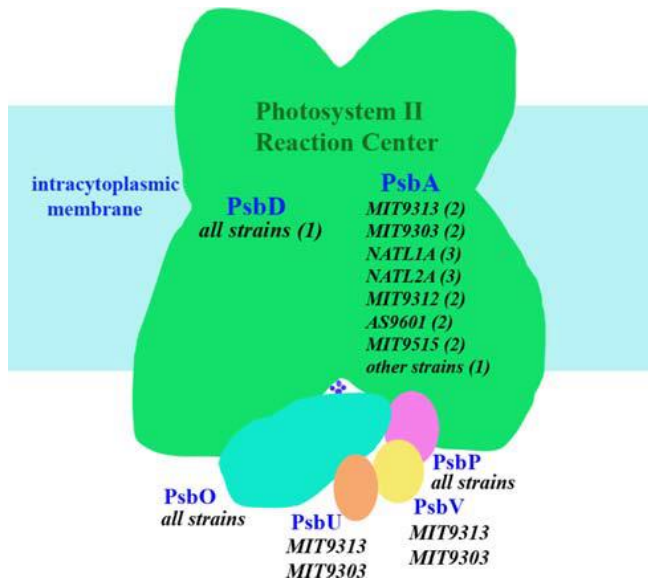
Fig. 8: A schema of Photosystem II with core proteins (PsbA and PsbD with number of their genes in parentheses) and associated extrinsic proteins creating oxygen-evolving complex in different *Prochlorococcus* strains (Ting et al. 2009).

Although the structure and function of OEC proteins are known, the process of oxygen evolution has been poorly studied in *Prochlorococcus marinus*. Only in one paper, published by Mimuro et al. (2011), the oxygen-evolving activity for three *Prochlorococcus* strains was reported so far. However, results describing gross and net oxygen primary production are not available probably due to the high sensitivity of this phototroph to sudden disturbances, such a concentrating and mechanical stirring which are usually the necessary steps used in the standard method of oxygen measurements. As our laboratory has many experiences with *Prochlorococcus* cultivation and with various methods of determining the rates of oxygen evolution, we performed a series of measurements, collected and analysed the data of comparative oxygen evolution in major

marine cyanobacteria and prepared them for publication (Partensky et al. 2018).

1.6.5 High-light stress

The ocean is a dynamic environment in which phytoplankton must cope with rapid changes in resources, particularly irradiance which can exceed photosynthetic requirements of the phytoplankton. Changes in irradiance level can be rapid due to the mixing in the water column. Thus, phytoplankton can move vertically through a large depth/irradiance gradient. High irradiance can lead to photoinhibiton and loss of function of the photosynthetic apparatus. This can happen when PQ pool becomes over-reduced or during charge recombination between PSII acceptor and donor side. Over-reduction of the PQ pool leads to the generation of singlet oxygen species, which can damage core of PSII (Six et al. 2007, Berg et al. 2011). This leads to the decrease in PSII photochemical efficiency, in the oxygen evolution and in the rate of carbon fixation. To protect photosynthetic apparatus and to avoid photoinhibition, cyanobacteria possess several photoprotective mechanisms, which can be divided according to the level of regulation. The dissipation of excess photon energy is controlled either at the level of light-harvesting, i.e. by state transitions (quick disconnection of phycobilisomes from PSII and their movement on the thylakoid membrane towards PSI), by energy quencher known as the orange carotenoid protein (OCP) in some cyanobacteria, by high-light inducible proteins (HLIP), or by non-photochemical quenching of chlorophyll *a* fluorescence (Bhaya et al. 2002, Bailey et al. 2005, Six et al. 2007, Kaňa et al. 2012, Kulk et al. 2013, Kirilovsky and Kerfeld 2016). The second level of defence against high-light damage is at the level of electron transport by alternative electron transport, i.e. by diverting electrons from the main linear electron transport chain to external acceptors, and/or by launching the cyclic electron flow around PSI (Mullineaux 2014a, Mullineaux 2014b). These general mechanisms decrease the probability of formation of oxygen

reactive species and damaging of photosynthetic apparatus in cyanobacteria.

As mentioned earlier, *Prochlorococcus* light-harvesting system significantly differ from other cyanobacteria, thus it has evolved different strategies how to cope with high levels of irradiance. Study Bailey et al. (2005) has shown that *Prochlorococcus* is capable of forming rapidly reversible non-photochemical quenching of chlorophyll *a* fluorescence. Two strains, HL adapted PCC 9511 and LL adapted SS120 were tested showing significantly higher values of NPQf for HL adapted strain. This is probably connected to the depth and light levels where these strain thrive. Strain PCC 9511 living in turbulent mixing water in the surface of ocean is exposed to fluctuating irradiance thus it regulates light-harvesting through NPQf.

Prochlorococcus possess a photoprotective xanthophyll pigment zeaxanthin (Goericke and Repeta 1992) in large amounts. This pigment is able to dissipate excess energy as a heat. As was shown by Kulk et al. (2011), the concentration of zeaxanthin increased with irradiance suggesting its photoprotective role in strain MED4. However, it is not known to be part of the Pcb antenna, instead it is thought to be present in lipid globules and acts as an photoprotective "umbrella" or sunscreen lotion.

Interestingly, genome analysis revealed that some *Prochlorococcus* strains possess LOV domain, part of OCP C-terminal domain and some other proteins interacting with OCP. OCP mediates energy and fluorescence quenching at the level of phycobilisomes. As *Prochlorococcus* do not possess phycobilisomes, the role of these genes remains unclear (Kirilovsky and Kerfeld 2013).

Many studies focused on the role of the high-light inducible proteins (HLIP) in the acclimation of photosynthetic organisms to photo-oxidative stress. They are members of protein family that includes Chlorophyll *a/b* (CAB)-binding light-harvesting antenna proteins (Hess et al. 2001). HLIP were first identified in cyanobacteria, however they were found also in eukaryotic algae (Reith and Munholland 1995) and in higher plants

(Jansson et al. 2000). Recently, they were shown to have photoprotective function (Staleva et al., 2015, Komenda and Sobotka 2016). *Prochlorococcus* has the greatest number of *hli* genes among cyanobacteria and it was shown that they are upregulated under high-light stress and nitrogen starvation (Steglich et al. 2006, Tolonen et al. 2006). Generally, it was found that genome of HL adapted strains contains many more *hli* genes in comparison to LL adapted strains, e.g. MED4 contains 22 *hli* genes, which is twofold higher than in MIT9313 with 9 or in SS120 with 12 *hli* genes. Interestingly, in contrast, NATL1 and NATL2 strains both LL adapted strains possess 41 *hli* genes, which is significantly more than contain HL strains. However, it was shown that these strains have remarkably similar properties as HL strains (Bhaya et al. 2002, Kettler et al. 2007). In general, these proteins are needed for active protection of photosystems and especially the Pcb antennae that surround them (Bibby et al. 2003) against high-light and UV stress. HLIPs may contribute to the ability of HL strains to growth successfully at higher intensities, notably at high latitude (Rocap et al. 2003, Partensky and Garczarek 2010).

The alternative electron flows are known for its function to remove the excess of electrons from photosynthetic linear electron pathway as a response to the high-light conditions. These alternative pathways are switched on either to prevent the damage of photosystems when linear electron transport is saturated or to regenerate proton-motive force for ATP synthesis. Cyanobacteria exhibit several modes of cyclic electron pathways around Photosystem I or they divert electrons through various valves to oxygen (Fig. 9).
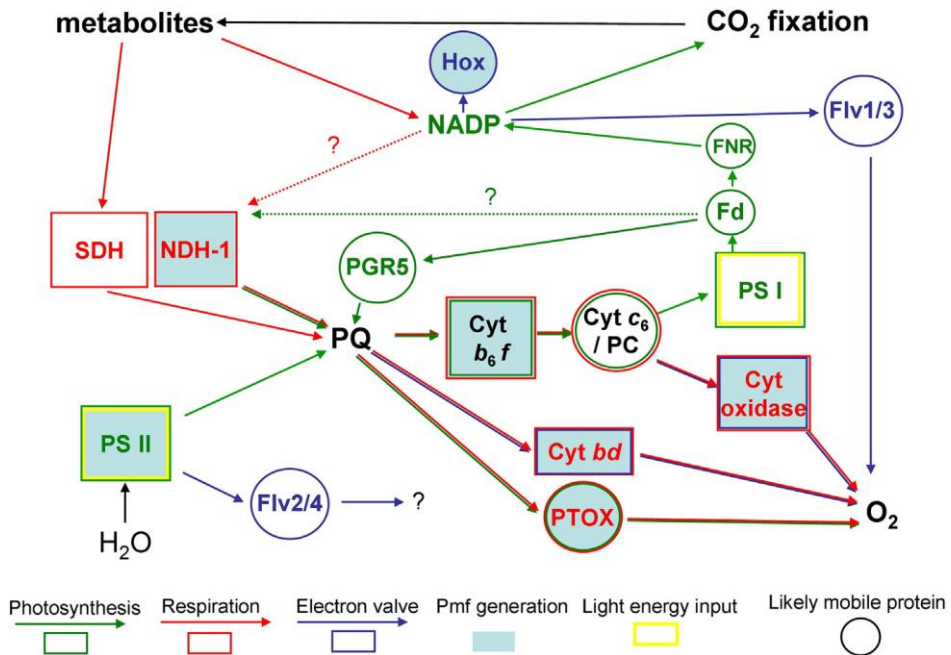
Fig. 9: Linear and cyclic electron transport pathways taking place in and around thylakoid membrane in cyanobacteria (Mullineaux et al. 2014b).

The presence of alternative electron pathways in *Prochlorococcus marinus* is much debated and their function is poorly known. Although several field and laboratory studies tried to investigate these electron flows, there is no direct evidence about their regulation so far. Mostly it is suggested that *Prochlorococcus* can use plastoquinol terminal oxidase (PTOX) pathway that redirects electrons from plastoquinone pool to oxygen. Metagenomics dataset revealed PTOX genes in HL strain MED4 (McDonald and Vanlerberghe 2005). Mackey et al. (2008) reported the possible activity of PTOX in maintaining of high photochemical efficiency and PSII reaction centers in oxidized state under high-light. Moreover, after treatment with propyl-gallate inhibitor (PGal), PSII electron flow decreased. By comparison, Kulk et al. (2013) published that using of PGal for inhibition of terminal oxidase in cells of the same strain

at high irradiances has no influence on loss of viability. Thus, the changes in the photo-physiology were probably related to the PSII level. In another study, Zinser et al. (2009) found that MED4 strain possesses NDH-I complex, which is involved in cyclic electron transport around PSI.

It is worth to note that existing studies observed possible involvement of alternative electron pathways only in one *Prochlorococcus* HL strain, which was exposed to high irradiances. However, these results provide only the indirect evidence about the participation of alternative electron pathways in metabolism of *Prochlorococcus* cells.

1.7 Estimation of oceanic primary production

Although the estimation of oceanic primary production is widely studied field, it remains challenging. Phytoplankton communities are a dynamic systems responding to continual changes in environment. Major ecological factors determining primary production are availability of nutrients, irradiance and grazing by zooplankton or viral infections. Phytoplankton drives the biogeochemical cycling of many elements and affects the functioning of aquatic ecosystems and climate on global scales. Therefore, it is important to understand the traits, which describe cell properties during resource-limited growth (Litchman and Klausmeier 2008).

For the estimation of phytoplankton photosynthetic production, labelling with inorganic ^{14}C is commonly used. This method developed by Steeman Nielsen in 1952 is reliable, sensitive and for its simple usage, it was rapidly applied for measurements of photosynthetic rates in aquatic systems. However, besides problems and concerns regarding its radioactivity, this technique is accompanied by an essential methodological concern regarding the incubation duration (Marra 2009, Laws 2013). This influences whether the incorporation of inorganic ^{14}C

provides an estimate of gross or net photosynthesis or the intermediate rate. To follow the fate of carbon in the cell, in study Halsey et al. (2010) ^{14}C method combining two time-dependent approaches of incubation was used in nitrogen-limited cultures of green alga *Dunaliella tertioclecta*. Short-term incubations (20 minutes) revealed different lifetime of the newly fixed carbon in the cell which depending on the nutrient limitation, i.e. specific growth rate. When the incorporation of the newly fixed carbon was tracked for 24 hours, it was found, that amount of carbon fixed by Rubisco, i.e. chlorophyll-specific gross carbon primary production (GPC[b]) is similar among nitrogen-limited cultures. Moreover, it was found out that amount of newly fixed carbon retained in biomass, i.e. chlorophyll-specific net carbon primary production (NPC[b]) was approx. 35% of GPC[b] in all cultures independently of nitrogen limitation. Nevertheless, the rest of carbon that does not contribute to the biomass was a transient carbon pool, which displayed decline in its kinetics over 24 hours. Several studies confirmed the decline in kinetics of chlorophyll-specific ^{14}C-based production over 24 hours. Moreover, it was revealed that the decline is affected by growth rate, i.e. the lifetime of transient carbon pool varies as a consequence of environmental stresses (Halsey et al. 2011, 2013, Pei and Laws 2013). With increasing nutrient limitation, i.e. with decreasing specific growth rate, the newly fixed carbon in the form of transient carbon was rapidly respired (in tens of minutes reached the levels of NPC[b]) and was used for ATP synthesis fuelling energetic demands of cell. Hence, ^{14}C method gives a good estimate of net photosynthesis at low growth rates. On the contrary, cells grown at high growth rates, i.e. nutrient non-limited catabolized the transient carbon pool very slowly (it takes approx. 8 hours until it reached the NPC[b]). This slow processing of newly fixed carbon is used for reductant regeneration. Thus, it was shown that transient carbon pool is catabolized according to cell requirements for ATP and NADPH.

According to these results, only the long-term ^{14}C method (24 hours) incubations) can serve as a reliable index of net carbon primary production. On the other hand, data obtained from the short-term

incubation method (20 or 40 minutes) used in the laboratories are not suitable for modelling primary production because then this method provides information about photosynthate utilization pathways. However, by combining these two time-dependent ^{14}C methods it is possible to put together model of carbon utilization, which reveals the discrepancy between GPC[b] and NPC[b] and growth-rate-dependent shifts in metabolic pathways.

Phytoplankton photosynthetic efficiency can be also expressed as a rate of oxygen normalized to chlorophyll (Laws 2013). Model of carbon utilization taken together with oxygen measurements and estimates of electron flow through PSII (Silsbe et al. 2015) allows to assemble photosynthetic efficiencies normalized either to chlorophyll or to spectral absorption (Halsey et al. 2013, 2014).

A recent study by Jones et al. 2017 introduced a novel approach to determine net primary production using rapid sorting flow cytometry combined with measurements of ATP and NADPH. The big advantage of this new method is in substitution of ^{14}C technique for estimation of NPP, which is based on samples incubations, and primarily in assessment of biomass and growth rate in the field. Oceanic NPP can be simply calculated using growth rate and phytoplankton carbon ($NPP = \mu * PC$). However, it turned out to be a methodological challenge to measure these two parameters in the field. For this reason, to determine phytoplankton abundance, chlorophyll concentration are routinely measured. Finally, to assess NPP, ^{14}C uptake data are related on chlorophyll (Laws 2013, Halsey et al. 2010).

Phytoplankton responds to varying environment, mainly to light and nutrient by adjusting of chlorophyll content. Decreasing growth irradiance causes increasing of amount of chlorophyll to ensure efficiently capture more light. Decreasing nitrogen concentration in environment causes reduction of N-rich pigment chlorophyll, which results in reduction of light-harvesting system (Halsey and Jones 2015, Graff et al. 2016). These changes are reflected by alterations of metabolic pathways and reallocation of photosynthetic energy to optimize growth. All these

factors together with described integrated models (Behrenfeld and Falkowski 1997) needs to be involved in calibrating satellite algorithms for quantifying global NPP (Behrenfeld et al. 2005, Halsey and Jones 2015).

2. Aim and hypothesis

Phytoplankton living in the ocean has to cope with dynamic changes of nutrient availability and irradiance intensity, which directly influence the process of photosynthesis. The overall aim of the thesis was to study mechanisms, which regulate allocation of photosynthetic primary production in cyanobacterium *Prochlorococcus marinus* under various environmental conditions, i.e. nitrogen limitation and light intensity, respectively. My research was based on the assumption of recent model describing the relationship between photosynthetic activity and primary production (Halsey et al. 2010). Thus, to study this relationship, it was necessary to assess basic physiological parameters of photosynthetic production and to quantify biochemical pools, i.e. where the fixed photosynthetic energy is allocated.

The research was based on (1) physiological approach – to analyse the utilization of photosynthetic energy and regulation of metabolism (photosynthesis, i.e. oxygen evolution, respiration, and carbon allocation) and on (2) molecular approach – to investigate how the unique structure of the oxygen-evolving cluster influences the photosynthetic activities.

Specific hypothesis and aims

(h1) **Effect of nitrogen limitation on the photosynthetic energy utilization.**
We tested the changes in cellular properties and in gross and net carbon primary production in dependence on growth rate that was manipulated by availability of nitrogen. Two distinct strains of *Prochlococcus marinus* (HL vs. LL adapted strain) were grown at three different specific growth rates in nitrogen-limited continuous cultures. We described the influence of N limitation on Photosystem II performance, on its functional absorption cross section and maximal photosynthetic efficiency, and on the amount of newly fixed carbon, i.e. the amount of assimilated carbon

by Rubisco and the amount of carbon stored in the biomass. We have revealed that the newly fixed carbon is utilized differently depending on the specific growth rate. Obtained data were compared with results known for eukaryotic algae (Papers I and III).

(h2) **The carbon allocation in acclimated cells changes in proportion to the degree of nutrient stress by nitrogen limitation.**
We determined the relative macromolecular biomass composition and its changes in HL and LL adapted strains of *Prochlorococcus marinus* grown in three different steady-state nitrogen-limited cultures. Changes in biomass composition depending on the N limitation were compared with data known for eukaryotic algae (Papers I and III).

(h3) **The functional adaptation of oxygen-evolving complex does not limit oxygen evolution in *Prochlorococcus*.**
We investigated oxygen evolution in different strains with varying composition of the oxygen-evolving complex. In four marine picocyanobacteria acclimated to low, medium and high light, we measured the rates of oxygen evolution and thermoluminescence. As these cyanobacteria vary in structure of OEC, i.e. some strains lack two subunits of OEC we wanted to know if this functional adaptation was efficient. We hypothesized that the reduced form of OEC is sufficient to ensure proper oxygen evolution (Paper II).

(h4) **LL and HL adapted strains of *P. marinus* exhibited distinct metabolisms.**
We evaluated and compared the photo-physiology and photosynthetic energy utilization in two distinct strains of *P. marinus*, i.e. HL and LL adapted strains growing similarly in N-limited continuous cultures. We hypothesized that LL adapted strain is more efficient in conversion of photosynthetic energy into biomass in comparison to HL adapted strain. Possible role of mixotrophy is discussed (Paper III).

3. Methods

3.1 Model organisms

Four marine picocyanobacteria were used in this work. HL adapted *Prochlorococcus marinus* strain PCC 9511 (Papers I, II, III), two LL adapted strains MIT9313 (Papers I, II, III) and SS120 (Paper II), and *Synechococcus* WH7803 (Paper II). These cyanobacteria, although closely related, were selected for their distinct genome and physiology. Phylogeny and evolutionary relationship among these strains are summarized in Fig. 10. The basic summary and comparison of their distinct characteristic are listed in the Table 1.
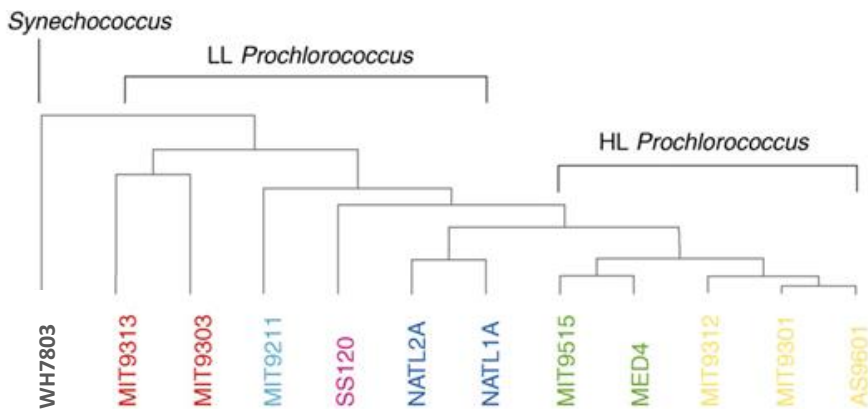
Fig. 10: The position of marine picocyanobacteria used in this work in the phylogenetic tree. Branching order of the isolates is based on *rpoB* gene (β subunit of RNA polymerase) (Coleman and Chisholm 2007).

Table 1: An overview of the major genetic and photosynthetic characteristics of picocyanobacteria used in this work.

	WH7803	MIT9313	SS120	PCC 9511	
Genome feature	2.366.980	2.410.873	1.751.080	1.657.990	chromosome size (bp)
	2.586	2.330	1.930	1.763	number of genes
	60	50	36	30	GC content (%)
Photobiology	0	2	8	1	*pcb* genes
	αβ	αβ	αβ	α	phycoerythrin subunits
	8-14	12	9	22	*hli* genes
N acquisition	+	+	+	+	ammonium
	+	+	-	-	nitrite
	+	+	-	-	amino acids
CCM		SbtA	SbtA	SbtA	Ci transporters
	BicA	BicA	BicA	BicA	
	+	+	-	+	CA
OEC	+	+	+	+	PsbO
	+	+	+	+	PsbP
	+	+	-	-	PsbU
	+	+	-	-	PsbV

Cyanobacteria were cultivated in continuous (Papers I and III) and semi-continuous cultures (Paper II) under constant light with appropriate intensity. Cultures grew for at least 10-15 generations to ensure full acclimation. Depending on growth rate, i.e. N-limitation, cultures grew 3-14 weeks.

HL adapted strain PCC 9511 and LL adapted strain MIT9313 were grown in chemostat mode (Fig. 11). The culture set up was based on the maintenance of appropriate cell suspension volume with continuous flow of fresh media through the culture.
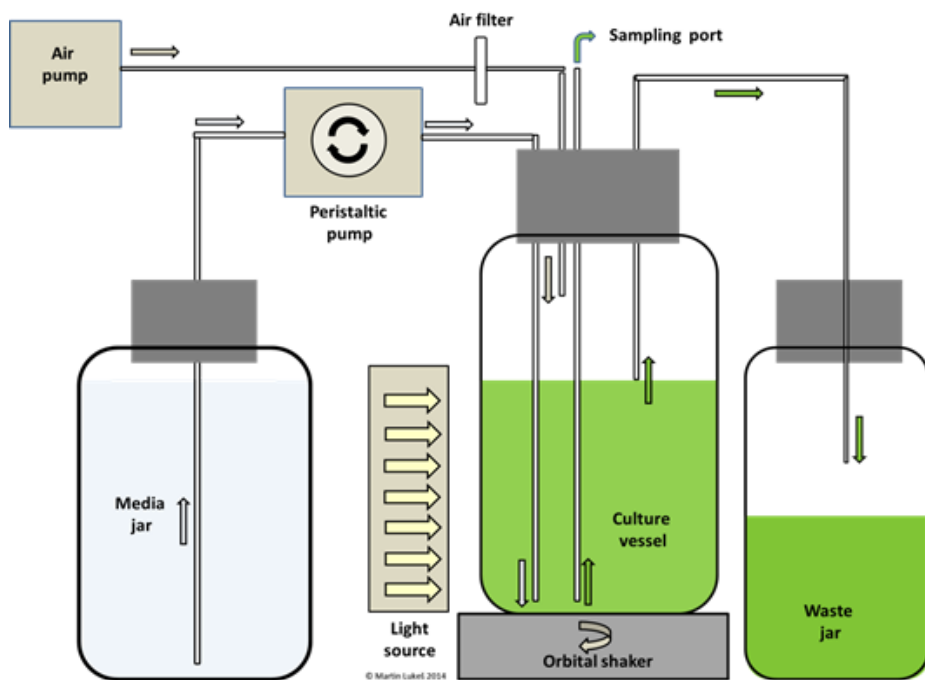
Fig. 11: A schema of the continuous culture used in this work.

Cultures were cultivated in 1L Erlenmeyer flasks which were placed on orbital shaker under constant temperature and continuous constant suitable growth irradiance, and aerated. Both cultures were grown under three different specific growth rates, which corresponded to the concentration of ammonium in the medium (Paper I and III, respectively). To determine oxygen evolution rates in four distinct marine picocyanobacteria (see Table 1), cultures were grown to the acclimated state and diluted 2-3 days prior to measurements to bring them into mid-exponential phase. Cultures were cultivated under constant temperature and under three different irradiance to test the influence of growth irradiances and high-light stress (Paper II).

3.2 Methods

^{14}C labelling

^{14}C labelling is a generally used method for estimation of primary production. It is based on inoculation of culture with labelled sodium bicarbonate. We used two approaches of ^{14}C incorporations to follow the fate and utilization of carbon within the cell (details see in Papers I and III).

Instrumentation: Tri-Carb 2810 TR liquid scintillation analyser, PerkinElmer, USA.

Oxygen evolution measurements

Membrane inlet mass spectrometry was used for measuring of production and consumption of oxygen. Conjunction with tracer $^{18}O_2$ which was added to the cell suspension during the measurement, allows observing consumption of oxygen $^{18}O_2$ and evolution of $^{16}O_2$ due to the water-splitting during the light exposure. This method enables to measure net and gross O_2 production as well as light-dependent O_2 consumption (Paper I).

Oxygen evolution was also measured by optically based oxygen sensor - optode. The principle of this method consists in the effect of dynamic luminescence quenching by molecular oxygen. The key advantage is that during measurements, oxygen is not consumed and cultures do not have to be mechanically stirred. (Paper II)

Instrumentation: Prisma QMS-200 quadrapole mass spectrometer, Pfeiffer Vacuum, USA; NeoFox system, Ocean optics Inc., USA.

Electron transport rate

Fast repetition rate chlorophyll variable fluorescence technique allows for rapid measuring of photochemical efficiency and light absorption, which enables to calculate the electron transfer rates through Photosystem II (details in Paper I).

Instrumentation: Fluorometer FL3500, Photon System Instrument, CZ.

Fourier transform infrared spectroscopy

We investigated the biochemical composition of cells using FTIR spectroscopy. This method enables semi-quantitative determination of the amount of cellular biochemical pools i.e. carbohydrates, proteins and lipids according to distinct vibrational frequencies of specific chemical bonds in these molecules (Papers I and III).

Instrumentation: Nicolet IS10, Thermo Scientific, USA, with Si 384-well plate, Bruker, USA.

Thermoluminescence

We used thermoluminescence to record photons emitted during charge recombination in active PSII reaction centers which allows us to calculate the abundance of active PSII centers and the energetics of charge recombination in PSII (Paper II).

Intrumentation: Thermoluminescence System TL 200/PMT, Photon Systems Instruments, CZ.

Gene expression

We checked the presence of genes encoding proteins creating OEC (see details in Paper II).

Instrumentation: Biosystem GeneAmp 5700, Life Technologies Inc., Applied Biosystems, USA.

4. Overview of my research

My thesis is based upon two published papers, and one manuscript in preparation. Paper I focuses on photo-physiology of cells and carbon allocation patterns in *P. marinus* strain PCC 9511 grown in nitrogen-limited continuous cultures (h1, h2). Paper II evaluates photosynthetic performances of four marine picocyanobacteria possessing various structures of oxygen-evolving complex under three acclimation irradiances (h3). Paper III (manuscript in preparation) compares cellular properties and carbon metabolism (h1, h2) between high-light and low-light adapted strains of *P. marinus* in nitrogen-limited continuous cultures (h4).

Paper I

Carbon use efficiencies and allocation strategies in Prochlorococcus marinus strain PCC 9511 during nitrogen-limited growth.

We studied cell properties including carbon allocation dynamics in the globally abundant and important cyanobacterium *Prochlorococcus marinus* strain PCC 9511 grown at three different growth rates in nitrogen-limited continuous cultures.

With increasing nitrogen limitation, cellular divinyl chlorophyll *a* and the functional absorption cross section of Photosystem II decreased, although maximal photosynthetic efficiency of PSII remained unaltered across all N-limited growth rates. Chl-specific gross and net carbon primary production were also invariant with nutrient-limited growth rate, but only 20% of Chl-specific gross carbon primary production was retained in the biomass across all growth rates. In nitrogen-replete cells, 60% of the assimilated carbon was incorporated into the protein pool while only 30% was incorporated into carbohydrates. As N limitation increased new carbon became evenly distributed between these two pools.

While many of these physiological traits are similar to those measured in other algae, there are also distinct differences, particularly the lower overall efficiency of carbon utilization. The latter provides new information needed for understanding and estimating primary production, particularly in the nutrient-limited tropical oceans where *P. marinus* dominates the phytoplankton community composition.

Paper II

Comparison of photosynthetic performances of marine picocyanobacteria with different configurations of the oxygen-evolving cluster.

The extrinsic PsbU and PsbV proteins are known to play a critical role in stabilizing the Mn_4CaO_5 cluster of the PSII oxygen-evolving complex (OEC). However, most isolates of the marine cyanobacterium *Prochlorococcus* naturally miss these proteins, even though they have kept the main OEC protein, PsbO. A structural homology model of the PSII of such a natural deletion mutant strain (*P. marinus* MED4) did not reveal any obvious compensation mechanism for this lack.

To assess the physiological consequences of this unusual OEC, we compared oxygen evolution between *Prochlorococcus* strains missing *psbU* and *psbV* (PCC 9511 and SS120) and two marine strains possessing these genes (*Prochlorococcus* sp. MIT9313 and *Synechococcus* sp. WH7803). While the low light-adapted strain SS120 exhibited the lowest maximal O_2 evolution rates (P_{max} per divinyl-chlorophyll *a*, per cell or per Photosystem II) of all four strains, the high light-adapted strain PCC 9511 displayed even higher P^{Chl}_{max} and P^{PSII}_{max} at high irradiance than *Synechococcus* sp. WH7803. Furthermore, thermoluminescence glow curves did not show any alteration in the B-band shape or peak position that could be related to the lack of these extrinsic proteins. This suggests an efficient functional adaptation of the OEC in these natural deletion mutants, in which PsbO alone is seemingly sufficient to ensure proper oxygen evolution.

Our study also showed that *Prochlorococcus* strains exhibit negative net O_2 evolution rates at the low irradiances encountered in minimum oxygen zones, possibly explaining the very low O_2 concentrations measured in these environments, where *Prochlorococcus* is the dominant oxyphototroph.

Paper III (manuscript in preparation)
Carbon metabolism differs in low-light and high-light ecotypes of Prochlorococcus marinus.

Prochlorococcus marinus is very important oceanic cyanobacterium living in the oligotrophic regions of oceans contributing up to 50% to the total primary productivity. We investigated photo-physiology and dynamics of newly fixed carbon in steady state cultures of low-light adapted strain *P. marinus* MIT9313 growing under three nitrogen-limited growth rates. We monitored Photosystem II characteristics, including the maximal and effective photochemical efficiency of PSII, the functional absorption cross section and changes in DV-Chl *a* concentrations. To assess gross and net carbon primary production and to follow the carbon utilization within the cell, the carbon assimilation was measured continuously over 24 h.

Increasing nitrogen limitation caused decrease in amount of DV-Chl *a*, reduction of the proportional size of PSII and reduction of the protein pool. However, the maximal and effective photochemical efficiency of PSII as well as Chl-specific net and gross carbon primary production remained unaffected. Approximately, 28% of newly fixed carbon was retained in the biomass across all growth rates.

Our results were compared to those known for physiologically and genetically distinct HL adapted strain PCC 9511. Taken these models together, we observed similar patterns in the adaptation of PSII and in biomass composition with increasing nitrogen limitation. Although the Chl-specific net and gross carbon primary production were not affected

by N limitation, the amount of newly fixed carbon by Rubisco as well as amount of carbon retained in biomass were significantly higher in LL adapted strain. Moreover, we found that time-dependent catabolism of newly fixed carbon significantly differ suggesting that cell needs to cover ATP demands.

Generally, from changes in the light-harvesting systems together with well-adapted genome and with possible role of mixotrophy we concluded that LL strain MIT9313 might be more efficient in converting of light energy into biomass.

5. Conclusions and future prospects

Oxygenic photosynthetic microorganisms, cyanobacteria and algae convert the light energy to the energy of chemical bonds and constitute the base of biological carbon cycle in aquatic environment. Phytoplankton produce approx. a half of global photosynthetic production annually. Thus, from the global aspect, the correct quantification of primary production of phytoplankton is necessary.

Regulation of photosynthesis and primary production of globally abundant and important cyanobacterium *Prochlorococcus marinus* under nitrogen and light stress was investigated in this thesis. Concentration of nitrogen and light availability in the ocean are the key conditions driving changes at the cellular level affecting all metabolic pathways which at the end determine also the species composition of phytoplankton in the oceans. Thus, in our laboratory experiments we simulated the reduced concentrations of nitrogen in medium and various irradiance levels to reveal the response and acclimation of cells to these conditions, and to obtain spectrum of parameters describing photosynthetic energy utilization. By estimating aquatic primary production from time-dependent ^{14}C measurements, it was found that substantial fraction of newly fixed carbon is in the cell in the form of transient carbon pool. This pool consists of the long-lived form of carbon, slowly catabolized and utilized for regeneration of reductants, which are used for protein and lipid synthesis. On the other hand, the transient carbon pool can also be short-lived. In this case, it is rapidly respired and used for ATP creation. As was previously shown, the processing of transient carbon pool is influenced by growth rate, which is related to the nutrient status of the cell (Halsey et al. 2010, 2011). Thus, to assess primary production in oceans, we need to understand first how phytoplankton metabolism responds to the changing conditions in the ocean. The gathering of such information and collecting data are useful for their application in the further development and improvement of algorithms used in the global models of primary production.

Most studies focused on the assessment of photosynthetic energy utilization in phytoplankton dealt with eukaryotic algae (Halsey et al. 2013, 2014, 2015, 2016). Only one study focused on cyanobacterial energy metabolism (Kunath et al. 2012). My work aimed at increasing our understanding of regulation of efficiency of conversion of photosynthetic energy into the biomass in ecologically relevant cyanobacteria. In order to achieve this goal, I have combined methods of physiology and molecular biology. Physiological approaches (cell density, Photosystem II Chl *a* characteristics, the electron transport rate through PSII, gas exchange measurements) were followed by molecular insights (analyses of ^{14}C content in the cell, quantification of D2 protein, 3D modelling of PSII) and assessment of gene expression (*psbO*, *psbP*, *psbU*, *psbV*).

In the studies dealing with carbon use efficiencies we described model of carbon utilization in HL and LL adapted strains of *P. marinus* in three nitrogen-limited continuous cultures (**I**, **III**). Our results confirmed changes in light-harvesting system and in pigmentation in dependence on N limitation. Interestingly, as photosynthetic efficiency was unaltered across specific growth rates, it enables to cells to assimilate (GPC[b]) and to retain similar amount of newly fixed carbon in biomass (NPC[b]) independently of N limitation. In line with previous studies dealing with eukaryotic algae (Halsey et al. 2010, 2011), we also revealed the source and extent of discrepancy between net and gross carbon primary production in both *P. marinus* strains. We found that most of newly fixed carbon in the cell was in the form of transient carbon pool which utilization was growth rate specific in the case of HL adapted strain PCC 9511. These results confirmed hypothesis that transient carbon pool can be long-lived supporting reductant formation or short-lived and thus quickly respired to fuel ATP. On the other hand, in the case of LL adapted strain MIT9313 it did not seem that the catabolism of transient carbon pool was affected by growth rate as markedly as in PCC 9511. In all three N-limited growth rates, this pool was very rapidly respired. However, this might be caused by very low specific growth rates. Our observations did not prove existence of any alternative electron transport.

We also showed that carbohydrate pool became enlarged with increasing limitation at the expense of protein pool in both *P. marinus* strains. These experiments provided crucial insights into the metabolism of key microorganism of oligotrophic oceans.

Our second study focused on the process of photosynthetic oxygen evolution in *P. marinus*. To our knowledge, this is the first study, which evaluates oxygen evolution rates among physiologically and genetically distinct strains of *P. marinus*. To this part of experiments, also cyanobacterium *Synechococcus* sp. WH7803 was included as it is the most related cyanobacterium to the *P. marinus*. We tested oxygen evolution rates of four marine picocyanobacteria possessing various composition of oxygen-evolving complex at various light levels. We revealed that despite of reduction of OEC complex through genome streamlining, the HL adapted strain PCC 9511 displayed usual and even higher oxygen evolution rates in comparison to other cyanobacteria having standard OEC. The possible compensatory mechanisms for lack of important extrinsic proteins in strains with reduced OEC structure were discussed.

A study comparing HL and LL adapted strains in terms of carbon metabolism was performed (**III**). We found that LL adapted strain growing in continuous cultures responded to the N limitation very similarly as HL adapted strain, i.e. changes at the level of light-harvesting system and in the redistribution of carbon allocation between protein and carbohydrate pool. As already mentioned, we revealed that transient carbon pool is catabolised very quickly for ATP creation in all three specific growth rates. Moreover, we observed significantly higher gross and net carbon primary production. The fraction of newly fixed carbon, which was retained in the biomass, reached 28% of GPC[b]. Interestingly, by comparing with HL adapted strain the NPC[b] was about 8% higher suggesting higher efficiency in photosynthetic energy utilization. This might be related to the specific physiological characteristics, i.e. multiplication of *pcb* genes, larger functional absorption cross sections of PSII, and also to the environmental conditions, i.e. higher concentration

of nutrients in the natural environment, ability to take up more N sources and glucose uptake.

To summarize, the most important conclusions of my research related to the initial hypotheses h1-h4 include:

(h1)   Effect of nitrogen limitation on the photosynthetic energy utilization.

We have confirmed that increasing nitrogen limitation influence not only light-harvesting system at the PSII level and biochemical composition of cells, but also the utilization of newly fixed carbon. The usage of this carbon either to supply ATP or NADPH was shown to be strongly growth rate dependent in HL adapted strain PCC 9511 but not in LL adapted strain MIT9313.

(h2)   The carbon allocation in acclimated cells changes in proportion to the degree of nutrient stress by nitrogen limitation.

We revealed the clear pattern in carbon allocation into the biomass during N-limited growth in both HL and LL adapted strains. N replete cells stored carbon mainly to the protein pool. However, with increasing N limitation, protein pool was reduced and carbon was redistributed to the carbohydrates.

(h3)   The functional adaptation of oxygen-evolving complex does not limit oxygen evolution in *Prochlorococcus*.

We assessed oxygen evolution rates in four marine picocyanobacteria grown under three different light conditions and proved that streamlined oxygen-evolving complex in two of them has no effect on proper function of this complex.

(h4)   HL and LL adapted strains of *P. marinus* exhibited distinct carbon metabolisms.

We revealed differences in time-dependent catabolism of newly fixed carbon between HL and LL adapted strains. LL adapted strain respired carbon very quickly to supply ATP demands probably. We also demonstrated possible higher efficiency of photosynthetic energy utilization.

Due to the burning of fossil fuels, anthropogenic emission constitute up approx. 10% of the global primary productivity. The increased concentration of CO_2 in the atmosphere is causing global change with several possible consequences for aquatic primary production: besides acidification of seawater, it is suggested that due to increased temperature and stratification, ocean regions poor in nutrients will expand. In these oligotrophic areas, cyanobacterium *Prochlorococcus* dominates, thus our results may contribute to the broader knowledge about regulation of photosynthesis and primary production in important cyanobacteria under ecologically relevant conditions. Therefore, these results may help with quantification of primary production and potentially they might contribute to the modelling of global primary production using remote sensing.

References

Badger MR, Hanson D and Price GD (2002) Evolution and diversity of CO_2 concentrating mechanisms in cyanobacteria. Functional Plant Biology 29: 161-173.

Badger MR and Price (2003) CO_2 concentrating mechanism in cyanobacteria: molecular components, their diversity and evolution. Journal of Experimental Biology 54: 609-622.

Badger MR, Price GD, Long BM and Woodger FJ (2006) The environmental plasticity and ecological genomics of the cyanobacterial CO_2 concentrating mechanism. Journal of Experimental Botany 57: 249-265.

Bailey S, Mann NH, Robinson C, Scanlan DJ (2005) The occurrence of rapidly reversible non-photochemical quenching of chlorophyll *a* fluorescence in cyanobacteria. FEBS Letters 579: 275-280.

Balint I, Bhattacharya J, Perelman A, Schatz D, Moskovitz Y *et al*. (2006) Inactivation of the extrinsic subunit of photosystem II, PsbU, in *Synechococcus* PCC 7942 results in elevated resistance to oxidative stress. FEBS Letters 580: 2117-2122.

Behrenfeld JM, Boss E, Siegel DA and Shea DM (2005) Carbon-based ocean productivity and phytoplankton physiology from space. Global Biogeochemical cycles 19: GB1006.

Behrenfeld JM and Falkowski PG (1997) A consumer's guide to phytoplankton primary productivity models. Limnology and Oceanography 42: 1479-1491.

Berg GM, Shrager J, van Dijken G, Mills MM, Arrigo KR *et al.* (2011) Responses of *psbA*, *hli* and *ptox* genes to changes in irradiance in marine *Synechococcus* and *Prochlorococcus*. Aquatic Microbial Ecology 65: 1-14.

Berube PM, Biller SJ, Kent AG, Berta-Thompson JW, Roggensack SE *et al.* (2015) Physiology and evolution of nitrate acquisition in *Prochlorococcus*. The ISME Journal 9: 1195-1207.

Bhaya D, Dufresne A, Vaulot D, Grossman A (2002) Analysis of the *hli* gene family in marine and freshwater cyanobacteria. FEMS Microbiology Letters 215: 209-219.

Bibby TS, Mary I, Nield J, Partensky F and Barber J (2003) Low-light-adapted *Prochlorococcus* species possess specific antennae for each photosystem. Nature 424: 1051-1054.

Biller SJ, Berube PM, Berta-Thompson JW, Kelly L, Roggensack SE *et al*. (2014) Genomes of diverse isolates of the marine cyanobacterium Prochlorococcus. Scientific data 1.

Biller SJ, Berube PM, Lindell D and Chisholm SW (2015) *Prochlorococcus*: The structure and function of collective diversity. Nature Reviews Microbiology 13: 13-27.

Bruyant F and Babin M, Genty B, Prasil O, Behrenfeld MJ (2005) Diel variations in the photosynthetic parameters of *Prochlorococcus* strain PCC 9511: Combined effects of light and cell cycle. Limnology and Oceanography 50: 850-863.

Chisholm SW, Frankel SL, Goericke R, Olson RJ, Palenik B *et al*. (1992) *Prochlorococcus marinus* nov. gen. nov. sp.: an oxyphototrophic marine prokaryote containing divinyl chlorophyll *a* and *b*. Archives of Microbiology 157: 297-300.

Chisholm SW, Olson RJ, Zettler ER, Goericke R, Waterbury A (1988) A novel free-living prochlorophyte abundant in the oceanic euphotic zone. Nature 334: 340-343.

Coleman ML and Chisholm SW (2007) Code and context: *Prochlorococcus* as a model for cross-scale biology. Trends in Microbiology15: 398-407.

Coleman ML and Chisholm SW (2010) Ecosystem-specific selection pressures revealed through comparative population genomics. PNAS 107: 18634-18639.

Coleman ML, Sullivan MB, Martiny AC, Steglich C, Barry K *et al.* (2006) Genomic islands and the ecology and evolution of *Prochlorococcus*. Science 311: 1768-1770.

De Las Rivas J, Balsera M and Barber J (2004) Evolution of oxygenic photosynthesis: genome-wide analysis of the OEC extrinsic proteins. TRENDS in Plant Science 9: 18-25.

Delmont TO and Eren AM (2018) Linking pangenomes and metagenomes: the *Prochlorococcus* metapangenome. Peer J 6: e4320.

Domínguez-Martín MA, Gómez-Baena G, Díez J, López-Gruesco MJ, Beynon RJ *et al*. (2017) Quantitative proteomics shows extensive remodelling induced by nitrogen limitation in *Prochlorococcus marinus* SS120. mSystems 2.

Domínguez-Martín MA, López-Lozano A, Clavería-Gimeno R, Velázquez-Campoy A, Seidel G *et al*. (2017) Differential NtcA responsiveness to 2-oxoglutarate underlies the diversity of C/N balance regulation in *Prochlorococcus*. Frontiers in Microbiology 8: 2641.

Domínguez-Martín MA, López-Lozano A, Rangel-Zúniga OA, Díez J and Gárcía-Férnandez JM (2018) Distinct features of C/N balance regulation in *Prochlorococcus* sp. strain MIT9313. FEMS Microbiology Letters 365 (3).

Dufresne A, Garczarek L and Partensky F (2005) Accelerated evolution associated with genome reduction in a free-living prokaryote.Genome Biology 6: R14.

Dufresne A, Salanoubat M, Partensky F, Artiguenave F, Axmann IM *et al*. (2003) Genome sequence of the cyanobacterium *Prochlorococcus marinus* SS120, a nearly minimal oxyphototrophic genome. PNAS 100: 10020-10025.

El Alaoui S, Díez J, Humanes L, Toribio F, Partensky F *et al.* (2001) In vivo regulation of glutamine synthetase activity in the marine chlorophyll b-containing cyanobacterium *Prochlorococcus* sp. strain PCC 9511 (Oxyphotobacteria). Applied and Environmental Microbiology 67: 2202-2207.

El Alaoui S, Díez J, Toribio F, Gómez-Baena G, Dufresne A *et al.* (2003) Glutamine synthetase from the marine cyanobacteria

Prochlorococcus spp. characterization, phylogeny and response to nutrient limitation. Environmental Microbiology 5: 412-423.

Enami I, Okumura A, Nagao R, Suzuki T, Iwai M *et al*. (2008) Structures and functions of the extrinsic proteins of photosystem II from different species. Photosynthesis Research 98: 349-363.

Espie GS, Kimber MS (2011) Carboxysomes: cyanobacterial RubisCO comes in small packages. Photosynthesis Research 109: 7-20.

Falkowski PG, Laws EA, Barber RT, Murray JW (2003) Phytoplankton and their role in primary, new, and export production. In: Fasham MJR (eds) Ocean biogeochemistry. Global change - the IGBP series. Springer, Berlin, Heidelberg.

Ferreira KN, Iverson TM, Maghlaoui JB, Iwata S (2004) Architecture of the photosynthetic oxygen-evolving center. Science 303: 1831-1838.

Field CB, Behrenfeld MJ, Randerson JT, Falkowski P (1998) Primary production of the biosphere: integrating terrestrial and oceanic components. Science 281: 237-240.

Fisher NL, Halsey KH (2016) Mechanisms that increase the growth efficiency of diatoms in low light. Photosynthesis Research 129: 183-197.

Flombaum P, Gallegos JL, Gordillo RA, Rincón J, Zabala LL, *et al.* (2013) Present and future global distributions of the marine cyanobacteria *Prochlorococcus* and *Synechococcus*. PNAS 110: 9824-9829.

Flores E and Herrero A (1994) Assimilatory nitrogen metabolism and its regulation. In: Bryant DA (eds) The molecular biology of cyanobacteria. Advances in Photosynthesis, vol 1. Springer, Dordrecht.

García-Férnandez JM, Diez J (2004) Adaptive mechanisms of nitrogen and carbon assimilatory pathways in the marine cyanobacteria *Prochlorococcus*. Research in Microbiology 155: 795-802.

García-Férnandez JM, Tandeau de Marsac N and Diez J (2004) Streamlined regulation and gene loss as adaptive mechanisms in

Prochlorococcus for optimized nitrogen utilization in oligotrophic environmnets. Microbiology and Molecular Biology Reviews 68: 630-638.

Garczarek L, Hess WR, Holtzendorff, van der Staay GWM and Partensky F (2000) Multiplication of antenna genes as a major adaptation to low light in a marine prokaryote. PNAS 97: 4098-4101.

Garczarek L, van der Staay GWM, Thomas JC and Partensky F (1998) Isolation and characterization of Photosystem I from two strains of the marine oxychlorobacterium *Prochlorococcus*. Photosynthesis Research 56: 131-141.

Gieskes WW and Kraay GW (1983) Unknown chlorophyll *a* derivatives in the North Sea and the tropical Atlantic Ocean revealed by HPLC analysis. Limnology and Oceanography 28: 757-766.

Giordano M, Beardall J and Raven JA (2005) Mechanisms, environmental modulation, and evolution. Annual review of plant biology 56: 99-131.

Goericke R and Repeta DJ (1992) The pigments of *Prochlorococcus marinus*: the presence of divinyl chlorophyll *a* and *b* in a marine prokaryote. Limnology and Oceanography 37: 425-433.

Goericke R and Repeta DJ (1993) Chlorophylls *a* and *b* and divinyl chlorophylls *a* and *b* in the open subtropical North Atlantic Ocean. Marine ecology progress series 101: 307-313.

Goericke and Welschmeyer (1993) The marine prochlorophyte Prochlorococcus contributes significantly to phytoplankton biomass and primary production in the Sargasso Sea. Deep-Sea Research 40: 2283-2294.

Gómez-Baena G, Domínguez-Martín MA, Donaldson RP, García-Fernández JM, Díez J (2015) Glutamine synthetase sensitivity to oxidative modification during nutrient starvation in *Prochlorococcus marinus* PCC 9511. PlosOne 10: e0135322.

Gómez-Baena G, López-Lozano A, Gil-Martínez J, Lucena JM, Díez J *et al*. (2008) Glucose uptake and its effect on gene expression in *Prochlorococcus*. PlosOne 10: e3416.

Graff JR, Westberry TK, Milligan AJ, Brown MB, Dall´Olmo *et al.* (2016) Photoacclimation of natural phytoplankton communities. Marine Ecology Progress Series 542: 51-62.

Guillard RRL, Murphy LS, Foss P, Liaaen-Jensen S (1985) *Synechococcus* spp. as likely zeaxanthin-dominant ultraphytoplankton in the North Atlantic. Limnology nad Oceanography 30: 412-414.

Guskov A, Kern J, Gabdulkhakov A, Broser M, Zouni A *et al.* (2009) Cyanobacterial photosystem II at 2.9-Å resolution and the role of quinones, lipids, channels and chloride. Nature structural and Molecular Biology 16: 334-342.

Halsey KH and Jones B (2015) Phytoplankton strategies for photosynthetic energy allocation. Annual Review of Marine Science 7: 265-97.

Halsey KH, Milligan AJ, Behrenfeld MJ (2010) Physiological optimization underlies growth rate-independent chlorophyll-specific gross and net primary production. Photosynthesis Research 103: 125-137.

Halsey KH, Milligan AJ, Behrenfeld MJ (2011) Linking time-dependent carbon-fixation efficiencies in *Dunaliella tertiolecta* (Chlorophyceae) to underlying metabolic pathways. Journal of Phycology 47: 1-11.

Halsey KH, Milligan AJ, Behrenfeld MJ (2014) Contrasting strategies of photosynthetic energy utilization drive lifestyle strategies in ecologically important picoeukaryotes. Metabolites 4: 260-280.

Halsey KH, O'Malley RT, Graff JR, Milligan AJ and Behrenfeld MJ (2013) A common partitioning strategy for photosynthetic products in evolutionarily distinct phytoplankton species. New Phytologist 198: 1030-1038.

Hess WR, Partensky F, van der Staay GWM, García-Fernández JM, Börner T *et al.* (1996) Coexistence of phycoerythrin and a chlorophyll *a*/*b* antenna in a marine prokaryote. PNAS 93: 11126-11130.

Hess WR, Steglich C, Lichtlé C and Partensky F (1999) Phycoerythrins of the oxyphotobacterium *Prochlorococcus marinus* are associated to the thylakoid membrane and are encoded by a single large gene cluster. Plant Molecular Biology 40: 507-521.

Hess WR, Rocap G, Ting CS, Larimer F, Stilwagen S *et al*. (2001) The photosynthetic apparatus of *Prochlorococcus*: Insights through comparative genomics. Photosynthesis Research 70: 53-71.

Huang S, Wilhelm SW, Harvey HR, Taylor K, Jiao N and Chen F (2012) Novel lineages of *Prochlorococcus* and *Synechococcus* in the global oceans. The ISME Journal 6, 285–297.

Inoue-Kashino N, Kashino Y, Satoh K, Terashima I and Pakrasi HB (2005) PsbU provides a stable architecture for the oxygen-evolving system in cyanobacterial photosystem II. Biochemistry 44: 12214-1228.

Ito H and Tanaka A (2011) Evolution of a divinyl chlorophyll-based photosystem in *Prochlorococcus*. PNAS 108: 18014-18019.

Jakob T, Wagner H, Stehfest K, Wilhelm C (2007) A complete energy balance from photons to new biomass reveals a light- and nutrient-dependent variability in the metabolic costs of carbon assimilation. Journal of Experimental Botany 58: 2101-2112.

Jansson S, Andersson J, Jung-Kim S and Jackowski G (2000) An *Arabidopsis thaliana* protein homologous to cyanobacterial highlight-inducible proteins. Plant Molecular Biology 42: 345-351.

Johnson PW and Sieburth JMcN (1979) Chroococcoid cyanobacteria in the sea: A ubiquitous and diverse phototrophic biomass. Limnology and Oceanography 24: 928-935.

Johnson ZI, Zinser ER, Coe A, McNulty NP, Malcolm E *et al*. (2006) Niche partitioning among Prochlorococcus ecotypes along ocean-scale environmental gradients. Science 311: 1737-1740.

Kamennaya NA and Post AF (2011) Characterization of cyanate metabolism in marine *Synechococcus* and *Prochlorococcus* spp. Applied and Environmental Microbiology 77: 291-301.

Kamiya N and Shen JR (2003) Crystal structure of oxygen-evolving photosystem II from *Thermosynechococcus vulcanus* at 3.7-Å resolution. PNAS 100: 98-103.

Kaňa R, Kotabová E, Komárek O, Šedivá B, Papageorgiou GC, Govindjee, Prášil O (2012) The slow S to M fluorescence rise in cyanobacteria is due to a state 2 to state 1 transition. BBA: 1237-1247.

Kashtan N, Roggensack SE, Berta-Thompson JW, Grinberg M, Stepanauhaskas R *et al*. (2017) Fundamental differences in diversity and genomic population structure between Atlantic and Pacific *Prochlorococcus*. The ISME Journal 11: 1997-2011

Kawakami K, Umena Y, Kamiya N, Shen JR (2011) Structure of the catalic, inorganic core of oxygen-evolving photosystem II at 1.9 Å resolution. Journal of Photochemistry and Photobiology B: Biology 104: 9-18.

Kent AG, Dupont CL, Yooseph S and Martiny AC (2016) Global biogeography of *Prochlorococcus* genome diversity in the surface ocean. The ISME Journal 10: 1856-1865.

Kettler GC, Martiny AC, Huang K, Zucker J, Coleman ML *et al*. (2007) Patterns and implications of gene gain and loss in the evolution of *Prochlorococcus*. PlosGenetics 3: e231.

Kimura A, Eaton-Rye JJ, Morita EH, Nishiyama Y and Hidenori H (2002) Protection of the oxygen-evolving machinery by the extrinsic proteins of photosystem II is essential for development of cellular thermotolerance in *Synechocystis* sp. PCC 6803. Plant Cell Physiology 43: 932-938.

Kirilovsky D and Kerfeld CA (2013) The orange carotenoid protein: a blue- green light photoactive protein. Photochemical and Photobiological Sciences 7.

Kirilovsky D and Kerfeld CA (2016) Cyanobacterial photoprotection by the orange carotenoid protein. Nature Plants 2: 16180.

Komenda J and Sobotka R (2016) Cyanobacterial high-light-inducible proteins – Protectors of chlorophyll-protein synthesis and assembly. BBA 1857: 288-295.

Kulk G, van de Poll WH, Visser RJW and Buma AGJ (2011) Distinct differences in photoacclimation potential between prokaryotic and eukaryotic oceanic phytoplankton. Journal of Experimental Marine Biology and Ecology 398: 63-72.

Kulk G, van de Poll WH, Visser RJW and Buma AGJ (2013) Low nutrient availability reduces high-irradiance-induces viability loss in oceanic phytoplankton. Limnology and Oceanography 58: 1747- 1760.

Kupriyanova EV, Sinetova MA, Cho SM, Park Y-I, Los DA *et al*. (2013) CO_2-concentrating mechanism in cyanobacterial photosynthesis: organization, physiological role, and evolutionary origin. Photosynthesis Research 117: 133-146.

LaRoche J, van der Staay GWM, Partensky F, Ducret A, Aebersold R *et al*. (1996) Independent evolution of the prochlorophyte and green plant chlorophyll a/b light-harvesting proteins. PNAS 93: 15244-15248.

Laws EA (2013) Evaluation of in situ phytoplankton growth rates: A synthesis of data from varied approaches. Annual Review of Marine Science 5: 247-268.

Laws EA, Sakshaug E, Babin M, Dandonneau Y, Falkowski P *et al*. (2002) Photosynthesis and primary productivity in marine ecosystems: Practical aspects and application of techniques. JGOFS report 36.

Lindell D, Erdner D, Marie D, Prášil O and Koblížek M *et al.* (2002) Nitrogen stress response of *Prochlorococcus* strain PCC 9511 (Oxyphotobacteria) involves contrasting regulation of *ntcA* and *amt1*. Journal of Phycology 38: 1113-1124.

Litchman E and Klausmeier CA (2008) Trait-based community ecology of phytoplankton. Annual Review of Ecology Evolution and Systematics 39: 615-639.

Lokstein H, Steglich C, Hess WR (1999) Light-harvesting antenna function of phycoerythrin in *Prochlorococcus marinus*. BBA 1410: 97-98.

Mackey KRM, Paytan A, Grossman AR and Bailey S (2008) A photosynthetic strategy for coping in a high-light, low-nutrient environment. Limnology and Oceanography 53: 900-913.

Malmstrom RR, Rodrigue S, Huang KH, Kelly L, Kern SZ *et al*. (2013) Ecology of uncultered *Prochlorococcus* clades revealed through single-cell genomics and biogeographic analysis. The ISME Journal 7: 183-198.

Marra J (2009) Net and gross primary productivity: weighing in with ^{14}C. Aquatic Microbial Ecology 56: 123-131.

Martiny AC, Kathuria S, Berube P (2009) Widespread metabolic potential for nitrite and nitrate assimilation among *Prochlorococcus* ecotypes. PNAS 106: 10787-10792.

McDonald AE and Vanlerberghe GC (2005) Alternative oxidase and plastoquinol terminal oxidase in marine prokaryotes of the Sargasso Sea. Gene 349: 15-24.

Mimuro M, Murakami A, Tomo T, Tsuchiya Watabe K *et al*. (2011) Molecular environments of divinyl chlorophylls in *Prochlorococcus* and *Synechocystis*: Differences in fluorescence properties with chlorophyll replacement. BBA 1807: 471-481.

Moore LR and Chisholm SW (1999) Photophysiology of the marine cyanobacterium Prochlorococcus: Ecotypic differences among cultured isolates. Limnology and Oceanography 44: 628-638.

Moore LR, Coe A, Zinser ER, Saito MA, Sullivan MB *et al*. (2007) Culturing the marine cyanobacterium *Prochlorococcus*. Limnology and Oceanography: Methods 5: 353-362.

Moore LR, Post AF, Rocap G, Chisholm SW (2002) Utilization of different nitrogen sources by the marine cyanobacteria *Prochlorococcus* and *Synechococcus*. Limnology and Oceanography 47: 989-996.

Moore LR, Rocap G, Chisholm SW (1998) Physiology and molecular phylogeny of coexisting *Prochlorococcus* ecotypes. Nature 393: 464-467.

Morel A, Ahn Y-H, Partensky F, Vaulot D and Claustre H (1993) *Prochlorococcus* and *Synechococcus*: A comparative study of their optical properties in relation to their size and pigmentation. Journal of Marine Research 51: 617-649.

Mullineaux CW (2014a) Electron transport and light-harvesting switches in cyanobacteria. Frontiers in Plant Science 5: 7.

Mullineaux CW (2014b) Co-existence of photosynthetic and respiratory activities in cyanobacterial thylakoid membranes. BBA 1837: 503-511.

Munoz-Marín MdC, Gómez-Baena G, Díez J, Beynon RJ, González-Ballester D *et al.* (2017) Glucose uptake in *Prochlorococcus*: Diversity of kinetics and effects on the metabolism. Frontiers in Microbiology 8: 327.

Munoz-Marín MdC, Luque I, Zubkov MV, Hill PG, Díez J *et al.* (2013) *Prochlorococcus* can use the Pro1404 transporter to take up glucose at nanomolar concentrations in the Atlantic Ocean. PNAS 110: 8597-8602.

Nishiyama Y, Los DA, Hayashi H and Murata N (1997) Thermal protection of the oxygen-evolving machinery by PsbU, an extrinsic protein of photosystem II, in *Synechococcus* species PCC 7002. Plant Physiology 115: 1473-1480.

Palenik B and Haselkorn R (1992) Multiple evolutionary origins of prochlorophytes, the chlorophyll *b*-containing prokaryotes. Nature 355: 265-267.

Palinska KA, Laloui W, Bédu S, Loiseaux-de Goër S, Castets AM *et al.* (2002) The signal transducer P_{II} and bicarbonate acquisition in *Prochlorococcus marinus* PCC 9511, a marine cyanobacterium naturally deficient in nitrate and nitrite assimilation. Microbiology 148: 2405-2412.

Partensky F and Garczarek L (2010) *Prochlorococcus*: advantages and limits of minimalism. Annual Review of Marine Science 2: 305-331.

Partensky F, Hess WR and Vaulot D (1999) *Prochlorococcus*, a marine photosynthetic prokaryote of global significance. Microbiology and Molecular Biology Reviews 63: 106-127.

Pei S and Laws EA (2013) Does the 14C method estimate net photosynthesis? Implications from batch and continuous culture studies of marine phytoplankton. Deep-Sea Research I 82: 1-9.

Pennisi E (2017) Making waves. Science 355: 1006-1009.

Price GD (2011) Inorganic carbon transporters of the cyanobacterial CO_2 concentrating mechanism. Photosynthesis Research 109: 47-57.

Price GD, Badger MR, Woodger FJ, Long BM (2008) Advances in understanding the cyanobacterial CO_2-concentrating-mechanism (CCM): functional components, Ci transporters, diversity, genetic regulation and prospects for engineering into plants. Journal of Experimental Botany 59: 1441-1461.

Reith ME and Munholland J (1995) Complete nucleotide sequence of the *Porphyra purpurea* chloroplast genome. Plant Molecular Biology 13: 333-335.

Rippka R, Coursin T, Hess W, Lichtlé C, Scanlan DJ *et al.* (2000) *Prochlorococcus marinus* Chisholm et al. 1992 subs. pastoris subsp. nov. strain PCC 9511, the first axenic chlorophyll a_2/b_2-containing cyanobacterium (Oxyphotobacteria). International Journal of Systematic and Evolutionary Microbiology 50: 1833-1847.

Rocap G, Larimer FW, Lamerdin J, Malfatti S, Chain P *et al.* (2003) Genome divergence in two *Prochlorococcus* ecotypes reflects oceanic niche differentiation. Nature 424: 1042-1047.

Scott KM, Hen-Sax M and Harmer TL, Longo DL, Frame CH *et al*. (2007) Kinetic isotope effect and biochemical characterization of form IA RubisCO from the marine cyanobacterium

Prochlorococcus marinus MIT9313. Limnology and Oceanography 52: 2199-2204.

Shen JR, Ikeuchi M and Inoue Y (1997) Analysis of the *psb*U gene encoding the 12-kDa extrinsic protein of photosystem II and studies on its role by deletion mutagenesis in *Synechocystis* sp. PCC 6803. The Journal of Biological Chemistry 272: 17821-17826.

Shen JR, Vermaas W and Inoue Y (1995) The role of cytochrome c-550 as studied through reverse genetics and mutant characterization in *Synechocystis* sp. PCC 6803. The Journal of Biological Chemistry 270: 6901-6907.

Silsbe GM, Oxborough K, Suggett DJ, Forster RM, Ihnken S *et al.* (2015) Toward autonomous measurements of photosynthetic electron transport rates: An evaluation of active fluorescence-based measurements of photochemistry. Limnology and Oceanography Method 13: 138-155.

Six C, Finkel ZV, Irwin AJ, Cambell DA (2007) Light variability illuminates niche-partitioning among marine picocyanobacteria. PlosOne 12: e1341.

Staleva H, Komenda J, Shukla MK, Šlouf V, Kaňa R *et al.* (2015) Mechanism of photoprotection in the cyanobacterial ancestor of plant antenna proteins. Nature chemical biology 11: 287-291.

Steeman-Nielsen E (1952) The use of radio-active carbon (C^{14}) for measuring organic production in the sea. ICES Journal of Marine Science 18: 117-140.

Steglich C, Frankenberg-Dinkel N, Penno S and Hess WR (2005) A green light-absorbing phycoerythrin is present in the high-light-adapted marine cyanobacterium *Prochlorococcus* sp. MED4. Environmental Microbiology 7: 1611-1618.

Steglich C, Futschik M, Rector T, Steen R and Chisholm SW (2006) Genome-wide analysis of light sensing in *Prochlorococcus*. Journal of Bacteriology 188: 7796-7806.

Steglich C, Post AF and Hess WR (2003) Analysis of natural populations of *Prochlorococcus* spp. in the northern Red Sea using phycoerythrin gene sequences. Environmental Microbiology 5: 681-690.

Tabita FR (1999) Microbial ribulose 1,5-bisphosphate carboxylase/ oxygenase: A different perspective. Photosynthesis Research 60: 1-28.

Tabita FR, Satagopan S, Hanson TE, Kreel NE and Scott SS (2008) Distinct form I, II, II, and IV Rubisco proteins from the three kingdoms of life provide clues about Rubisco evolution and structure/function relationships. Journal of Experimnetal Botany 59: 1515-1524.

Thornton LE, Ohkawa H, Roose JL, Kashino Y, Keren N *et al*. (2004) Homologs of plant PsbP and PsbQ proteins are necessary for regulation of Photosystem II activity in the cyanobacterium *Synechocystis* 6803. The Plant Cell 16: 2164-2175.

Ting CS, Dusenbury KH, Pryzant RA, Higgins KW, Pang CJ *et al*. (2014) The *Prochlorococcus* carbon dioxide-concentrating mechanism: evidence of carboxyzome-associated heterogeneity. Photosynthesis Research 123: 45-60.

Ting CS, Hsich C, Sundararaman S, Mannella C and Marko M (2007) Cryo-electron tomography reveals the comparative three-dimensional architecture of *Prochlorococcus*, a globally important marine cyanobacterium. Journal of Bacteriology189: 4485-4493.

Ting CS, Ramsey ME, Wang YL, Frost AM, Jun E, Durham T (2009) Minimal genomes, maximal productivity: comparative genomics of photosystem and light-harvesting complexes in the marine cyanobacterium, *Prochlorococcus*. Photosynthesis Research 101: 1-19.

Ting CS, Rocap G, King J, Chisholm SW (2001) Phycobiliprotein genes of the marine photosynthetic prokaryote *Prochlorococcus*: evidence for rapid evolution of genetic heterogeneity. Microbiology 147: 3171-3182.

Ting CS, Rocap G, King J, Chisholm SW (2002) Cyanobacterial photosynthesis in the ocean: the origins and significance of divergent light-harvesting strategies. Trends Microbiol 10: 134-142.

Tolonen AC, Aach J, Lindell D, Johnson ZI, Rector T *et al*. (2006) Global gene expression of *Prochlorococcus* ecotypes in response to changes in nitrogen availability. Molecular System Biology 2.

Umena Y, Kawakami K, Shen JR, Kamiva N (2011) Crystal structure of oxygen-evolving photosystem II at 1.9Å resolution. Nature 473: 55-60.

Urbach E, Robertson DL and Chisholm SW (1992) Multiple evolutionary origins of prochlorophytes within the cyanobacterial radiation. Nature 355: 267-270.

Vaulot D, Marie D, Olson RJ, Chisholm SW (1995) Growth of *Prochlorococcus* a photosynthetic prokaryote, in the equatorial Pacific Ocean. Science 268: 1480-1482.

Veerman J, Bentley FK, Eaton-Rye JJ, Mullineaux CW, Vasiľev S and Bruce D. (2005) The PsbU subunit of photosystem II stabilizes energy transfer and primary photochemistry in the phycobilisome photosystem II assembly of Synechocystis sp. PCC 6803. Biochemistry 44: 16939-16948.

Veldhuis MJW and Kraay GW (1990) Vertical distribution and pigment composition of a picoplanktonic prochlorophyte in the subtropical North Atlantic: a combined study of HPLC-analysis of pigments and flow cytometry.Marine Ecology Progress Series 68: 121-127.

West NJ and Scanlan DJ (1999) Niche-partitioning of *Prochlorococcus* populations in a stratified water column in the Eastern North Atlantic Ocean. Applied and Environmental Microbiology 65: 2585–2591.

Wiethaus J, Busch AWU, Dammeyer T, Frankenberg-Dinkel N (2010) Phycobiliproteins in Prochlorococcus marinus: Biosynthesis of pigments and their assembly into proteins. European Journal of Cell Biology 89: 1005-1010.

Yelton AP, Acinas SG, Sunagawa S, Bork P, Pedrós-Alió C *et al*. (2016) Global genetic capacity for mixotrophy in marine picocyanobacteria. The ISME Journal 10: 2946-2957.

Zinser ER, Lindell D, Johnson ZI, Futschik ME, Steglich C *et al*. (2009) Choreography of the transcriptome, photophysiology, and cell cycle of a minimal photoautotroph, *Prochlorococcus*. PLoS One 4: 1-18.

Zubkov MV, Fuchs BM, Tarran GA, Burkhill PH and Amann R (2003) High rate of uptake of organic nitrogen compounds by *Prochlorococcus* cyanobacteria as a key to their dominance in oligotrophic oceanic waters. Applied and Environmental Microbiology 69: 1299-1304.

RESEARCH ARTICLES

CrossMark

Carbon use efficiencies and allocation strategies in *Prochlorococcus marinus* strain PCC 9511 during nitrogen-limited growth

Kristina Felcmanová[1,2] · **Martin Lukeš**[1,2] · **Eva Kotabová**[1] · **Evelyn Lawrenz**[1] · **Kimberly H. Halsey**[3] · **Ondřej Prášil**[1,2]

Abstract We studied cell properties including carbon allocation dynamics in the globally abundant and important cyanobacterium *Prochlorococcus marinus* strain PCC 9511 grown at three different growth rates in nitrogen-limited continuous cultures. With increasing nitrogen limitation, cellular divinyl chlorophyll *a* and the functional absorption cross section of Photosystem II decreased, although maximal photosynthetic efficiency of PSII remained unaltered across all N-limited growth rates. Chl-specific gross and net carbon primary production were also invariant with nutrient-limited growth rate, but only 20% of Chl-specific gross carbon primary production was retained in the biomass across all growth rates. In nitrogen-replete cells, 60% of the assimilated carbon was incorporated into the protein pool while only 30% was incorporated into carbohydrates. As N limitation increased, new carbon became evenly distributed between these two pools. While many of these physiological traits are similar to those measured in other algae, there are also distinct differences, particularly the lower overall efficiency of carbon utilization. The latter provides new information needed for understanding and estimating primary production, particularly in the nutrient-limited tropical oceans where *P. marinus* dominates phytoplankton community composition.

Introduction

Phytoplankton biomass in the oceans represents approximately 0.2% of the global photosynthetically active carbon biomass (Field et al. 1998). Despite this fact, oceans contribute 45–50% of global net primary production (NPP), equating to roughly 50 petagrams of carbon per year (Falkowski et al. 1998; Field et al. 1998). Accurate measurements of phytoplankton primary production are critical to understand and predict how marine ecosystems will respond to climate change. Furthermore, advancing ocean biogeochemistry and ecosystem models require quantitative descriptions of phytoplankton properties during resource-limited growth (Litchman and Klausmeier 2008; Follows and Dutkiewicz 2011).

Prochlorococcus marinus is a globally important and extensively studied cyanobacterium (Hess et al. 2001; Ting et al. 2002; Partensky and Garczarek 2010). With an average cell diameter of 0.6 µm, it is the smallest known unicellular phototroph (Chisholm et al. 1988), and is ubiquitously distributed in the euphotic zone in tropical and subtropical oligotrophic waters between 40°N and 40°S with cell densities ranging from 10^4 to 10^5 cells ml^{-1} (Partensky et al. 1999). Thus, *P. marinus* is the most abundant photosynthetic organism in the world playing a crucial role in global

✉ Ondřej Prášil
  prasil@alga.cz

1 Institute of Microbiology, Czech Academy of Sciences, v. v. i., Novohradská 237, Třeboň 37981, Czech Republic

2 Department of Experimental Plant Biology, Faculty of Science, University of South Bohemia, Branišovská 31, České Budějovice 37005, Czech Republic

3 Department of Microbiology, Oregon State University, Nash Hall, Corvallis, OR 97330, USA

✦ Springer

primary production and carbon cycling (Chisholm et al. 1988; Partensky et al. 1999).

Prochlorococcus contributes an estimated 13–48% of NPP in the equatorial Pacific Ocean (Vaulot et al. 1995) and an estimated 8.5% of ocean NPP (Flombaum et al. 2013). NPP is defined as the rate of photosynthetically fixed C available for other trophic levels, and it can be calculated as the product of phytoplankton growth rate and cell carbon when those values are available. However, while phytoplankton carbon is now measureable (Graff et al. 2012), methods to reliably determine growth rate remain out of reach. In contrast, cell chlorophyll (Chl) and light absorption are relatively simple to measure in the field and by remote sensing. Therefore, estimates of marine primary production are commonly derived using photosynthetic efficiencies [rates of carbon fixation or oxygen production per unit Chl or normalized to absorbed light (Silsbe et al. 2015)]. However, phytoplankton adjust their Chl content depending on nutrient availability. This cellular plasticity can cause the Chl:C ratio to vary by an order of magnitude and causes major uncertainties in global estimates of primary production (Siegel et al. 2013).

Rates of carbon production are commonly measured using ^{13}C or ^{14}C-radiolabeled sodium bicarbonate. Chl-specific ^{14}C-uptake rates have been used extensively to estimate net carbon primary production (NPC) and are also used to calibrate algorithms of NPC based on satellite retrievals (Behrenfeld and Falkowski 1997). However, Chl-specific ^{14}C-uptake rates vary depending on incubation duration and growth rate and can range between gross and net carbon production (Laws et al. 2002; Marra 2009). This variability is caused by the relative distribution of photosynthetically assimilated carbon among different metabolic pathways, such as various catabolic and biosynthesis pathways. Ultimately, the lifetime of newly assimilated carbon (the time it takes for assimilated carbon to be converted back to CO_2) depends on the metabolic pathway that dominates under certain environmental conditions (Halsey et al. 2011).

In this study, we investigated the effects of nitrogen limitation on metabolic processes underlying gross and net carbon primary production and other cell properties in *P. marinus*. In recent studies on eukaryotic algae, Halsey et al. (2010, 2013, 2014) discovered that chlorophyll-specific gross and net carbon primary production (GPC^{b} and NPC^{b}) were independent of nutrient-limited growth rates. We tested whether these behaviors are also expressed in the cyanobacterium *P. marinus*. We used ^{14}C-uptake measurements of varying duration to assess GPC^{b} and NPC^{b}, fluorometry to examine Photosystem II activity (maximal photosynthetic efficiency of PSII F_V/F_M, and functional absorption cross section of Photosystem II σ_{PSII}), and Fourier transform infrared (FTIR) spectroscopy to determine the biochemical composition of *P. marinus* grown at different steady-state nutrient-limited growth rates under constant saturating light (see Table 1 for detailed definitions of the production measurements made in this study). We found that *P. marinus* uses the same general carbon allocation strategies as many eukaryotic algae. However, a key difference is that the efficiency of carbon conversion into biomass is significantly lower in this globally important cyanobacterium compared to the eukaryotes (Halsey et al. 2013, 2014). Our results provide important cell properties of *Prochlorococcus* under steady-state nutrient limitation and information about the photo-physiology and photosynthetic energy use efficiency of *P. marinus* that can be directly applied to global estimates of net primary production that take into account community composition.

Materials and methods

Culture conditions

Prochlorococcus marinus strain PCC 9511 (Pasteur Culture Collection of Cyanobacteria; Pasteur Institute, Paris, France) was grown at 20 °C in chemostat mode in artificial sea water PCR-S11 medium (Rippka et al. 2000) made

Table 1 Abbreviations and definitions of production measurements

Abbreviation	Definition	Units
F_V/F_M	Maximum photochemical efficiency of open RCIIs	Unitless
Φ_{PSII}	Effective photochemical efficiency of RCIIs in actinic light	Unitless
P^b_{max}	Maximum Chl-specific carbon fixation rate	µmol C (mg DV-Chl a h)$^{-1}$
α^b	Light-limited slope of the PE curve	µmol C (mg DV-Chl a)$^{-1}$ h^{-1} (µmol quanta m^{-2} s^{-1})$^{-1}$
E_k	Light saturation point	µmol quanta m^{-2} s^{-1}
P^b_{Eg}	Chl-specific carbon fixation rate at the growth irradiance	µmol C (mg DV-Chl a h)$^{-1}$
GPC^b	Chl-specific gross carbon primary production	µmol C (mg DV-Chl a h)$^{-1}$
NPC^b	Chl-specific net carbon primary production	µmol C (mg DV-Chl a h)$^{-1}$

of Red Sea salt (Red Sea Fish Pharm, Israel) and supplemented with $(NH_4)_2SO_4$ concentrations of 400, 200, and 100 μM to achieve specific growth rates (μ) of 0.3, 0.2, and 0.1 day^{-1}, respectively. The maximum specific growth rate (0.3 day^{-1}) corresponded to the N-replete culture. Cultures attained steady-state growth by continuous flow of medium into and out of the culture using peristaltic pumps at pre-set rates; accordingly, μ was set by the dilution rate determined as

$$\mu = \frac{\text{Flow rate}}{\text{Culture volume}}. \tag{1}$$

Cultures were maintained at each growth condition for at least 10–15 generations (i.e., 3–14 weeks, depending on growth rate) to ensure full acclimation prior to sampling (LaRoche et al. 2010). Cells were considered to be at steady-state once measurements of intrinsic fluorescence (F_0) or divinyl chlorophyll a (DV-Chl a) (see below) were constant for 3–4 consecutive days. For each nitrogen-limited growth rate, triplicate 700 ml cultures were grown in 1 l Erlenmeyer flasks, aerated, and continuously illuminated by fluorescent light bulbs (PILA LF 36W/33–640, Poland) with a photon flux density ~50 μmol quanta m^{-2} s^{-1} measured using a spherical quantum sensor (Walz ULM 500, Germany). Growth under continuous irradiance limited the range of growth rates achieved compared to those previously reported for $P.$ $marinus$ cells growing under light–dark cycles. We used constant light conditions to ensure that cell division was asynchronous and there was no diel rhythm in photosynthesis, thus providing us the advantage of reproducible sampling. $P.$ $marinus$ was unable to maintain growth at continuous irradiances >50 μmol quanta m^{-2} s^{-1} (data not shown), which resulted in bleaching of cultures probably due to accumulated photo-damage. Nevertheless, the light conditions used in this study for $P.$ $marinus$ were similar to the study by Lindell et al. (2002) that investigated nitrogen metabolism in $Prochlorochoccus$ strain PCC 9511.

Culture monitoring

Daily measurements of F_0 or DV-Chl a concentration were used to monitor each culture. F_0 was measured in fluorometer FL3000 (Photon System Instrument, Czech Republic) after acclimating cells for 10 min to darkness. To determine DV-Chl a, cells of triplicate culture samples were filtered onto 25-mm glass fiber filters with a particle retention of 0.4 μm (MN GF 5, Macherey–Nagel, Germany). Filters were extracted in 100% methanol and stored at −20 °C for 24 h. The absorption spectra of the extracts were measured spectrophotometrically (spectrophotometer UV 500, ChromSpec, CZ), and DV-Chl a was quantified using the equation for Chl a assessment in Porra (2006).

Cell density

Number of cells was measured using a flow cytometer A50 (Apogee Flow systems, UK) equipped with a blue laser (488 nm) and analyzed using FlowJo software (Flowjo LLC, USA) using standard procedures for data analysis according to Shapiro (2005).

Elemental composition

For cellular carbon and nitrogen analysis (C:N), 1, 2, and 3 ml samples were filtered in triplicate onto pre-combusted (5 h at 550 °C) MN GF 5 filters, wrapped in tin capsules and stored at −70 °C until analysis with a CN Elemental Analyzer vario MICRO cube (Elementar Analysensysteme GmbH, Germany) as described in Nelson and Sommers (1996). A filter blank was subtracted from raw values.

Photosystem II Chl a fluorescence characteristics

Chl a fluorescence was measured using a fluorometer FL3000 (Photon System Instruments, Czech Republic). Cells were dark acclimated for 10 min prior to measurements to oxidize all PSII reaction centers. F_0 was measured using low-intensity blue measuring light (455 nm). A multiple turnover saturating flash (duration 850 ms, intensity 2100 μmol quanta m^{-2} s^{-1}, 635 nm) was applied to reduce all reaction centers and raise fluorescence to its maximum (F_M). The maximum photochemical efficiency of open RCIIs was calculated as the ratio of F_V/F_M, where F_V (variable fluorescence) corresponds to $F_M - F_0$. Cells were then exposed to an actinic light (205 μmol quanta m^{-2} s^{-1}, 635 nm) for 145 s. The effective photochemical efficiency of PSII in actinic light (Φ_{PSII}) was determined as F_q'/F_M', where F_M' is the maximum fluorescence in light-adapted state and $F_q' = F_M' - F'$, where F' is the steady-state fluorescence in the light (Kromkamp and Forster 2003).

Measurements of electron transport rate

The electron transport rate (ETR) through Photosystem II was determined by fast repetition rate fluorescence using a custom-designed FL3500 fluorometer (Photon Systems Instruments, Czech Republic). After a 10 min dark acclimation period, a series of 100 blue (463 nm) flashlets of 1 μs duration was applied to induce single turnover of all RCII. Changes in fluorescence were then measured during sequential exposure to 11 different intensities (0–1023 μmol photons m^{-2} s^{-1}) of blue actinic light. The resulting fluorescence light curves were fitted to the model of Kolber et al. (1998) to derive the maximum and minimal fluorescence, the effective PSII cross section (σ_{PSII}), and the connectivity between photosystems (p). These parameters

were then used to calculate the ETR according to Suggett et al. (2010):

$$ETR = \sigma_{PSII} \times n_{PSII} \times \frac{F'_q/F'_m}{F_v/F_m} \times \Phi_{RCII} \times E, \qquad (2)$$

where n_{PSII} represents the ratio of functional reaction centers of PSII to total chlorophyll a. The value $1/n_{PSII} = 500$ (mol chl a/mol RCII) was used (see Suggett et al. 2010 for details). Φ_{RCII} is the quantum yield of photochemistry within RCII [taking constant values of 1 mol e$^-$ (mol photons^{-1})], and E is the intensity of the actinic light. We used a custom-designed fluorometer, so an instrument-specific K_r coefficient for n_{PSII} assessment has not been determined. Therefore, relative numbers of active RCII, instead of absolute numbers, were derived from F_0 and σ_{PSII} (Oxborough et al. 2012; Silsbe et al. 2015).

Short-term ^{14}C-uptake rates

To assess photosynthesis versus irradiance (PE) relationships, uptake of ^{14}C-bicarbonate at light intensities ranging from 0.5 to 500 µmol quanta m^{-2} s^{-1} was measured in a temperature-controlled photosynthetron-type incubator. For each PE curve, a 45 ml culture aliquot was inoculated with 5 µCi inorganic ^{14}C (NaH^{14}CO$_3$, MP Biomedicals, CA, USA), aliquoted into scintillation vials (1 ml each), and incubated for 20 min. After incubation, samples were acidified with 50 µl 1 N HCl and degassed for 24 h. Three 1 ml samples inoculated with ^{14}C were kept in the dark for 20 min, acidified, and degassed. After 24 h of degassing, EcoLite scintillation cocktail (MP Biomedicals, CA, USA) was added to each sample to determine their radioactive decay using a Tri-Carb 2810 TR liquid scintillation analyzer (PerkinElmer, MA, USA). To obtain the total activity of NaH^{14}CO$_3$ added, three 50 µl samples were added to vials containing 50-µl ethanolamine, 900 µl culture media, and 5 ml of EcoLite scintillation cocktail and capped immediately and counted. PE curves were modeled according to nonlinear least-squares regression described by (Jassby and Platt 1976)

$$P^b = P^b_{max}\left[1 - \exp\left(\frac{\alpha^b \times E}{P^b_{max}}\right)\right], \qquad (3)$$

where P^b is the Chl-specific rate of carbon fixation [µmol C (mg DV-Chl a h)$^{-1}$], P^b_{max} is the maximum Chl-specific C fixation rate [µmol C (mg DV-Chl a h)$^{-1}$], α^b is the light-limited slope of the PE curve [µmol C (mg DV-Chl a)$^{-1}$ h^{-1} (µmol quanta m^{-2} s^{-1})$^{-1}$], and E is the irradiance

(µmol quanta m^{-2} s^{-1}). The light saturation point E_k (µmol quanta m^{-2} s^{-1}) was defined as

$$E_k = \frac{P^b_{max}}{\alpha^b}. \qquad (4)$$

Samples for measuring dissolved organic carbon (DOC) were prepared with ^{14}C as described above and incubated for 20 min at 0 and 500 µmol quanta m^{-2} s^{-1}. Samples were then filtered through an MN GF 5 filter to separate dissolved from particulate matter, acidified, and degassed as described above.

Time dependence of ^{14}C-uptake

To determine the kinetics of ^{14}C-uptake over time, a 100 ml aliquot of culture was transferred to a small sterile temperature-controlled chemostat with the same light conditions and a flow rate adjusted to maintain the same specific growth rate as the stock chemostat by accounting for the reduced volume in Eq. (1). Freshly prepared bovine carbonic anhydrase (Sigma-Aldrich, St. Louis, MO, USA) was added to the culture (5 U ml^{-1}) to ensure immediate isotopic equilibrium between HCO$_3^-$ and CO$_2$. After 2 min, the culture was inoculated with NaH^{14}CO$_3$ (1 µCi ml^{-1}). Sampling for ^{14}C-uptake rate started 2 min after inoculation with ^{14}C and continued regularly over 24 h by taking 1.1 ml samples at each time point using a syringe and transferring the sample to a 2-ml Eppendorf tube. Two 0.5 ml subsamples were transferred to scintillation vials, acidified and degassed for 24 h. At each time point, two additional 50 µl samples were taken to determine the total remaining activity, and treated as total activity samples described above. Five milliliter of scintillation cocktail was added to each sample after 24 h and then measured by liquid scintillation counting.

Generalized model of carbon utilization

Carbon allocation in cells growing at all three growth rates was modeled by calculating the fraction of newly fixed carbon that is partitioned into either a short-half-life or long-half-life pool as described in detail in Halsey et al. (2013).

Gas exchange measurements

Photosynthesis and light-dependent respiration rates at 20 °C were measured using a MIMS (Membrane Inlet Mass Spectrometer). The instrument, experimental procedures, and data analysis were identical to Milligan et al. 2007 with the following exceptions: because *Prochlorococcus* photosynthetic activity is inhibited by stirring or shaking, we have added the isotope label by mixing 1 ml of ^{18}O$_2$

saturated medium with 5 ml of cell suspension. The actinic illumination was provided by a laboratory white LED light source adjusted to 50 µmol quanta m^{-2} s^{-1} inside the measuring chamber.

Fourier transform infrared spectroscopy

To determine the macromolecular composition of cells growing at each nitrogen-limited growth rate, 30 ml of the cell suspension was harvested by centrifugation at 8000×g for 10 min at 20 °C. Cells were washed twice with ammonium formate (28 g l^{-1}), re-suspended in 50 µl of ammonium formate, and spread on a Si 384-well plate (Bruker, Billerica, MA, USA). Samples were measured on a Nicolet IS10 (Thermo Scientific, Waltham, MA, USA) spectrometer equipped with a microarray reader and a deuterated triglycine sulfate (DTGS) detector. Absorbance spectra were collected in the spectral range from 400 to 4000 cm^{-1} at a spectral resolution of 4 cm^{-1} and 64 scans were co-added and averaged. A Blackman–Harris three-term apodization function was used, with a zero-filling factor of two. Omnic software (Nicolet) was used for measurement and data processing. Spectra were normalized to the maximum of an amide I absorption band at 1645 cm^{-1} and absorption maxima of lipids (1735 cm^{-1}) to protein (amide I) and lipid to carbohydrate (1152 cm^{-1}) were used for comparison (Giordano et al. 2001).

Statistics

Data were statistically analyzed by linear regression using MS EXCEL 2010. One-way ANOVA analysis [Dunn's Method to detect significant differences ($p < 0.05$)] and nonlinear least-squares regressions were performed by SigmaPlot 11 (Systat Software, CA, USA).

Results

Growth and cell properties

Continuous cultures of *P. marinus* were established with three steady-state N-limited specific growth rates (0.1, 0.2, and 0.3 day^{-1}). The maximum achieved growth rate of N-replete culture (0.3 day^{-1}) in our experiments was less than the maximal growth rate reported under light–dark regimes of illumination [0.69 day^{-1} in synchronized cyclostats with diel light (Bruyant et al. 2005) and 0.63 day^{-1} under a 12:12 light:dark cycle (Kulk et al. 2012)]. The slower growth under continuous irradiance has been observed in several species (Brand and Guillard 1981). Recently, we reported slower growth in alga *Chromera velia* grown under light–dark cycles than

under continuous irradiance with the same light dose (Quigg et al. 2012). This has several possible reasons. Under continuous irradiance, cell cycles are not synchronized. While under light–dark cycles DNA replication and cell division occur in the dark phase, in continuous light replicated DNA is damaged and growth is inhibited. Also, in our study of *Prochlorococcus*, we used an artificial seawater-based medium with defined nitrogen concentrations instead of the natural seawater-based medium with undefined nitrogen concentrations used in the studies achieving faster growth rates. Nevertheless, the growth rates we established are comparable to those reported in other research on *P. marinus*, where $\mu = 0.38$ day^{-1} under a 12:12 L:D regime (Fu et al. 2007) and $\mu = 0.19$–0.38 day^{-1} under a dynamic irradiance (Kulk et al. 2011; Zorz et al. 2015) were observed. The range of growth rates used in our experiments allowed us to investigate the effects of steady-state nutrient limitation on cell properties and photosynthetic energy use in *P. marinus*.

Cellular DV-Chl a decreased with increasing nitrogen limitation ($p < 0.05$). Thus, DV-Chl$a$:C and DV-Chl$a$:N also decrease significantly ($p < 0.05$, Table 2). On the other hand, ratios of C:N increased slightly but not significantly with increasing N limitation (Table 2).

Photosystem II Chl *a* fluorescence characteristics

F_V/F_M and Φ_{PSII} remained almost invariant across all steady-state N-limited growth rates, suggesting that cells maintained fully functional active photosystems and photosynthetic electron transport regardless of the degree of nutrient limitation. The functional absorption cross section of PSII (σ_{PSII}) was significantly larger in N-replete cells growing at 0.3 day^{-1} than in N-limited cells growing at 0.2 and 0.1 day^{-1} (Table 3), ($p < 0.05$). Thus, *Prochlorococcus* cells decreased the size of their light-harvesting antennae with increasing N limitation. However, the

Table 2 Cellular DV-Chl a content and elemental composition of steady-state nitrogen-limited cultures of *P. marinus* ($n = 4$, ± standard deviations)

Variables	N-limited growth rate (day^{-1})		
	0.1	0.2	0.3
DV-Chl a (fg/cell)	0.3 ± 0.2*	0.9 ± 0.1*	1.5 ± 0.2*
DV-Chl$a$:C (×10^{-2}) (µg/µg)	0.7 ± 0.1*	1.8 ± 0.5	3.1 ± 0.7*
DV-Chl$a$:N (µg/µg)	0.07 ± 0.01*	0.13 ± 0.04†	0.22 ± 0.05*·†
C:N (µg/µg)	8.3 ± 1.2	8.1 ± 0.9	7.2 ± 0.5

Statistically significant changes are indicated with asterisks and daggers ($p < 0.05$)

Table 3 Photophysiological fluorescence characteristics of steady-state nitrogen-limited *P. marinus* ($n = 4$, ±standard deviations)

Variables	N-limited growth rate (day^{-1})		
	0.1	0.2	0.3
F_V/F_M	0.63 ± 0.03	0.66 ± 0.02	0.62 ± 0.01
Φ_{PSII}	0.49 ± 0.05	0.54 ± 0.05	0.5 ± 0.04
σ_{PSII} (A^2 PSII^{-1})	174 ± 19.9*	162 ± 14.5†	250 ± 5.4*,†
n_{PSII} (PSII DV-Chl a^{-1}) relative units	2.78 ± 1.77	1.15 ± 0.54	0.87 ± 0.18
n_{PSII} (PSII cell^{-1}) relative units	3.1 ± 2.5	4.6 ± 3.6	5.0 ± 1.3

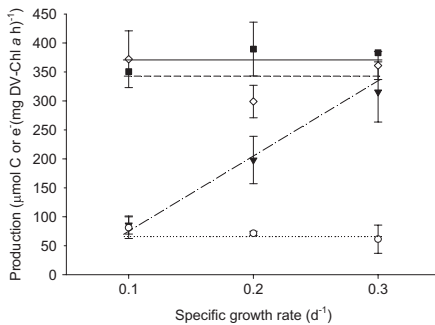Statistically significant changes are indicated with asterisks and daggers ($p < 0.05$)

Fig. 1 Relationships between the photosynthetic electron transfer rate (*open diamond* and *dashed line*), DV-Chl *a* specific gross carbon primary production (GPC^b, *filled square* and *solid line*), carbon fixation rate at the growth irradiance (P^b_{Eg}, *filled inverted triangle* and *dash-dotted line*), and net carbon primary production (NPC^b, *open circle* and *dotted line*), in *P. marinus* as a function of N-limited growth rate. Each data point is the average from at least three measurements (where none are visible, the *error bars* are smaller than the size of the *symbol*)

Table 4 Variables describing PE curves measured in steady-state nitrogen-limited *P. marinus* ($n = 3$, ±standard deviations)

Variables	N-limited growth rate (day^{-1})		
	0.1	0.2	0.3
P^b_{max} [µmol C (mg DV-Chl a h)$^{-1}$]	214 ± 4*	316 ± 4*	558 ± 6*
α^b [µmol C (mg DV-Chl a)$^{-1}$ h^{-1} (µmol quanta m^{-2} s^{-1})$^{-1}$]	3 ± 0.1*	6 ± 0.2*	11 ± 0.3*
E_k (µmol quanta m^{-2} s^{-1})	71 ± 0.8*	53 ± 1.5	51 ± 1.8
P^b_{Eg} [µmol C (mg DV-Chl a h)$^{-1}$]	86 ± 16*	198 ± 41*	315 ± 52*
P^b_C (day^{-1})	0.17 ± 0.03*	1.02 ± 0.21*	2.18 ± 0.46*
DOC% of P^b_{max}	19 ± 3.2*	7 ± 1.1	6 ± 2.5

Statistically significant changes are indicated with asterisks ($p < 0.05$)

decrease in effective PSII antenna size was not linearly proportional to the nutrient-dependent decline in growth rate and in chlorophyll concentration. We hypothesize that this nonlinearity in σ_{PSII} dependence on the growth rate and pigmentation reflects the removal of the packaging effect (i.e., pigment self-shading) in the N-limited cells growing at 0.2 and 0.1 day^{-1}. Relative n_{PSII} normalized to DV-Chl *a* increased with increasing nutrient limitation, but, conversely, when normalized to cell density, relative n_{PSII} decreased (Table 3). Photosynthetic electron transfer rates through PSII at the growth irradiance did not change across steady-state N-limited growth rates and averaged 344 ± 39 µmol e$^-$ (mg DV-Chl a h)$^{-1}$ (Fig. 1).

Short-term ^{14}C-uptake incubations

Chl-specific 20 min ^{14}C-uptake measurements were used to estimate photosynthesis as a function of irradiance (PE curves) and to gain information about how nutrient limitation influences carbon metabolism. From the fits of the measured data, we determined the initial light-limited slope (α^b) and the light-saturated rate of carbon fixation (P^b_{max}). Both P^b_{max} and α^b increased linearly ($r^2 = 0.96$) with μ (Table 4; Fig. 2). The consequence of the observed covariance in P^b_{max} and α^b is that the light saturation index (E_k) was almost identical for $\mu = 0.3$ and 0.2 day^{-1} (Behrenfeld et al. 2004), and E_k was only slightly higher in the severely nitrogen-limited cells with $\mu = 0.1$ day^{-1} (Table 4). From the PE curves generated from 20 min incubations, we also determined P^b_{Eg}, which is the Chl-specific carbon fixation rate at the growth irradiance (50 µmol quanta m^{-2} s^{-1}). P^b_{Eg} increased linearly with μ ($r^2 = 0.99$) and differed significantly among N-limited cultures ($p < 0.05$), (Table 4; Fig. 1). At first approximation, since P^b_{Eg} was measured at the growth irradiance, it should provide quantitative information about the amount of fixed C available for cell metabolism and growth. However, due to the duration of the incubation (20 min), P^b_{Eg} represents the balance between (a) new C fixed by photosynthesis and retained by the cell and (b) new C fixed and oxidized back to CO_2 during the incubation. In severely N-limited cells, P^b_{Eg} matched the NPC^b value, but P^b_{Eg} was similar to GPC^b in N-replete cells (Fig. 1). Short-term (20 min)
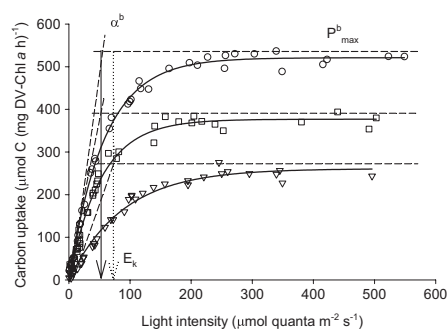
Fig. 2 Carbon uptake rate as a function of irradiance for *P. marinus* steady-state cultures grown at 0.3 day⁻¹ (*open circle*), 0.2 day⁻¹ (*open square*), and 0.1 day⁻¹ (*open inverted triangle*) obtained from 20 min ¹⁴C-uptake measurements. Data fitting is represented by *solid lines*. Parameters α^b and P^b_{max} are characterized by drawn *short dashed lines* to show the light saturation index E_k (*solid arrow* for cultures grown at 0.3 day and 0.2 day⁻¹, *dashed arrow* for culture grown at 0.1 day⁻¹)

Fig. 3 Kinetics of carbon production based on ¹⁴C-uptake measurements of increasing duration and the generalized model of carbon utilization for cells growing at 0.3 day⁻¹ (*open circle and solid line*), 0.2 day⁻¹ (*filled inverted triangle and dashed line*), and 0.1 day⁻¹ (*open square and dotted line*). The rates of decline occurring in the ¹⁴C-based production show growth rate-dependent kinetics of carbon utilization. The *solid horizontal line* is gross carbon primary production determined from the 2 min ¹⁴C-uptake incubation, and the *dotted horizontal line* is net carbon primary production determined from cellular carbon and DV-chlorophyll *a* and matches the 24 h ¹⁴C-uptake values for cells at all growth rates. Each data point is the average of three measurements, error bars are standard deviations with $n = 3$ (where not visible, the *error bars* are smaller than the size of the *symbol*)

carbon fixation provided a fairly good estimate of growth rate (=P^b_{Eg}×DV-Chl *a*/C) in the slowest growing cells (0.17 day⁻¹ in cells growing at 0.1 day⁻¹), but increasingly overestimated growth rate by five- and sevenfold in cells growing at 0.2 and 0.3 day⁻¹, respectively (Table 4). The amount of DOC excreted into the medium was <10% of P^b_{max} in N-replete cells (μ=0.3 day⁻¹) and in less N-limited cells (μ=0.2 day⁻¹), but was 20% of P^b_{max} in severely N-limited cells (μ=0.1 day⁻¹) (Table 4).

Time-dependent ¹⁴C-uptake

Because previous work showed that metabolic processing of newly fixed carbon can be influenced by nutrient limitation and therefore can impact the kinetics of carbon turnover, we also determined the time dependency of the net rate of C assimilation in *P. marinus*. Chl-specific ¹⁴C-based production was measured following incubations that ranged from 2 min to 24 h using the method introduced by Halsey et al. (2011) (Fig. 3). Measurements of C-production obtained 2 min after isotope addition were similar for cultures grown at the three N-limited growth rates and averaged 374 ± 21 μmol C (mg DV-Chl *a* h)⁻¹, providing a good estimate of GPC^b. Chl-specific ¹⁴C-uptake rates decreased with time. The kinetics describing the decline of the Chl-specific ¹⁴C-uptake rates changed depending on N limitation. In the most severely N-limited cells, Chl-specific ¹⁴C-uptake declined by 50% of the initial rate after only 4 min. In contrast, it took 10 min in less N-limited cells and 120 min in N-replete cells for Chl-specific

¹⁴C-uptake to decline to 50% of the initial rate. Following 24 h, approximately 80% of newly fixed carbon had been catabolized to CO_2 regardless of growth rate. After 24 h, Chl-specific ¹⁴C-uptake matched NPC^b in cells growing at all growth rates. NPC^b was invariant with growth rate and averaged 71 ± 10 μmol C (mg DV-Chl *a* h)⁻¹.

We applied a generalized model of algal carbon allocation and mobilization (Halsey et al. 2013) to our data describing the kinetics of ¹⁴C-production (Fig. 3). This model is based on the idea that newly fixed carbon is allocated to two different carbon pools that vary in their rate of carbon oxidation back to CO_2 in proportion to growth rate. The model gave a strong fit to the data for cells growing at the slower two growth rates (r^2=0.97), but was a poorer fit for the fastest growing cells (r^2=0.86). Optimized half-lives for the two carbon pools were 18 s and 2.8 h.

Fourier transform infrared spectroscopy

We used FTIR to determine the relative contributions of different macromolecular carbon pools in *P. marinus* growing at different nutrient-limited growth rates (Pistorius et al. 2009). The biomass of faster growing cells (μ=0.3 day⁻¹) was more biochemically reduced (i.e., containing higher amounts of proteins than slower growing cells). More severe N limitation caused carbohydrates to increase

from 32 to 43% of the total carbon content while protein content decreased from 61 to 46%, ($p < 0.05$) and lipid content remained nearly constant (Fig. 4).

Discussion

This study examined the physiological responses of *P. marinus* strain PCC 9511 to nutrient limitation. We focused on understanding how the degree of nutrient limitation affected resource allocation in this globally important cyanobacterium and whether these allocation strategies are distinct from those determined in other eubacterial and eukaryotic phototrophs.

Parameters describing the pigmentation (Table 2) show that cells decrease cellular DV-Chl *a* with increasing nitrogen limitation. Light-harvesting pigments are rich in nitrogen and are therefore downregulated with decreasing ammonium availability. This adjustment also caused the DV-Chl *a*:C and DV-Chl *a*:N ratios to decrease linearly with decreasing growth rate. Such linearity has been observed before, and the slope of the DV-Chl *a*:C vs. nutrient-limited growth rate relationship in *P. marinus* is comparable to the corresponding relationships in eukaryotic algae (Laws and Bannister 1980; Halsey and Jones 2015). This new information for numerically abundant *P. marinus* increases the robustness of the Chl:C parameter to constrain production models. Interestingly, F_V/F_M and Φ_{PSII} in acclimated *P. marinus* cells were not affected by nitrogen limitation (Table 3) supporting the results of Parkhill et al. (2001). Thus, *P. marinus* alters its light-harvesting

Fig. 4 Relative macromolecular biomass composition of steady-state nitrogen-limited *P. marinus* determined by FTIR semi-quantitative analysis ($n = 4$, ±standard deviations). Changes in protein (**) and carbohydrates (***) content in cells grown at 0.1 and 0.3 day^{-1} were statistically significant from one another ($p < 0.05$)

photosynthetic apparatus to maintain maximal photosynthetic efficiency at the level of PSII in response to nutrient availability. Such alterations of the light-harvesting system include adjusting the effective absorption cross section (σ_{PSII}). In the nitrogen-limited cells (i.e., cells growing at $\mu = 0.1$ and 0.2 day^{-1}), the very low cellular DV-Chl *a* content was reflected by a reduced σ_{PSII} and higher relative n_{PSII} compared to cells growing at 0.3 day^{-1}. However, changes in relative n_{PSII} related to DV-Chl *a* (Table 3) were driven by the decreasing concentration of DV-Chl *a* within the cell. Interestingly, the cellular density of PSII reaction centers decreased markedly with decreasing growth rate (Table 3). This result, taken together with the smaller protein pool (Fig. 4) in nitrogen-limited cells, suggested crucial changes in the PSII light-harvesting antennae (Herzig and Falkowski 1989). These changes allow cells to maintain maximal photosynthetic efficiency and photosynthetic electron transport across all growth rates (Table 3; Fig. 1).

Basic parameters describing PE relationships in N-limited *P. marinus* (P^b_{max}, α^b, and P^b_{Eg} see Table 4) decreased linearly with increasing N limitation. E_k thus remained constant in cells growing at 0.3 and 0.2 day^{-1}, a phenomenon known as E_k-independent variability. This behavior is caused by differences in how newly fixed carbon is allocated to carbon metabolic pathways depending on growth rate. In very slowly growing cells, severely limited by nitrogen, the lifetime of newly fixed carbon is much shorter compared to faster growing cells (Halsey et al. 2010, 2011). Interestingly, P^b_{max} measured in N-replete cells (Table 4) nearly matched dawn values in *P. marinus* PCC 9511 grown under cyclostat conditions (Bruyant et al. 2005). Similarly, P^b_{max} in severely N-limited cells was similar to the midnight values in the Bruyant et al. (2005) study. Thus, the dawn- and night-time physiology of *P. marinus* growing under a diel cycle appear to express the metabolic behaviors of fast and slow-growing cells, respectively. These observations comparing photo-physiology of laboratory-based culture studies are particularly useful when interpreting measurements on natural communities to understand their nutrient or growth status.

The particular stage of the cell cycle through which a cell is progressing also influences how newly fixed carbon is allocated to different carbon metabolic pathways. During the division phase (S-G2-M), cells direct the majority of new carbon to long-term storage compounds (long-lived carbon forms) (Halsey et al. 2013). Thus, P^b_{max} peaked in the afternoon in synchronized *Prochlorococcus* MED4, coinciding with the division phase of the cell cycle (Zinser et al. 2009). Slightly less than half of the cells in our *P. marinus* culture growing at 0.3 day^{-1} divided each day, whereas only about a tenth of the cells growing at 0.1 day^{-1} divide each day. Thus, the growth rate-dependent increases in P^b_{max} and α^b (Table 4) reflect the increasing proportion
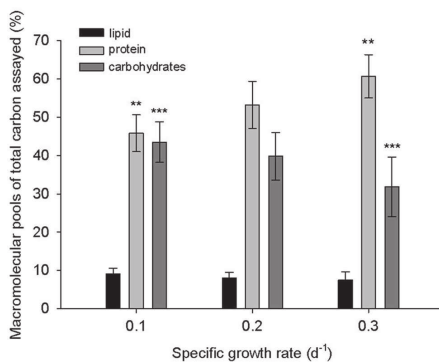
of cells that are entering the division phase and diverting new carbon to longer-lived storage forms.

The rate of photosynthetic electron transport through PSII (ETR$_{PSII}$) was not significantly different from GPC^b across all three N-limited growth rates (Fig. 1). This result indicates that under the growth conditions employed in this study, essentially all photosynthetically derived electrons passing through thylakoid membrane from PSII towards PSI are used for carbon fixation via the Calvin cycle. This result was surprising because previous work on *P. marinus* PCC 9511 postulated that a significant portion of photosynthetically derived electrons are diverted away from the Calvin cycle and instead directed to oxygen-consuming pathways, such as the Mehler reaction and terminal oxidase activity, to generate sufficient ATP to fuel metabolism (Behrenfeld et al. 2008). To verify our findings that these pathways were not operating in our cultures, we used $^{18}O_2$ as a tracer of respiration and monitored its loss rates in the light and dark using MIMS. If these alternative, oxygen-consuming pathways were operating in our *P. marinus* cultures, $^{18}O_2$ would have been consumed more rapidly in the light than in the dark (Halsey et al. 2010); however, no differences in the $^{18}O_2$ loss rates were observed in cells grown at any of the three nitrogen-limited growth rates (Fig. S1).

One possibility for the contrasting results of these studies is that in all of our cultures, regardless of growth rate, sufficient newly fixed carbon flows through cellular catabolic pathways (glycolysis and respiration) to satisfy the ATP demands of the cells. This scenario is especially plausible because the growth rates were slow [0.1–0.3 day^{-1}, compared to 0.69 day^{-1} in the Behrenfeld et al. (2008) report]. Thus, the proportion of new carbon allocated to short-lived pathways (respiration) was likely sufficient for all ATP requirements in our cultures, but it was insufficient to cover the energetic costs in cells growing faster than 0.3 day^{-1}. Therefore, in fast growing cells, alternative pathways (Mehler and terminal oxidase activity) may be required but not in the slow-growing cells in our experiments. It is worth noting that phytoplankton isolated from the oligotrophic open ocean, including *P. marinus* MED4, exhibited alternative oxidase activity. This activity is highest under high-light conditions (Mackey et al. 2008). Moreover, plastoquinol terminal oxidase proteins (McDonald and Vanlerberghe 2005) and NAD(P)H dehydrogenase complexes which function in PSI cyclic electron transport were found in MED4 (Zinser et al. 2009). These findings obtained from field (McDonald and Vanlerberghe 2005; Mackey et al. 2008) and laboratory research (Behrenfeld et al. 2008; Zinser et al. 2009) suggest that *P. marinus* may activate and use alternative electron pathways in response to high light to avoid photo-damage. However, to our knowledge, oxygen-consuming alternative pathways have not yet been directly measured in *Prochlorococcus*,

and those alternative pathways were only a small fraction of gross photosynthesis in the cyanobacterium, *Microcystis aeruginosa* (Kunath et al. 2012).

It should be noted here that despite many trials, we have not yet been able to quantitatively measure the rates of oxygen evolution in *Prochlorococcus* that match the measured rates of ETR or C assimilation. For some unknown reason, the maximal gross rates of O_2 evolution [110–145 μmol O_2 (mg DV-chl *a* h)$^{-1}$] measured either using a Clark electrode or MIMS were several times lower than the rates of ETR or GPC^b. Further experiments are under way to elucidate whether this is due to the mechanical stress caused by unavoidable concentrating and stirring of *Prochlorococcus* cell suspensions, or whether it is inherently caused by some structural or functional modification of Photosystem II in this organism with highly streamlined genome (e.g., Rocap et al. 2003).

The rate of carbon fixation through the Calvin cycle is GPC and the rate of carbon accumulation into biomass is NPC. Consistent with previous observations in eukaryotic algae (Halsey et al. 2010, 2013, 2014), our results showed that neither GPC^b nor NPC^b were affected by nitrogen limitation in *P. marinus*. We found that NPC^b constituted approximately 20% of GPC^b. The remaining 80% of GPC^b is known as a transient carbon pool. The primary product of the Calvin cycle is glyceraldehyde 3-phosphate and allocation of this product to different metabolic pathways is species specific (Palmucci et al. 2011; Giordano et al. 2015), and as discussed above, can also vary depending on nitrogen availability (Kaffes et al. 2010; Palmucci et al. 2011; Giordano et al. 2015; Halsey et al. 2010, 2011, 2013).

The parameter P^b_{Eg}, together with time-dependent ^{14}C measurements, can reveal information about how cells alter carbon allocation in response to different environmental conditions. P^b_{Eg} matched NPC^b values in cells growing at $\mu = 0.1$ day^{-1} (Fig. 1). Thus, in these very slowly growing cells, 80% of the carbon fixed during the 20-min incubation (the difference between GPC^b and NPC^b) was "short-lived" transient carbon that was catabolized back to CO_2. On the other hand, P^b_{Eg} matched GPC^b in cells growing at $\mu = 0.3$ day^{-1} because carbon fixed during the incubation is long-lived. The growth rate-dependent lifetimes of the transient carbon pool are clearly resolved in Fig. 3 and are remarkably similar to the behaviors in other nutrient-limited algae. Nevertheless, the generalized model of carbon utilization did not fully capture the kinetics of carbon production in *P. marinus* growing at 0.3 day^{-1}. The data show that newly fixed carbon in cells growing at 0.3 day^{-1} is longer lived than the model predicts and suggests that other processes are functioning to regulate carbon use in this bacterium.

To better understand how carbon use in *P. marinus* differs from other algae, we also compared biomass composition of *P. marinus* across nutrient-limited growth rates.

The fate of new carbon differs depending on the environment because cellular requirements for the major macromolecules, lipids, proteins, and carbohydrates, can vary with nutrient availability (Jakob et al. 2007). In general, eukaryotic cells cultivated in continuous culture respond to decreased growth rate due to increased N limitation by reducing carbon flow to lipids and accumulating carbohydrates (Halsey and Jones 2015). In *P. marinus*, we also found a significant increase in carbon allocated into carbohydrates in cells growing at 0.1 compared to 0.3 day^{-1} (Fig. 4). However, lipid content did not change significantly and was only 8–10% of the total carbon pool compared to 45–70% in green algae (Halsey and Jones 2015; Fig. 3), likely reflecting the lack of internal membrane bound organelles in the cyanobacterium. The protein pool, which is typically maintained even at very slow growth rates (Morris 1980) became smaller with N limitation. Overall, the carbon allocation patterns in *P. marinus* grown under nitrogen limitation were equivalent to those observed in the model diatom *P. tricornutum* (Jakob et al. 2007).

One of the open questions in the field of aquatic primary productivity is whether relatively simple and rapid measurements of ETR, derived from chlorophyll variable fluorescence can substitute traditional methods employing incorporation of C isotopes in quantitative determination of primary productivity (for review, see Suggett et al. 2010). For several decades, researchers have tried to parametrize and understand the underlying mechanisms causing the observed variability between ETR and C fixation. Such variability can be quantified as the electron requirement for carbon fixation ($\Phi_{e,C}$=ETR/C fixation, Lawrenz et al. 2013). Our results indicate, that when C assimilation is determined by short-term incubations (20–120 min), a major source of the variability in $\Phi_{e,C}$ seems to be environmentally driven changes in utilization of C products. Our and recent work (reviewed in Halsey and Jones 2015) show that rates of C fixation determined in such a way can attain almost any value between GPC^b (for nutrient-replete) and NPC^b (for nutrient-stressed cultures). On the other hand, in all cases reported here, ETR provided accurate estimates of GPC^b and more importantly, a vehicle for determining NPC^b. Therefore, at least for *Prochlorococcus*, aquatic net primary production can be derived directly from measurements of ETR. Further research is, however, needed to prove validity of this hypothesis for other organisms and other environmental stresses.

This work quantitatively describes the photosynthetic energy budget in the globally abundant cyanobacterium *P. marinus* strain PCC 9511. To our knowledge, this is only the second cyanobacterium for which an accounting of photosynthetic energy from gross to net photosynthesis has been done. GPC^b in *P. marinus* [374$\pm$21 µmol C (DV-Chl a h)$^{-1}$] was similar to the value for *D. tertiolecta*

[319$\pm$17 µmol C (Chl a h)$^{-1}$] (Halsey et al. 2010). However, only 20% of GPC^b was retained as NPC^b in *P. marinus*, compared to ~35% in the green alga and in a diatom (Halsey et al. 2013). Interestingly, NPC^b was only 18% of GPC^b in *M. aeruginosa*, to our knowledge the only other cyanobacterium for which these data have been collected during nitrogen-limited growth (Kunath et al. 2012). On the other hand, under light-limited growth, CO_2 conversion into biomass was at least as efficient in *Synechocystis* sp. as in the green alga, *Chlorella sorokiniana* (Schuurmans et al. 2015). These data suggest the possibility that under nitrogen limitation, cyanobacteria are generally less efficient in converting photosynthetic energy into biomass. This decreased energetic efficiency could be related to the fact that in cyanobacteria, photosynthetic and respiratory electron transport operate simultaneously in the plasma membrane, and moreover, these two processes share some of the same electron transfer components. Other photosynthetic electron transport pathways, such as those that contribute to light-dependent oxygen consumption (e.g., Mehler and/or midstream oxidase activities) and cyclic electron transport, can serve to supplement ATP generation, thereby decreasing reliance on carbon catabolism. Eukaryotes reliably direct ~20% of gross photosynthetic flow to light-dependent respiratory pathways during steady-state growth (Halsey and Jones 2015). However, reports so far show that cyanobacteria use these pathways only at super-saturating irradiances (Kunath et al. 2012; Schuurmans et al. 2015) or under iron limitation (Bailey et al. 2008), although electron cycling around PSII may be an important mechanism to support additional ATP generation in cyanobacteria (Ananyev et al. 2016). Finally, our results may also imply that primary and secondary endosymbiotic events leading to the evolution of eukaryotic algae afforded a greater efficiency of photosynthetic energy use.

References

Ananyev G, Gates C, Dismukes GC (2016) The oxygen quantum yield in diverse algae is controlled by partitioning of flux between linear and cyclic electron flow within photosystem II. Biochim Biophys Acta-Bioenerg 1857:1380–1391

Bailey S, Melis A, Mackey KRM, Cardol P, Finazzi G et al (2008) Alternative photosynthetic electron flow to oxygen in marine *Synechococcus*. Biochim Biophys Acta-Bioenerg 1777:269–276

Behrenfeld JM, Falkowski PG (1997) A consumer's guide to phytoplankton primary productivity models. Limnol Oceanogr 42:1479–1491

Behrenfeld JM, Prášil O, Babin M, Bruyant F (2004) In search of physiological basis for covariations in light-limited and light-saturated photosynthesis. J Phycol 40:4–25

Behrenfeld JM, Halsey KH, Milligan AJ (2008) Evolved physiological responses of phytoplankton to their integrated growth environment. Phil Trans R Soc B 363:2687–2703

Brand LE, Guillard RRL (1981) The effects of continuous light and light intensity on the reproduction rates of twenty-two species of marine phytoplankton. J Exp Mar Biol Ecol 50:119–132

Bruyant F, Babin M, Genty B, Prášil O, Behrenfeld JM et al (2005) Diel variations in the photosynthetic parameters of *Prochlorococcus* strain PCC 9511: combined effects of light and cell cycle. Limnol Oceanogr 50:850–863

Chisholm SW, Olson RJ, Zettler ER, Goericke R, Waterbury A (1988) A novel free-living prochlorophyte abundant in the oceanic euphotic zone. Nature 334:340–343

Falkowski PG, Barber RT, Smetacek V (1998) Biogeochemical controls and feedbacks on ocean primary production. Science 281:200–206

Field CB, Behrenfeld MJ, Randerson JT, Falkowski P (1998) Primary production of the biosphere: integrating terrestrial and oceanic components. Science 281:237–240

Flombaum P, Gallegos JL, Gordillo RA, Rincón J, Zabala LL et al (2013) Present and future global distributions of the marine cyanobacteria *Prochlorococcus* and *Synechococcus*. Proc Natl Acad Sci 110:9824–9829

Follows MJ, Dutkiewicz S (2011) Modeling diverse communities of marine microbes. Annu Rev Mar Sci 3:427–451

Fu FX, Warner ME, Zhang Y, Feng Y, Hutchins DA (2007) Effects of increased temperature and CO_2 on photosynthesis, growth, and elemental ratios in marine *Synechococcus* and *Prochlorococcus* (cyanobacteria). J Phycol 43:485–496

Giordano M, Kansiz M, Heraud P, Beardall J, Wood B, McNaughton D (2001) Fourier transform infrared spectroscopy as a novel tool to investigate changes in intracellular macromolecular pools in the marine microalga *Chaetoceros muellerii* (Bacillariophyceae). J Phycol 37:271–279

Giordano M, Palmucci M, Norici A (2015) Taxonomy and growth conditions concur to determine the energetic suitability of algal fatty acid complements. J Appl Phycol 27:1401–1413

Graff JR, Milligan AJ, Behrenfeld MJ (2012) The measurement of phytoplankton biomass using flow-cytometric sorting and elemental analysis of carbon. Limnol Oceanogr Method 10:910–920

Halsey KH, Jones B (2015) Phytoplankton strategies for photosynthetic energy allocation. Annu Rev Mar Sci 7:265–297

Halsey KH, Milligan AJ, Behrenfeld MJ (2010) Physiological optimization underlies growth rate-independent chlorophyll-specific gross and net primary production. Photosynth Res 103:125–137

Halsey KH, Milligan AJ, Behrenfeld MJ (2011) Linking time-dependent carbon-fixation efficiencies in *Dunaliella tertiolecta* (Chlorophyceae) to underlying metabolic pathways. J Phycol 47:1–11

Halsey KH, O'Malley RT, Graff JR, Milligan AJ, Behrenfeld MJ (2013) A common partitioning strategy for photosynthetic products in evolutionarily distinct phytoplankton species. New Phytol 198:1030–1038

Halsey KH, Milligan AJ, Behrenfeld MJ (2014) Contrasting strategies of photosynthetic energy utilization drive lifestyle strategies in ecologically important picoeukaryotes. Metabolites 4:260–280

Herzig R, Falkowski PG (1989) Nitrogen limitation in *Isochrysis galbana* (Haptophyceae). I. Photosynthetic energy conversion and growth efficiencies. J Phycol 25:462–471

Hess WR, Rocap G, Ting CS, Larimer F, Stilwagen S, Lamerdin J, Chisholm SW (2001) The photosynthetic apparatus of *Prochlorococcus*: Insight through comparative genomics. Photosynth Res 70:53–71

Jakob T, Wagner H, Stehfest K, Wilhelm C (2007) A complete energy balance from photons to new biomass reveals a light- and nutrient-dependent variability in the metabolic costs of carbon assimilation. J Exp Bot 58:2101–2112

Jassby AD, Platt T (1976) Mathematical formulation of the relationship between photosynthesis and light for phytoplankton. Limnol Oceanogr 21:540–547

Kaffes A, Thoms S, Trimborn S, Rost B, Langer G et al (2010) Carbon and nitrogen fluxes in the marine coccolithophore *Emiliana huxleyi* grown under different nitrate concentrations. J Exp Mar Biol Ecol 393:1–8

Kolber ZS, Prášil O, Falkowski PG (1998) Measurements of variable chlorophyll fluorescence using fast repetition rate techniques: defining methodology and experimental protocols. Biochim Biophys Acta-Bioenerg 1367:88–106

Kromkamp JC, Forster RM (2003) The use of variable fluorescence measurements in aquatic ecosystems: differences between multiple and single turnover measuring protocols and suggested terminology. Eur J Phycol 38:103–112

Kulk G, Van de Poll WH, Visser RJW, Buma AGJ (2011) Distinct differences in photoacclimation potential between prokaryotic and eukaryotic oceanic phytoplankton. J Exp Mar Biol Ecol 398:63–72

Kulk G, de Vries P, Van de Poll WH, Visser RJW, Buma AGJ (2012) Temperature-dependent growth and photophysiology of prokaryotic and eukaryotic oceanic picophytoplankton. Mar Ecol Prog Ser 466:43–55

Kunath C, Jakob T, Wilhelm C (2012) Different phycobilin antenna organizations affect the balance between light use and growth rate in the cyanobacterium *Microcystis aeruginosa* and in the cryptophyte *Cryptomonas ovata*. Photosynth Res 111:173–183

LaRoche J, Rost B, Engel A (2010) Bioassays, batch culture and chemostat experimentation. In Riebesell U (ed) Guide to best practices for ocean acidification research and data reporting. Publication Office of the European Union, Luxembourg, pp 81–94

Lawrenz E, Silsbe G, Capuzzo E, Ylostalo P, Forster RM et al (2013) Predicting the electron requirement for carbon fixation in seas and oceans. PLoS ONE 8:e58137

Laws EA, Bannister TT (1980) Nutrient- and light-limited growth of *Thalassiosira fluviatilis* in continuous culture with implications for phytoplankton growth in the ocean. Limnol Oceanogr 25:457–473

Laws EA, Sakshaug E, Babin M, Dandonneau Y, Falkowski P et al (2002) Photosynthesis and primary productivity in marine ecosystems: practical aspects and application of techniques. JGOFS Report No. 36, Bergen

Lindell D, Erdner D, Marie D, Prášil O, Koblížek M et al (2002) Nitrogen stress response of *Prochlorococcus* strain PCC 9511 (Oxyphotobacteria) involves contrasting regulation of *ntcA* and *amt1*. J Phycol 38: 1113–1124

Litchman E, Klausmeier CA (2008) Trait-based community ecology of phytoplankton. Annu Rev Ecol Evol Syst 39:615–639

MacKey KRM, Paytan A, Grossman AR, Bailey S (2008) A photosynthetic strategy for coping in a high-light, low nutrient environment. Limnol Oceanogr 53:900–913

Marra J (2009) Net and gross primary productivity: weighing in with [14]C. Aquat Microb Ecol 56:123–131

McDonald AE, Vanlerberghe GC (2005) Alternative oxidase and plastoquinol terminal oxidase in marine prokaryotes of the Sargasso Sea. Gene 349:15–24

Milligan AJ, Berman-Frank I, Gerchman Y, Dismukes GC, Falkowski PG (2007) Light-dependent oxygen consumption in nitrogen-fixing cyanobacteria plays a key role in nitrogenase protection. J Phycol 43:845–852

Morris I (1980) Paths of carbon assimilation in marine phytoplankton. In: Falkowski PG primary productivity in the sea. Springer, New York, pp 139–159

Nelson DW, Sommers LE (1996) Total carbon, organic carbon, and organic matter. In: Sparks DL (eds) Methods of soil analysis, part 2: chemical methods. SSSA Book Series No. 5, SSSA, Madison, pp 961–1010

Oxborough K, Moore CM, Suggett DJ, Lawson T, Chan JG, Geider RJ (2012) Direct estimation of functional PSII reaction centre concentration and PSII electron flux on a volume basis: a new approach to the analysis of Fast Repetition Rate fluorometry (FRRF) data. Limnol Oceanogr Method 10:142–154

Palmucci M, Ratti S, Giordano M (2011) Ecological and evolutionary implications of carbon allocation in marine phytoplankton as a function of nitrogen availability: a Fourier transform infrared spectroscopy approach. J Phycol 47:313–323

Parkhill JP, Maillet G, Cullen JJ (2001) Fluorescence-based maximal quantum yield for PSII as a diagnostic of nutrient stress. J Phycol 37:517–529

Partensky F, Garczarek L (2010) *Prochlorococcus*: advantages and limits of minimalism. Annu Rev Mar Sci 2:305–331

Partensky F, Hess WR, Vaulot D (1999) *Prochlorococcus*, a marine photosynthetic prokaryote of global significance. Microbiol Mol Biol Rev 63:106–127

Pistorius AM, DeGrip WJ, Egorova-Zachernyuk TA (2009) Monitoring of biomass composition from microbiological sources by means of FT-IR spectroscopy. Biotechnol Bioeng 103:123–129

Porra RJ (2006) Spectrometric assays for plant, algal and bacterial chlorophylls. In: Grimm B (ed) Chlorophylls and bacteriochlorophylls biochemistry, biophysics, function and applications. Springer, Berlin, pp 95–107

Quigg A, Kotabova E, Jaresova J, Kana R, Setlik J et al (2012) Photosynthesis in *Chromera velia* represents a simple system with high efficiency. PLoS ONE 7:e47036

Rippka R, Coursin T, Hess W, Lichtlé C, Scanlan DJ et al (2000) *Prochlorococcus marinus* Chisholm et al. 1992 subs. pastoris subsp. nov. strain PCC 9511, the first axenic chlorophyll a_2/b_2-containing cyanobacterium (Oxyphotobacteria). Int J Syst Evol Microbiol 50:1833–1847

Rocap G, Larimer FW, Lamerdin J, Malfatti S, Chain P et al (2003) Genome divergence in two *Prochlorococcus* ecotypes reflects oceanic niche differentiation. Nature 424:1042–1047

Schuurmans RM, van Alphen P, Schuurmans JM, Matthijs HCP, Hellingwerf KH (2015) Comparison of the photosynthetic yield of cyanobacteria and green algae: different methods give different answers. PLoS ONE 10:e0139061

Shapiro HM (2005) Data analysis. In: Practical flow cytometry. Wiley, New York, pp 225–256

Siegel DA, Behrenfeld MJ, Maritorena S, McClain CR, Antoine D et al (2013) Regional to global assessments of phytoplankton dynamics from the SeaWiFS mission. Remote Sens Environ 135:77–91

Silsbe GM, Oxborough K, Suggett DJ, Forster RM, Ihnken S et al (2015) Toward autonomous measurements of photosynthetic electron transport rates: an evaluation of active fluorescence-based measurements of photochemistry. Limnol Oceanogr Method 13:138–155

Suggett DJ, Moore MC, Geider RJ (2010) Estimating aquatic productivity from active fluorescence measurement. In: Suggett DJ (ed) Chlorophyll a fluorescence in aquatic sciences: methods and applications. Springer, Dordrecht, pp 103–127

Ting CS, Rocap G, King J, Chisholm SW (2002) Cyanobacterial photosynthesis in the ocean: the origins and significance of divergent light-harvesting strategies. Trends Microbiol 10:134–142

Vaulot D, Marie D, Olson RJ, Chisholm SW (1995) Growth of *Prochlorococcus*, a photosynthetic prokaryote, in the equatorial Pacific Ocean. Science 268:1480–1482

Zinser ER, Lindell D, Johnson ZI, Futschik ME, Steglich C et al (2009) Choreography of the transcriptome, photophysiology, and cell cycle of a minimal photoautotroph, *Prochlorococcus*. PLoS ONE 4:1–18

Zorz JK, Allanach JR, Murphy CD, Roodvoets MS, Campbell DA, Cockshutt AM (2015) The RUBISCO to photosystem II ratio limits the maximum photosynthetic rate in picocyanobacteria. Life 5:403–417
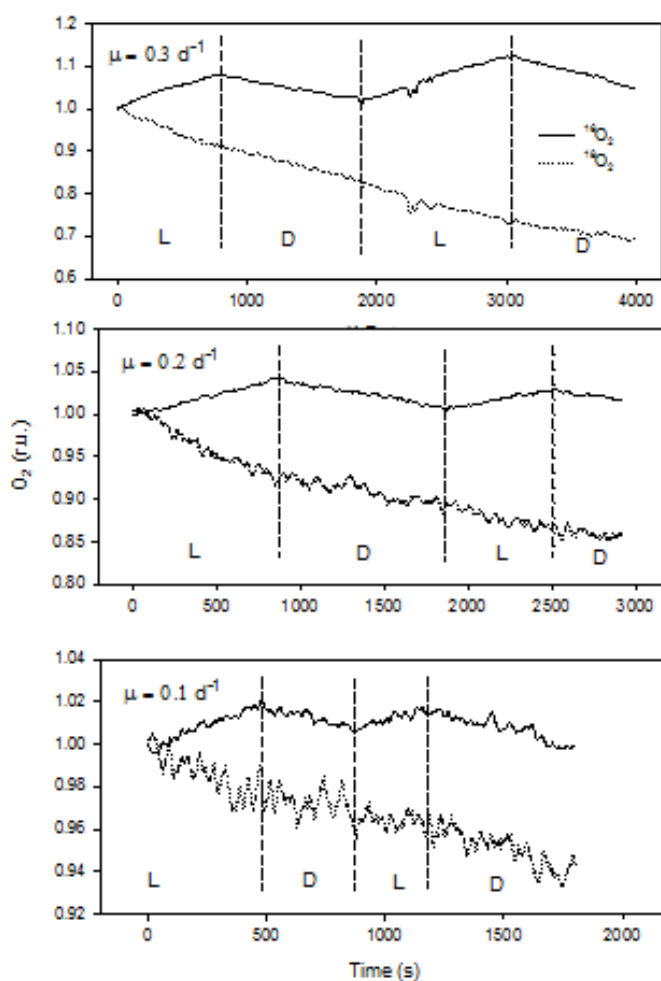
Fig. S1. Example of light-dependent changes of oxygen concentration obtained by MIMS in N-limited *Prochlorococcus* cell suspensions grown at different rates: 0.3 d^{-1} (top panel), 0.2 d^{-1} (middle panel) and 0.1 d^{-1} (lower panel). In each panel, changes in the concentration of $^{16}O_2$ (full lines) and $^{18}O_2$ (dotted lines) are shown. The vertical dash lines indicate periods when cell suspensions were illuminated by actinic light (L) or kept in the dark (D). Both oxygen isotope kinetic traces are uncalibrated and shown as relative values.

PAPER II

Comparison of photosynthetic performances of marine picocyanobacteria with different configurations of the oxygen-evolving complex

Partensky F., Mella-Flores D., Six C., Garczarek L., Czjzek M., Marie D., Kotabová E., Felcmanová K. and Prášil O.

(2018)

ORIGINAL ARTICLE

CrossMark

Comparison of photosynthetic performances of marine picocyanobacteria with different configurations of the oxygen-evolving complex

Frédéric Partensky[1,2] · **Daniella Mella-Flores[1,2,3,4]** · **Christophe Six[1,2]** · **Laurence Garczarek[1,2]** · **Mirjam Czjzek[1,5]** · **Dominique Marie[1,2]** · **Eva Kotabová[6]** · **Kristina Felcmanová[6,7]** · **Ondřej Prášil[6,7]**

Abstract

The extrinsic PsbU and PsbV proteins are known to play a critical role in stabilizing the Mn_4CaO_5 cluster of the PSII oxygen-evolving complex (OEC). However, most isolates of the marine cyanobacterium *Prochlorococcus* naturally miss these proteins, even though they have kept the main OEC protein, PsbO. A structural homology model of the PSII of such a natural deletion mutant strain (*P. marinus* MED4) did not reveal any obvious compensation mechanism for this lack. To assess the physiological consequences of this unusual OEC, we compared oxygen evolution between *Prochlorococcus* strains missing *psbU* and *psbV* (PCC 9511 and SS120) and two marine strains possessing these genes (*Prochlorococcus* sp. MIT9313 and *Synechococcus* sp. WH7803). While the low light-adapted strain SS120 exhibited the lowest maximal O_2 evolution rates (P_{max} per divinyl-chlorophyll *a*, per cell or per photosystem II) of all four strains, the high light-adapted strain PCC 9511 displayed even higher P^{Chl}_{max} and P^{PSII}_{max} at high irradiance than *Synechococcus* sp. WH7803. Furthermore, thermoluminescence glow curves did not show any alteration in the B-band shape or peak position that could be related to the lack of these extrinsic proteins. This suggests an efficient functional adaptation of the OEC in these natural deletion mutants, in which PsbO alone is seemingly sufficient to ensure proper oxygen evolution. Our study also showed that *Prochlorococcus* strains exhibit negative net O_2 evolution rates at the low irradiances encountered in minimum oxygen zones, possibly explaining the very low O_2 concentrations measured in these environments, where *Prochlorococcus* is the dominant oxyphototroph.

Introduction

The chlorophyll biomass of warm, open ocean ecosystems is largely dominated by tiny photosynthetic cells (< 2–3 μm), collectively called the 'picophytoplankton' (Stockner 1988). In vast oceanic areas, up to 99% of the oxyphototrophic cells constituting this size fraction are cyanobacteria, a group

largely dominated by the *Prochlorococcus* and *Synechococcus* genera (Campbell and Vaulot 1993; Campbell et al. 1994). Together these two photosynthetic prokaryotes are thought to contribute for 32 to 80% of primary production in oligotrophic areas (Li et al. 1992; Li 1994; Liu et al. 1997) and up to 25% of the global marine primary productivity (Flombaum et al. 2013).

Because of their ecological importance and tiny sizes (about 1 and 0.6 μm equivalent cell diameters, respectively), *Prochlorococcus* and *Synechococcus* have been privileged targets for genome sequencing and numerous complete genomes are now available for each genus, representing a large spectrum of genetic diversity, physiological types and ecological niches (Kettler et al. 2007; Dufresne et al. 2008; Scanlan et al. 2009; Biller et al. 2014). The comparison of *Prochlorococcus* genomes has revealed that a dramatic reduction of genome size and G + C content has affected

Frédéric Partensky and Daniella Mella-Flores have contributed equally to this paper

Electronic supplementary material The online version of this article (https://doi.org/10.1007/s11120-018-0539-3) contains supplementary material, which is available to authorized users.

✉ Frédéric Partensky
  frederic.partensky@sb-roscoff.fr

Extended author information available on the last page of the article

Springer

many lineages in this genus, including most low light-adapted (LL) and all high light-adapted (HL) clades (Rocap et al. 2003; Dufresne et al. 2005; Partensky and Garczarek 2010; Batut et al. 2014). For instance, the HLI strain MED4 has one of the smallest genomes known so far for an oxyphototroph (1.66 Mbp) and a very low G + C content (30.8%) and comparable genome characteristics were found in the LLII strain SS120 (1.75 Mbp; G + C% = 36.4%). In contrast, strain MIT9313, a member of the LLIV clade located at the base of the *Prochlorococcus* radiation, has a genome size (2.41 Mbp) and G + C content (50.7%) more similar to marine *Synechococcus* spp. (genome size ranging from 2.2 to 3.0 Mbp and G + C% between 52.5–66.0%; Dufresne et al. 2008; Scanlan et al. 2009). Thus, genome streamlining seemingly occurred after the differentiation of the *Prochlorococcus* genus from its common ancestor with marine *Synechococcus* spp. (Dufresne et al. 2005). This process was accompanied by a reduction of cell size and individual cell components, such as carboxysomes, photosynthetic membranes or even the cell wall (Ting et al. 2007) and likely plays a critical role in the fitness of *Prochlorococcus* to oligotrophic environments (Dufresne et al. 2008; Partensky and Garczarek 2010).

When compared to marine *Synechococcus*, all *Prochlorococcus* strains with a streamlined genome lack a number of genes, such as those encoding glycolate oxidase or an ABC transporter involved in the uptake of the compatible solute glucosylglycerol (Scanlan et al. 2009; Partensky and Garczarek 2010). Most genes encoding phycobilisomes, a type of light-harvesting complexes found in most cyanobacteria including all marine *Synechococcus* spp., have been also lost in *Prochlorococcus* spp.—apart from some phycoerythrin remnants (Hess et al. 1996)—and the major photosynthetic antenna in the latter genus is therefore constituted of membrane-intrinsic Chl-binding proteins, termed Pcb (Partensky and Garczarek 2003) or CBP (Chen et al. 2008). Although most other photosynthetic genes have been retained and are generally well conserved in *Prochlorococcus*, all strains with streamlined genomes lack *psb32*, coding for a protein thought to protect photosystem II (PSII) from photodamage and to accelerate its repair (Wegener et al. 2011), as well as *psbU* and *psbV*, encoding two small extrinsic proteins of the oxygen-evolving complex (OEC; De Las Rivas et al. 2004).

The OEC is the part of the PSII where the water-splitting reaction takes place at the level of the Mn_4CaO_5 cluster (hereafter Mn cluster; Kawakami et al. 2011). According to the structure of *Thermosynechococcus elongatus* PSII, PsbU (a.k.a. PSII 12 kDa extrinsic protein) and PsbV (a.k.a. cytochrome c_{550}) together with the main OEC protein PsbO form a large protein cap in the lumenal side of PSII that shields the Mn cluster from the bulk aqueous phase (Zouni et al. 2001; Ferreira et al. 2004; Guskov et al. 2009). This structural organization is consistent with a role of these extrinsic proteins in stabilizing PSII. Indeed, it has been reported that deletion of PsbU and PsbV proteins may affect PSII stability in several ways. In *Synechocystis* sp. PCC 6803, *psbV*-less mutants were unable to grow in the absence of Ca^{2+} and Cl^-, while cyanobacterial and red algal *psbU*-less mutants showed a decreased growth in the same condition, suggesting that these genes help in maintaining the proper ion environment for oxygen evolution, presumably by acting in the affinity of PSII for Ca^{2+} and Cl^- (Shen et al. 1997; Enami et al. 2000; Okumura et al. 2001, 2007; Inoue-Kashino et al. 2005). Additionally, these deletion mutants exhibited a drop of oxygen evolution (a 40% and 81% decrease in *Synechocystis* sp. PCC 6803 *psbV*- and *psbU*-less mutants, respectively; Shen et al. 1995, 1997) concomitant with a destabilization of PSII complex, as manifested by the decreased proportion of assembled PSII centres in *psbV*-less mutants (Shen et al. 1995, 1997; Kimura et al. 2002) and the impairment of the donor side of PSII in mutants lacking *psbU* (Inoue-Kashino et al. 2005). It has also been reported that the presence of PsbU and PsbV protects PSII against dark inactivation (Shen et al. 1998; Veerman et al. 2005) and contributes to the thermal stability of the OEC function (Nishiyama et al. 1997, 1999). Moreover, PsbU was shown to protect PSII against photodamage (Inoue-Kashino et al. 2005) and oxidative stress (Balint et al. 2006).

Considering the critical roles that PsbU and PsbV are thought to play in cyanobacterial OEC, one may wonder whether the loss of these genes in all *Prochlorococcus* lineages except members of the LLIV clade has consequences on the ability of these natural mutants to evolve oxygen. Here, oxygen evolution was compared at several growth irradiances between two *Prochlorococcus* strains lacking *psbU* and *psbV* (*P. marinus* SS120 and PCC 9511) and two marine picocyanobacterial strains that have retained these genes (*Prochlorococcus* sp. MIT9313 and *Synechococcus* spp. WH7803). Structural homology modelling of the PSII of MED4 (a strain very closely related to PCC 9511; Rippka et al. 2000) was also used to look for possible compensation mechanism such as extension of other PSII subunits.

Materials and methods

Strains and culture condition

The four clonal picocyanobacterial strains used in this study were retrieved either from the Roscoff Culture Collection (http://roscoff-culture-collection.org/) or the Pasteur Culture Collection (cyanobacteria.web.pasteur.fr/). *Prochlorococcus* sp. MIT9313 (RCC407), *P. marinus* PCC 9511, *P. marinus* SS120 (RCC156) and *Synechococcus* sp. WH7803 (RCC752) were grown at 22 °C in 0.2 μm filtered PCR-S11 medium (Rippka et al. 2000) supplemented with

1 mM NaNO$_3$ (nitrates are used only by WH7803) under continuous light provided by Sylvania Daylight 58W/154 fluorescent neon tubes. Cultures were acclimated for > 30 generations at several irradiances (see results) and diluted 2–3 days prior to measurements of Photosynthesis vs. Irradiance (P–E) curves, to ensure that cultures were in early to mid-exponential phase and exhibited a balanced growth (Brand et al. 1981) and optimal photosynthetic performances (Glibert et al. 1986). The physiological status of cultures was monitored just prior to experiments by measuring the PSII fluorescence quantum yield (F$_V$/F$_M$) using a Pulse Amplitude Modulated (PAM) fluorometer (PhytoPAM, Walz, Effeltrich, Germany), as previously described (Six et al. 2007; Garczarek et al. 2008) and no samples with F$_V$/F$_M$ lower than 0.43 were retained for the experiment (mean F$_V$/F$_M$ = 0.58 ± 0.07; n = 22). For oxygen evolution analysis, exponentially growing cultures were concentrated between 10- and 20-fold by gentle centrifugation at 3900×g for *Synechococcus* cells and 5450×g for *Prochlorococcus* for 7 min at 22 °C, using an Eppendorf 5804R centrifuge (Hamburg, Germany) and aliquots were taken from the concentrate for flow cytometry, chlorophyll assays and immunoblotting. Each experiment was replicated four to six times.

Gene expression

In order to check for the expression of *psbO* and, when present, *psbU* and *psbV* genes in the different strains, an independent set of cultures was performed under the standard LL culture conditions (18 µmol photons m^{-2} s^{-1}). A 150 mL volume was sampled from each culture strain, immediately cooled down to about 2–4 °C by swirling the sample in liquid nitrogen and harvested by centrifugation (7 min at 4 °C, 17,700×g, Eppendorf 5804R) in the presence of 0.03% (v/v) of pluronic acid (Sigma-Aldrich). Cell pellets were then resuspended in 300 µL Trizol (Invitrogen, Carlsbad, CA), frozen in liquid nitrogen and stored at −80 °C until extraction. Frozen cells in Trizol were then thawed for 15 min in a water bath set at 65 °C with regular vortexing. This step was followed by two chloroform extractions (0.2 mL of chloroform per mL of Trizol) before purification using the miRNeasy kit (Qiagen, Valencia, CA). A DNase treatment (DNAse I FPLC purified, GE Healthcare Bio-Sciences, Uppsala, Sweden) was performed for 30 min at room temperature. Purified RNAs were eluted in 35 µL of RNase-free water and stored at −80 °C. Primers for reverse transcription and real-time PCR (RT-PCR) were designed using Primer Express (Applied Biosystem, v2.0; Online Resource_Table_S1). The cDNA was obtained by reverse transcription of 100 ng of RNA and 8 pmol of the reverse primer. RNA was denatured for 10 min at 70 °C in the presence of 20 U of RNase inhibitor (RNasine, Ambion, Austin, TX) before addition of a mix of SuperScriptII (Life Technologies Inc. Gibco-BRL, Grand Island, NY), 5X reaction buffer, 2 µM DTT and 0.25 mM of each dNTP. The reaction mix was incubated at 42 °C for 50 min followed by 15 min of cDNA denaturation at 72 °C. RT-PCR was done on a Biosystem GeneAmp 5700 (Life Technologies Inc., Applied Biosystems, Foster City, CA) using the SYBR Green PCR master mix (Applied Biosystem). Real-time PCRs were performed with the GeneAmp 5700 detection system (Perkin Elmer, Waltham, MA) using the SYBR Green PCR master mix (Applied Biosystems) on a 1:50th diluted cDNA in the presence of 300 nM primers. The PCR reaction program consisted of a sequence of 10 min at 95 °C followed by 40 cycles of 15 s at 95 °C and 1 min at 60 °C.

Oxygen evolution

Photosynthetic oxygen evolution was measured using a NeoFox system equipped with an oxygen optode connected to an optical fiber (Ocean Optics Inc., Dunedin, FL). Measurements were carried out on 2 mL aliquots of concentrated cultures placed into a cuvette, homogenized with a magnetic stirrer and maintained at 22 °C by circulation of thermostated water from a MultiTempIII temperature-controlled bath (GE Healthcare, Amersham Biosciences, Uppsala, Sweden). The temperature probe coupled with the Neofox system was also maintained at 22 °C in the same bath. Pilot measurements allowed us to check that oxygen rates were not modified by addition of 2 mM NaHCO$_3$, so they were not limited by availability of inorganic carbon. P–E curves were derived from measured rates of O$_2$ evolution obtained by exposing cells to a range of increasing actinic light levels, obtained using a KL 1500 LCD halogen light source (Schott, Mainz, Germany). Each illumination period (5–10 min) was followed by a comparable dark period used to measure respiration (see a representative experiment in Online Resource_Fig_S1). Oxygen-evolving rates (µmol O$_2$ mg Chl^{-1} h^{-1}) were determined by fitting P–E curves using the dynamic fit function of Sigmaplot (Systat Softwares, San Jose, CA) with the following equation (Platt and Jassby 1976):

$$P^x = P^x_m \cdot \tanh \left(\alpha^x \cdot E / P^x_m \right) - R^x, \tag{1}$$

where P^x is the net rate of oxygen evolution at an irradiance E (µmol photon m^{-2} s^{-1}), P^X_m is the maximal, light-saturated oxygen evolution rate, α^x is the initial light-limited slope of the P–E curve and R^x is the dark respiration rate. The x stands for the parameter used to normalize the data, i.e. (DV−) Chl *a*, cell or mole D2 (see below). The saturating irradiance E_k (µmol photon m^{-2} s^{-1}) was calculated using the equation:

$$E_k = P^{Chl}_m \big/ \alpha^{Chl} \tag{2}$$

and the compensation irradiance was determined as follows (Geider and Osborne 1992):

$$E_0 = R^{Chl} / \alpha^{Chl}. \tag{3}$$

Chlorophyll assays

Chlorophyll (Chl) concentrations were determined after extracting pigments in 100% cold methanol using a spectrophotometer UV − mc² (SAFAS, Monaco). For *Synechococcus*, Chl *a* concentrations were assessed using Chl *a* extinction coefficient (Roy et al. 2011). For *Prochlorococcus* strains, which contain unique divinyl derivatives of both Chl *a* and *b* (hereafter DV-Chl *a* and b; Goericke and Repeta 1992), concentrations were assessed using the equations of Porra (2002) for methanol, which we modified using the absorption values at the red peak of DV-Chl *a* (instead of A_{665} for Chl *a*) and 13 nm before the red peak for DV-Chl *b* (instead of A_{652} for Chl *b* in Porra's equation).

Flow cytometry

A 10 µL aliquot from each concentrated culture was diluted in 990 µL of fresh PCR-S11 medium in the presence of 0.25% glutaraldehyde grade II (Sigma- Aldrich, St Louis, MO, USA) for 20 min in the dark at room temperature, then flash frozen in liquid nitrogen and stored at -80 °C until analysis. Cyanobacterial concentration in cultures was determined using a BD FACS Canto flow cytometer (Becton Dickinson, San Jose, CA, USA), as previously described (Marie et al. 1999). Heterotrophic bacteria were also counted after DNA staining using SYBR Green (Marie et al. 1999) in order to check that contamination was minimal (always < 20% total cell counts) during oxygen measurements.

Quantitation of core photosystem proteins

In order to normalize the oxygen production per photosystem, we quantified the relative amounts of the D2 subunit of photosystem II, essentially as described by Pittera et al. (2014), except that they quantified D1. Briefly, cell pellets were resuspended in an extraction buffer and lysed, the total protein concentration was determined, then samples were denatured for 2 min at 80 °C in the presence of 50 mM dithiothreitol and loaded on a 4–12% acrylamide precast NuPAGE mini-gel (Invitrogen) along with D2 protein standards (Agrisera, Sweden), used to draw the calibration standard curve. After gel electrophoresis, proteins were transferred onto a methanol prehydrated polyvinylidene di-fluoride (PVDF) membrane (Sigma-Aldrich) for 70 min at 30 mA for two membranes, and then immediately immersed in Tween 20-tris-buffered saline (Tween-TBS; Sigma-Aldrich) buffer pH 7.6 (0.1% Tween 20, 350 mM sodium chloride, 20 mM Trizma base) containing 2% (w:vol) blocking agent (Amersham Biosciences) overnight

at 4 °C. The primary antibody PsbD (photosystem II D2 core subunit; Agrisera, Sweden) was diluted at 1:50,000 in Tween-TBS in the presence of 2% blocking agent and the membrane was soaked in this solution for 1 h with slow agitation at room temperature. After discarding the primary antibody solution and extensive washing in Tween-TBS, the anti-rabbit secondary antibody coupled to horseradish peroxidase (Biorad) diluted at 1:50,000 in Tween-TBS buffer containing 2% blocking agent was added for 1 h. The membrane was washed three times for 5 min in Tween-TBS buffer prior to revelation using an enhanced chemiluminescence reagent (ECL, Amersham Biosciences). Signals were measured using the ImageQuant software (GE Healthcare, Bio-Sciences, Uppsala, Sweden; for example western blots, see Online Resource_Fig_S2). Protein concentrations were determined by fitting the sample signal values on the recombinant D2 protein standard curve. Pilot experiments were performed to ensure that sample signals fell within the range spanned by the standard curve.

Thermoluminescence

Thermoluminescence (TL) glow curves were recorded using a TL 200/PMT instrument (Photon Systems Instruments, Drasov, Czech Republic), as described by Belgio et al. (2018). For each cyanobacterial strain studied, we first determined the volume of sample that provided linear response in terms of thermoluminescence (TL) intensity (usually 2–6 mL of culture). After sample collection, the determined volume of cell suspension was filtered through a Pragopor #6 nitrocellulose membrane filter (pore size: 0.4 µm; Pragochema, Czech Republic) and placed onto the sample holder. Samples were cooled down to 3 °C, where series of 1–5 saturating single turnover flashes (50 µs, 200 ms apart) were given 1 s prior to the start of the heating and recording phase. TL curves were then recorded from 3 to 65 °C with a heating rate of 0.5 °C s^{-1}. For all TL measurements reported here, the sensitivity of the TL detection system was kept the same in order to allow quantitative comparisons among studied strains. For the measurements in the presence of 10 µM DCMU, the inhibitor was added to suspension before filtering and the sample was cooled down to − 10 °C. TL was then measured from − 10 to 65 °C.

3D modelling of *P. marinus* MED4 PSII

The 3D structure of the whole PSII of *P. marinus* MED4 was performed using the MODELLER software (Eswar et al. 2007), based on sequence homologies with PSII proteins from *Thermosynechococcus elongatus* BP-1, for which the crystallographic structure was resolved at 2.9 Å (PDB access code: 3BZ1 and 3BZ2; Guskov et al. 2009). First, sequences of each PSII subunit of *T. elongatus* and *P. marinus* were

aligned using clustalW (Thompson et al. 1994). Alignments combined with the atomic coordinates of each subunit of *T. elongatus* in the 3D structure were used as entries for MODELLER (Webb and Sali 2014). Ten models were calculated for each subunit from *P. marinus* and the best model was assessed using the 'objective function' parameter of the MODELLER software. The best model for each subunit was then superimposed to the crystallographic structure of the corresponding subunit from *T. elongatus* using TURBO-FRODO (Roussel and Cambillau 1991) in order to reconstitute the whole 3D model of *P. marinus* PSII. The figure was then realized using PYMOL (DeLano 2002).

Results

Transcription of OEC genes

Since *psbU* and *psbV* genes are missing in the genome of *Prochlorococcus* strains MED4 and SS120 (Online Resource_Table_S2), we checked by RT-PCR whether these genes were effectively expressed in *Prochlorococcus* sp. MIT9313, using *Synechococcus* sp. WH7803 as positive control (Table 1). Expression of the core *psbO* gene, encoding the main protein of the OEC, was also measured in all strains. The number of PCR cycles needed to reach the threshold level (i.e. the number of cycles needed to detect a real signal from the samples) was much lower in the experimental sample with reverse transcription (+RT) than in the control (−RT), where it was sometimes too high (> 40) to be detectable (Table 1). These results clearly show that the *psbO* gene was highly expressed in all tested strains in standard culture conditions. Similarly, the large differences between +RT and −RT conditions for both *psbU* and *psbV* genes showed that these genes were strongly expressed in both *Synechococcus* sp. WH7803 and *Prochlorococcus* sp. MIT9313, allowing us to reject the hypothesis that these are pseudogenes in the latter strain, with the caveat that differences in the levels of expression at the mRNA and protein

levels are often observed in cyanobacteria (see e.g. Welkie et al. 2014).

Maximal oxygen evolution rates

In order to determine whether the absence of the PsbU and PsbV proteins in the RCII of *Prochlorococcus* strains SS120 and MED4 could affect their oxygen-evolving characteristics compared to strains possessing these proteins, light response curves were determined at three acclimation irradiances (LL = 18 µmol photons m^{-2} s^{-1}; ML = 75 µmol photons m^{-2} s^{-1} and HL = 163 µmol photons m^{-2} s^{-1}) for *P. marinus* PCC 9511 and *Synechococcus* sp. WH7803 strains and only the former two irradiances for the LL-adapted *Prochlorococcus* strains SS120 and MIT9313, which could not grow at the highest irradiance. Given the significant differences in cell size, number of PSII per unit biomass as well as in the nature and composition of the light-harvesting complexes between these four strains (Kana and Glibert 1987a; Moore and Chisholm 1999; Partensky et al. 1993; Six et al. 2007; Ting et al. 2007), P–E curves (Online Resource_Fig_S3–S5) and the corresponding maximal net O_2 evolution rates (P_m) were normalized per (DV-)Chl *a*, per cell and per PSII, in order to ease comparisons (Fig. 1a–c).

Maximal O_2 evolution rates per (DV−)Chl *a* (P^{Chl}_m) globally increased with increasing growth irradiance for all cyanobacterial strains except for MIT9313, which exhibited the highest rate among all three *Prochlorococcus* strains at LL (P^{Chl}_m = 342 mol O_2.[mol DV-Chl *a*]$^{-1}$ h^{-1}) but a lower rate at ML (Fig. 1a and Online Resource_Fig_S3). The record P^{Chl}_m value was observed at HL for PCC 9511 (959 mol O_2.[mol DV-Chl *a*]$^{-1}$.h^{-1}), showing that despite lacking PsbU/V, this strain is a very efficient oxyphototroph and is truly HL-adapted. It is worth noting that at the lowest irradiance tested (18 µmol photons m^{-2} s^{-1}), all picocyanobacterial strains globally consumed more oxygen than they emitted (Fig. 2a).

When rates were normalized per cell (Fig. 1b and Online Resource_Fig_S4), the highest P^{Cell}_m values were, as

Table 1 Expression of genes coding for the oxygen-evolving complex in the four picocyanobacterial strains used in this study

Gene	*P. marinus* PCC 9511		*P. marinus* SS120		*Prochlorococcus* sp. MIT9313		*Synechococcus* sp. WH7803	
	−RT	+RT	−RT	+RT	−RT	+RT	−RT	+RT
psbO	36	25.6	36.2	22.7	n.d.	28.9	n.d.	26.6
psbU	n.a.	n.a.	n.a.	n.a.	37.7	21.6	n.d.	23.2
psbV	n.a.	n.a.	n.a.	n.a.	37.3	23.1	37.5	26.4

Values correspond to the number of cycles needed to reach a fixed fluorescence threshold

Difference in the number of cycles without reverse transcription (-RT), i.e. DNA, and after reverse transcription (+ RT), i.e. mRNA, is proportional to the expression level

n.a. not applicable, *n.d.* not detected
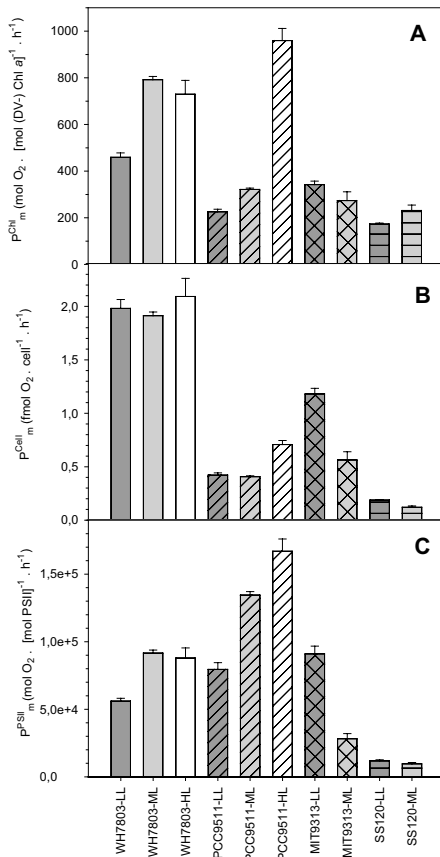
Fig. 1 Comparison of maximal rates of oxygen evolving (P_m) for the four tested marine picocyanobacterial strains grown at low, medium and/or high continuous growth irradiance (LL, 18 ± 3 µmol photons m^{-2} s^{-1}; ML, 75 ± 10 µmol photons m^{-2} s^{-1}; HL, 163 ± 12 µmol photons m^{-2} s^{-1}; the latter irradiance was only applicable for *Synechococcus* sp. WH7803 and *Prochlorococcus marinus* PCC 9511). **a** Values normalized per total Chl, i.e. Chl *a* only for *Synechococcus* sp. WH7803 and the sum of DV-Chl *a* and *b* for *Prochlorococcus* strains MED4, SS120 and MIT9313. **b** Values normalized per cell. **c** Values normalized per PSII (D2 protein). All measurements are average $\pm$ SD of 4 to 6 biological replicates

expected, observed for the two strains exhibiting the largest cell sizes, i.e. WH7803 and MIT9313 (Kana and Glibert 1987a; Ting et al. 2007). PCC 9511 was the sole strain for which P^{Cell}_m significantly increased with irradiance, while it dropped twofold between LL and ML for MIT9313.

When rates were normalized per PSII complex (Fig. 1c and Online Resource_Fig_S5), PCC 9511 exhibited the highest P^{PSII}_m value at both ML and HL with a regular increase between LL and HL, while for MIT9313 P^{PSII}_m was threefold lower at ML than LL. It is worth noting that the proportion of PSII per total protein tended to decrease with increasing growth irradiance (I_g) in the two HL-adapted strains (WH7803 and PCC 9511), while it was virtually unchanged between LL and ML in the two LL-adapted strains (Fig. 3). With the caveat that cultures exhibited a limited contamination by heterotrophic bacteria that could somewhat bias the measured amount of total proteins, the much lower maximal evolution rates per PSII measured for *P. marinus* SS120 compared to the two other *Prochlorococcus* strains (Fig. 1c) might be explained in part by the fact that the latter strain seemingly contains a particularly high number of PSII per total protein (Fig. 3), although the reason why its rates were also very low when normalized per cell (Fig. 1b) remains unclear. Altogether, our data suggest that (i) HL-adapted strains mainly acclimate to increasing I_g by reducing their total PSII number, whereas LL-adapted strains rather reduce the size of their PSII antennae and (ii) the PSII efficiency is much less affected by increases in I_g in HL- than in LL-adapted strains.

Other photosynthetic parameters

The low light capture efficiency per cell, as assessed by the initial light-limited slope of the P–E curve (α^{Cell}; Fig. 2b), was expectedly higher for the larger cell-sized strains, *Synechococcus* sp. W7803 and *Prochlorococcus* sp. MIT 9313. α^{Cell} tended to decrease between LL and ML in all strains, as a likely result from a decrease of the antenna size, but this trend was statistically significant only in the LL-adapted strain MIT9313.

The HL-adapted strains *Synechococcus* sp. WH7803 and *P. marinus* PCC 9511 displayed slightly higher saturation irradiances at LL (E_k > 150 µmol photons m^{-2} s^{-1}; Fig. 2c) than the LL-adapted strains MIT9313 and SS120 (< 150 µmol photons m^{-2} s^{-1}), but while E_k increased with irradiance in the former strains, it slightly decreased in the latter strains. The compensation irradiance (E_0) occurred at about one-fourth (26.4 ± 4.5%) of the E_k values in all strains (Fig. 2d).

Thermoluminescence

TL glow curves in the temperature range 10–50 °C result from thermally induced radiative back reactions within PSII, namely from the $S_{2/3}Q_B^-$ charge recombination (Rutherford et al. 1984). We measured the shapes and intensities of the TL glow curves of strains grown at LL in order to compare the energetics of the donor and acceptor sides of PSII and the
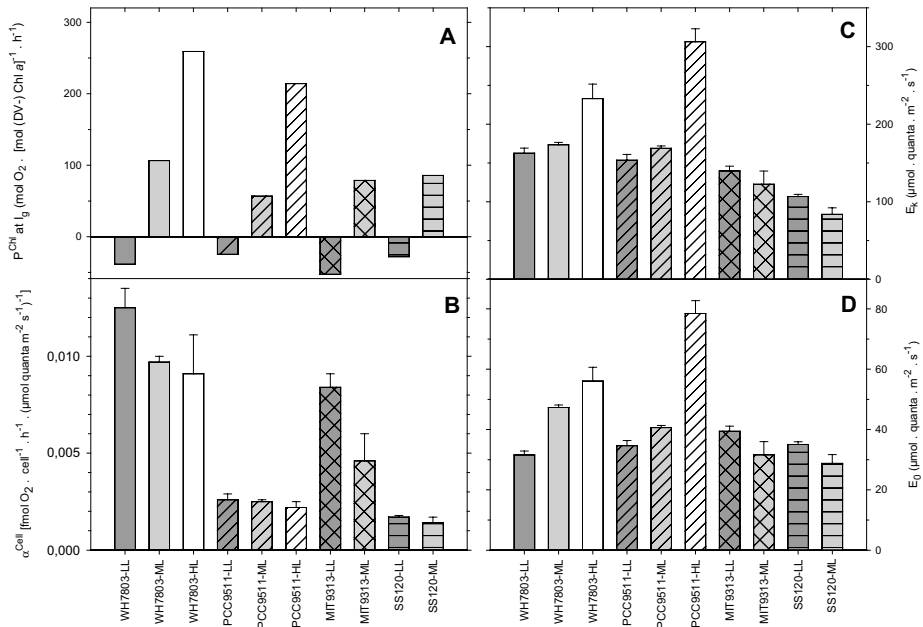
Fig. 2 Photosynthetic parameters derived from the light response curves of oxygen evolution for the four marine picocyanobacterial strains grown at low, medium or high continuous growth irradiance. **a** Oxygen-evolving rates normalized per total Chl at growth irradiance (P^{Chl} at I_g). **b** Photosynthetic capture efficiencies (α) per cell. **c** Saturating irradiance (E_k). **d** Compensation irradiance (E_0)
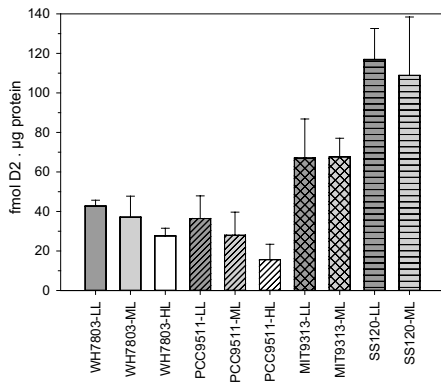
Fig. 3 Molar immunoquantitation of the D2 protein of photosystem II in the four marine picocyanobacterial strains grown at low, medium or high continuous growth irradiance. All measurements are average ± SD of 4 to 6 biological replicates

function of OEC in the studied strains. In the control strain *Synechococcus* sp. WH7803, the glow curve after 2 flashes (the so-called B-band) peaked at 30 °C (Fig. 4a). According to previous results on *Synechocystis* deletion mutants (Burnap et al. 1992; Shen et al. 1997, 1998), one could have expected that the absence of the PsbU or PsbV proteins in the *P. marinus* PCC 9511 and SS120 would result in the shift of the peak temperature of the glow curve to higher temperatures. However, the maxima of all three *Prochlorococcus* strains were either comparable to the control strain or even peaked at lower temperatures (Fig. 4a). Like for WH7803, the $S_{2/3}Q_B^-$ charge recombination in *Prochlorococcus* sp. MIT 9313 resulted in a B-band peaking in the 30–34 °C region, indicating that the recombination of charges stored on $S_2Q_B^-$ and $S_3Q_B^-$ occurs from identical energetic levels. The glow curves of *P. marinus* PCC 9511 were always composed of two bands, peaking around 15 and 32 °C, suggesting a heterogenous energetics of the $S_{2/3}Q_B^-$ charge recombination. Heterogeneity in recombination energetics was also observed in *P. marinus* SS120 (Fig. 4a) and in *Synechocystis* sp. PCC 6803 (data not shown). By adding
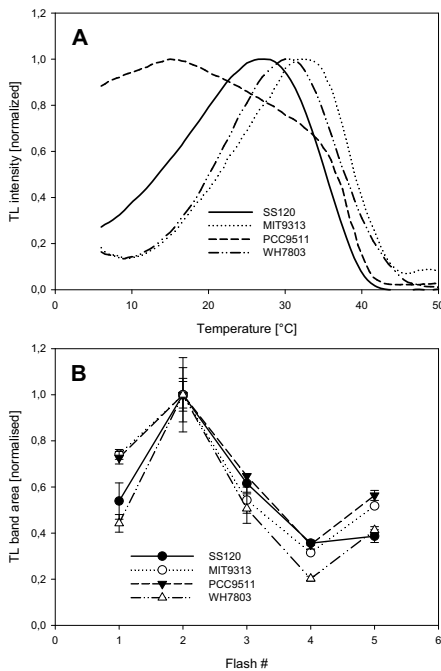
Fig. 4 Thermoluminescence parameters for the picocyanobacteria grown at LL. **a** Plot of normalized thermoluminescence (TL) intensity vs. temperature for the four marine picocyanobacterial strains studied: *Synechococcus* sp. WH7803 and *Prochlorococcus* strains MED4, SS120 and MIT9313. **b** Dependence of the intensity of the B-band on the number of excitation flashes. The intensity of the B-band was calculated as the integral of the TL signal from 10 to 50 °C and normalized to the maximal value reached after 2 flashes

DCMU, we checked that the band at lower temperature was not the Q-band ($S_2Q_A^-$ recombination). The TL glow curve in the presence of DCMU peaked at lower temperatures (-5 to +5 °C; data not shown). Such heterogeneity likely reflects different energetics of the $S_2Q_B^-$ (B2 band) and $S_3Q_B^-$ (B1 band) charge recombinations in studied organisms. The split in the B-band is typically observed when lumen pH < 7 (Ducruet and Vass 2009). However, in our experiments, the addition of an uncoupler (up to 10 mM NH_4Cl) did not change the shape of the composed B-band (data not shown). We also studied the oscillations of the B-band. Since the TL B-bands result from the $S_{2/3}Q_B^-$ charge recombination only, the overall intensity of the glow curve following excitation by series of single turnover flashes oscillates with period of 4 (Rutherford et al. 1984). Similarly to the oscillations of

the oxygen flash yields, these flash-induced oscillations of the TL B-band intensity stem from the initial distribution of the S-states and occupancy of the Q_B pocket in the dark and from the efficiency of transitions between different S-states. Usually, the intensity of the B-band is maximal after two flashes (Rutherford et al. 1984). As expected, in all studied strains, the TL was maximal after two excitation flashes and minimal after 4 flashes (Fig. 4b). One can also note that the B-band was significantly more intense after 1 and 5 excitation flashes in *P. marinus* PCC 9511 and MIT9313, respectively, than in the control *Synechococcus* sp. WH7803 strain (Fig. 4b) or the freshwater *Synechocystis* sp. PCC 6803 (data not shown), where the TL B-band intensity after 1 flash was always less than 45% of the maximum. This increased intensity of the TL glow curve after 1 flash can be interpreted as an increased proportion of PSII centres remaining in the S1 state in the dark in *Prochlorococcus* strains.

We also compared the integral intensity of the TL B-band after 2 pre-flashes normalized to the (DV-)Chl content (Online resource Fig. S6), the TL B-band intensity being a quantitative proxy for the actively recombining PSII reaction centres (Burnap et al. 1992). Similar to the (DV-)Chl-normalized maximal oxygen evolution rates (P^{Chl}_m) at LL (Fig. 1a), the highest Chl-normalized TL emission was detected in *Synechococcus sp.* WH7803, followed by *P. marinus* PCC 9511 and *P. marinus* SS120. However, for unclear reasons, the PSII recombination efficiency was unexpectedly low in *P. marinus* MIT9313, almost an order of magnitude lower than the control WH7803 (0.41 ± 0.12 a.u. and 3.56 ± 0.31 a.u., respectively).

Structural homology model of *P. marinus* MED4 PSII

The published 3D X-ray structure of *Thermosynechococcus elongatus* PSII (Guskov et al. 2009) was used to build a homology model for the PSII of *P. marinus* MED4, a close relative to *P. marinus* PCC 9511 (Rippka et al. 2000). Online Resource_Table_S2 compares the PSII gene content of the four picocyanobacterial strains used in this study and lists all genes included in the model. Comparison of a side view of this MED4 PSII structure (Fig. 5a, c) with the same model where PsbU and PsbV from *T. elongatus* are superimposed (Fig. 5b, d) shows that the Mn cluster of MED4 is directly exposed to the surrounding environment and no structural modifications of PSII proteins surrounding the Mn cluster seemingly compensate for the lack of PsbU and PsbV proteins. This is confirmed by sequence alignments of *T. elongatus* PSII subunits and their orthologs from *Prochlorococcus* and marine *Synechococcus* that show that, despite some intergenus variability in sequences of several minor subunits, most PSII proteins of *Prochlorococcus* strains with
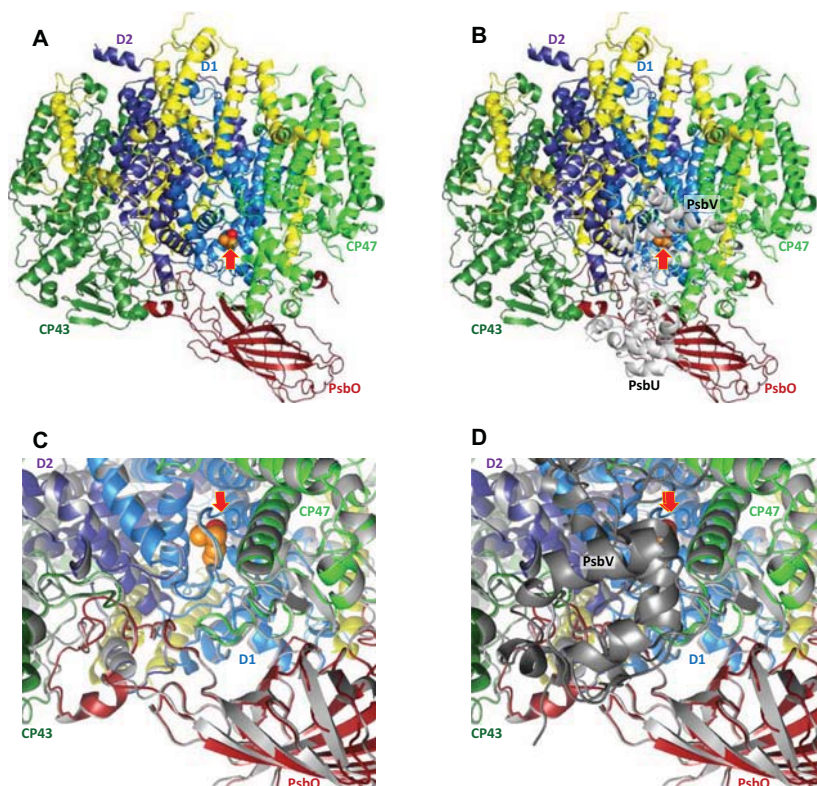
Fig. 5 a Luminal side view of the 3D structure of a PSII monomer from *Prochlorococcus marinus* MED4, modelled after *Thermosynechococcus elongatus* (Guskov et al. 2009). **b** Same but showing the location of the PsbU and PsbV proteins from *T. elongatus* that shield the Mn cluster. **c** Zoom on the oxygen-evolving complex (OEC) region with superimposition of the 3D structures of *P. marinus* MED4 (in colour) and *T. elongatus* (in grey). **d** Same as *C* but including the PsbV protein from *T. elongatus* (PsbU cannot be seen on this view). Only the major PSII proteins are annotated; all other intrinsic proteins are shown in yellow (see complete list in Online Resource_ Table_S2). The Mn cluster is represented by orange (Mn ions) and red (Ca^{2+} ion) spheres and its position indicated by a red arrow

streamlined genomes are of similar length than their counterparts in marine picocyanobacterial strains possessing PsbU/V (i.e. all *Synechococcus* spp. and/or *Prochlorococcus* sp. clade LLIV; data not shown). Notable exceptions are PsbM and PsbX, two minor PSII proteins that possess a specific extension (C- or N-terminal, respectively) in all streamlined strains (Online Resource_Figs._S7-S8). Yet, the localization of these two proteins on the cytoplasmic side of the PSII structure (Guskov et al. 2009) is way too far from the Mn cluster for these additional domains to compensate for the lack of PsbU and PsbV.

Discussion

Lack of two extrinsic OEC proteins does not affect *P. marinus* oxygen evolution rates

P–E curves and derived parameters showed that *P. marinus* strains PCC 9511 and SS120 can evolve oxygen at significant rates despite lacking *psbU* and *psbV* (Figs. 1, 2 and Online Resource_Fig_S3–S5), even though these two genes appear to be functional in the clade LLIV strain *Prochlorococcus* sp. MIT9313 (Table 1). This contrasts with previous studies on knockout mutants of these genes in freshwater

cyanobacteria, notably regarding the drop of oxygen evolution rates observed in *Synechocystis* sp. PCC 6803 *psbV*-less mutants (Shen et al. 1995, 1998). Yet, examination of a structural homology model of the 3D structure of PSII in *P. marinus* MED4 did not reveal any obvious extension of other PSII subunits located in the close vicinity of the Mn cluster that may compensate for the absence of these extrinsic proteins (Fig. 5a, c). In the PSII structure of *Thermosynechococcus vulcanus*, the PsbV C-terminus, and more specifically Tyr 137, is thought to be involved in an exit channel for protons arising from the deprotonation of D1-Tyr161 (a.k.a. Y_Z) to the lumen (Umena et al. 2011), suggesting that absence of PsbV in MED4 could affect the proton extrusion process. It is worth noting that PsbU and PsbV are also absent from green algae and higher plants, but they are replaced by PsbP and PsbQ (De Las Rivas et al. 2007). Surprisingly, most cyanobacteria possess distant PsbP and PsbQ homologs, usually called 'CyanoP' and 'CyanoQ', respectively (Kashino et al. 2002; Thornton et al. 2004; Roose et al. 2007; Enami et al. 2008), but their role and localization remain unclear, since they are not detected in PSII crystal structures (Guskov et al. 2009; Umena et al. 2011). While the *cyanoQ* gene is absent from all *Prochlorococcus* genomes, including members of the LLIV clade, *cyanoP* is a core gene in marine picocyanobacteria (Online Resource_Table_S2). CyanoP is thought to be a constitutive PSII protein that stabilizes charge separation (Sato 2010; Aoi et al. 2014). As previously noticed by Fagerlund and Eaton-Rye (2011), its closest homolog in *Arabidopsis* is not PsbP itself, but the PsbP-like protein encoded by *PPL1* (*At3g55330*), which is involved in the repair of photodamaged PSII (Ishihara et al. 2007). *In silico* protein docking experiments have suggested that, when CyanoQ is present, CyanoP is located on the lumenal face of the PSII complex, below the D2 protein and away from the other extrinsic proteins. However, in absence of CyanoQ, CyanoP might take its place in the immediate vicinity of PsbV (Fagerlund and Eaton-Rye 2011). So, we cannot exclude that in *P. marinus* MED4, which lacks PsbU, PsbV and CyanoQ altogether, CyanoP might have a role in shielding the Mn cluster. Another noticeable PSII protein present in all marine picocyanobacteria (Online Resource_Table_S2), but not in PSII crystals, is Psb27 (Nowaczyk et al. 2006). Like CyanoP (and CyanoQ), it possesses an N-terminal signal peptidase II motif, indicating that it is a lipoprotein. In *Synechocystis* PCC 6803, Psb27 is thought to facilitate the assembly of the Mn cluster by preventing the premature association of other extrinsic proteins (PsbO, PsbU, PsbV and CyanoQ). Psb27 is then replaced by these proteins upon assembly of the Mn cluster (Roose and Pakrasi 2008). Psb27 has been reported to occur in sub-stoichiometric amounts compared to other PSII subunits in *T. elongatus* (Michoux et al. 2014). If this is also the case in *Prochlorococcus* strains lacking PsbU and

PsbV, this would plead against a role of Psb27 in shielding of the Mn cluster. However, one cannot exclude that the absence of *psbU* and *psbV* in many *Prochlorococcus* strains might trigger an increased expression level for *psb27*, so that its product would be synthesized in stoichiometric amounts compared to other PSII components and could act as a constitutive OEC extrinsic protein. Examination of the whole transcriptome of *P. marinus* MED4 cells synchronized by a 14-h:10-h light–dark cycle (Zinser et al. 2009) indeed shows that *psb27* is strongly expressed and exhibits a diel cycle globally similar to *psbO*, with a maximum at the dark-to-light transition and a minimum in the afternoon, while *cyanoP* and *psb27* both reach their minimal diel expression level 2 h before *psbO* (4 pm *vs.* 6 pm, respectively; see http://proportal.mit.edu/).

Another possibility is that the missing PsbU and PsbV have been replaced by some *Prochlorococcus*-specific PSII protein(s) that could have been acquired early during the evolution of these lineages. The comparison of currently available genomes of marine picocyanobacteria shows that *Prochlorococcus* strains with a streamlined genome possess 21 specific proteins (absent from both *Prochlorococcus* spp. LLIV and *Synechococcus* spp. strains; Online Resource Table S3). However, examination of these sequences using LipoP (http://www.cbs.dtu.dk/services/LipoP/) shows that none contain a putative N-terminal signal peptidase II motif, indicative of lipoproteins (as found in CyanoP and CyanoQ), nor even a signal peptidase I motif (as found in PsbU and PsbV). A number of uncharacterized membrane proteins are, however, worth noting in this dataset, as they could potentially intrinsic PSII proteins specific of *Prochlorococcus* with streamlined genomes (Online Resource Table S3).

Proteins able to replace PsbU and/or PsbV might also have been acquired later during the evolution of the *Prochlorococcus* radiation, i.e. by the common ancestor of the HL branch shortly after its differentiation from other (LL-adapted) *Prochlorococcus* lineages. The rationale for this hypothesis is that a *psbU*-less mutant of *Synechocystis* sp. PCC 6803 was found to grow well under moderate light, but was highly susceptible to photoinhibition at high light, likely due to an accelerated rate of D1 degradation in this condition (Inoue-Kashino et al. 2005). The absence of the Mn cluster shield provided by PsbU might therefore not be harmful for *Prochlorococcus* cells living in a low light habitat like that occupied by LL-adapted *P. marinus* (such as SS120), while it would be deleterious in the upper mixed layer that is exposed to high irradiances, where thrive HL-adapted strains *P. marinus*, such as MED4 or PCC 9511. Comparative genomics analyses showed that sequenced members of the HL clades possess at least 76 specific genes (i.e. absent from all other marine picocyanobacteria), including one (PMM0736) for which LipoP detected a signal peptidase II motif (like in CyanoP and

CyanoQ) and nine others that exhibited (like for PsbU/V) a signal peptidase I motif (Online Resource Table S3). Proteomic analyses of PSII preparations are needed to check whether some of the abovementioned proteins are indeed linked to PSII and/or localized near the OEC.

Alternatively, compensatory mechanisms for the lack of extrinsic proteins in *Prochlorococcus* cells may simply rely on the occurrence in *Prochlorococcus* cells of an ion environment in the thylakoid lumen that could be different from that in freshwater cyanobacteria, especially regarding Ca^{2+} and Cl^-, a difference possibly linked to their different habitat. Indeed, both of these OEC cofactors were shown to be critical for the growth of a *Synechocystis* sp. PCC 6803 *psbU-* and psb*V*-less mutant, likely due to their protective role on the Mn cluster, by reducing its accessibility to solvent attacks (Shen et al. 1998; Inoue-Kashino et al. 2005).

Insights from the thermoluminescence analysis

TL has been used as a tool to study the role of extrinsic OEC proteins in model cyanobacteria (Balint et al. 2006; Burnap et al. 1992; Shen et al. 1997, 1998). The deletion of PsbU and PsbV was found to cause a shift of the B-band to higher temperatures and a lower intensity of the B-band, suggesting a stabilization of the S_2 state of the OEC and a decrease in the number of active PSII centres. Although each *Prochlorococcus* strain that we studied had distinct and characteristic shape of the B-band (Online Resource_Fig_S6), we did not observe any clear trend in B-band shape or peak position that could be explained by the absence of the extrinsic proteins, indicating that the OEC is fully functional in strains with streamlined genomes. When studying the oscillation patterns of the TL B-band (Fig. 4b), we noticed that, in all *Prochlorococcus* strains, the TL intensity after one flash was significantly higher than in all other cyanobacteria or microalgae studied in recent years in the Třeboň laboratory (data not shown). Since we still observed maxima after 2 flashes, we interpret this modification of the TL oscillation pattern not as a change of the Q_B/Q_B^- fraction but rather as an increase in the fraction of centres in S_1 state in the dark. TL intensity can be used also as a proxy for active PSII centres (Burnap et al. 1992). Such proxy is, however, only semi-quantitative because several pathways for the $S_{2/3}Q_B^-$ charge recombination exist within PSII and TL monitors only one of them, namely the radiative recombination resulting in the singlet P_{680}^*. Still, we observed reasonable correlation between the P^{Chl}_m and the (DV-)Chl-normalized TL intensity for three of the studied strains grown at LL (Online Resource Fig S6, inset). Yet, the reason for the much lower TL intensity observed in the MIT9313 strain remains unclear and would require further experimental work.

Comparison of *Prochlorococcus* oxygen evolution and carbon assimilation rates

While several previous studies reported carbon fixation rates in various *Prochlorococcus* strains (Bruyant et al. 2005; Partensky et al. 1993; Moore and Chisholm 1999; Zinser et al. 2009) and in *Synechococcus* sp. WH7803 (Kana and Glibert 1987b), the present study is to our knowledge the first one reporting in detail oxygen production in marine picocyanobacteria. A striking feature of P–E curves derived from incubations with $^{14}CO_2$ of both LL- and HL-adapted *Prochlorococcus* strains (but not *Synechococcus*) is the strong photoinhibitory effect of high irradiances, as indicated by a drop in P^{Chl} at irradiances ca. fourfold higher than the light saturation index E_k (Partensky et al. 1993; Moore and Chisholm 1999). In contrast, we observed little photoinhibition in the present study, even for the LL-adapted strains (Online Resource_Fig_S3–S5), though it is worth noting that MIT9313 cultures pre-acclimated to 75 ± 10 µmol quanta m^{-2} s^{-1} did show an altered O_2 emission after 4–5 min exposure to the highest tested irradiance; see Online Resource_Fig_S1. This difference is possibly due to the fact that the method used to measure O_2 evolution, typically 5–10 min exposure to light followed by a similar period in dark (Online Resource_Fig_S1), is much less stressing for *Prochlorococcus* cells than are measurements of CO_2 assimilation. For instance, for modelling P–E curves Moore and Chisholm (1999) exposed cells to a range of irradiances for 45 min.

The photosynthetic quotient, i.e. the number of moles O_2 produced per mole CO_2 assimilated, has not yet been determined for *Prochlorococcus*. However, since all *Prochlorococcus* strains studied here lack nitrate assimilation genes and cells essentially rely on ammonium as a nitrogen source (Kettler et al. 2007; Rocap et al. 2003; Moore et al. 2002), therefore avoiding the electron-consuming step of nitrate reduction, the photosynthetic quotient should theoretically not deviate much from 1.0 (Falkowski and Raven 2007). This makes possible direct comparisons between maximum photosynthetic rates for O_2 production and CO_2 consumption. Moore and Chisholm (1999) measured P^{Chl}_m values of ca. 134, 156 and 179 mol C mol Chl a^{-1} h^{-1} at LL, as compared in the present study to 226, 173 and 342 mol O_2 mol Chl a^{-1} h^{-1} at LL for PCC 9511 (a close relative of MED4), SS120 and MIT9313, respectively. Although P^{Chl}_m values obtained here for O_2 release were systematically higher than Moore and co-workers' for CO_2 assimilation, these discrepancies might be due in part to the different light conditions used in the two studies.

Ecological implications of *Prochlorococcus* oxygen evolution characteristics

The O₂ evolving measurements reported in the present study for different strains of marine picocyanobacteria at several growth irradiances should be very useful for assessing the contribution of these key phytoplankters to the global oxygen production of the world ocean and more generally their role in the biogeochemical cycle of oxygen. Our study also provides new insights to explain the paradoxical occurrence of virtually monoalgal populations of *Prochlorococcus* in waters of the Arabian Sea and the Eastern Tropical Pacific Ocean displaying O₂ concentrations lower than 20 μM, so-called 'oxygen minimum zones' (OMZ; Beman and Carolan 2013; Garcia-Robledo et al. 2017; Goericke et al. 2000; Lavin et al. 2010). OMZ generally occur along continental margins where high rates of phytoplankton productivity in the upper layer, coupled with poor ventilation and sluggish circulation, lead to an extensive, oxygen-deficient layer at depth, where the decomposition of sinking biological material provokes high microbial respiration rates (Helly and Levin 2004). Although most of the OMZ occur below the euphotic layer, the top of the OMZ can be reached by light and when this is the case, O₂ production by *Prochlorococcus* could be sufficient to feed aerobic processes (Ulloa et al. 2012). The maintenance of anoxic conditions despite vertical mixing and lateral advection was proposed to rely upon highly efficient O₂ scavenging by local microbial communities (Kalvelage et al. 2015). However, our data show that at the low irradiances reaching the top of the OMZ (typically 0.1 to 2% of the surface irradiance; (Goericke et al. 2000; Garcia-Robledo et al. 2017), corresponding to ca. 2–40 μmol quanta m^{-2} s^{-1} at solar noon), the net oxygen exchange rate of *Prochlorococcus* cells is expected to be less than or equal to zero (Online Resource_Fig_S3A). This could explain in part the very low oxygen levels measured in these layers. Phylogenetic analyses of *Prochlorococcus* populations thriving in OMZ showed that they predominantly belong to the LLIV clade and to two novel, uncultured low light-adapted clades called LLV and LLVI (Lavin et al. 2010). The latter clades are phylogenetically closely related to LLIV members and share a number of characteristics with them, such as a large G + C% compared to other *Prochlorococcus* lineages. It is therefore possible that, like MIT9313, their genome is not streamlined and that they possess a full set of OEC proteins, a hypothesis that will be confirmed by sequencing the genomes of LLV and LLVI representatives.

References

Aoi M, Kashino Y, Ifuku K (2014) Function and association of CyanoP in photosystem II of *Synechocystis* sp. PCC 6803. Res Chem Intermediat 40:3209–3217. https://doi.org/10.1007/s11164-014-1827-y

Balint I, Bhattacharya J, Perelman A, Schatz D, Moskovitz Y, Keren N, Schwarz R (2006) Inactivation of the extrinsic subunit of photosystem II, PsbU, in *Synechococcus* PCC 7942 results in elevated resistance to oxidative stress. FEBS Lett 580:2117–2122. https://doi.org/10.1016/j.febslet.2006.03.020

Batut B, Knibbe C, Marais G, Daubin V (2014) Reductive genome evolution at both ends of the bacterial population size spectrum. Nature Rev Microbiol 12:841–850. https://doi.org/10.1038/nrmicro3331

Belgio E, Trsková E, Kotabová E, Ewe D, Prášil O, Kana R (2018) High light acclimation of *Chromera velia* points to photoprotective NPQ. Photosynth Res 135:263–274. https://doi.org/10.1007/s11120-017-0385-8

Beman JM, Carolan MT (2013) Deoxygenation alters bacterial diversity and community composition in the ocean's largest oxygen minimum zone. Nature Commun 4:2705. https://doi.org/10.1038/Ncomms3705

Biller SJ, Berube PM, Berta-Thompson JW, Kelly L, Roggensack SE, Awad L, Roache-Johnson KH, Ding H, Giovannoni SJ, Rocap G, Moore LR, Chisholm SW (2014) Genomes of diverse isolates of the marine cyanobacterium *Prochlorococcus*. Nature Scient Data 1:140034. https://doi.org/10.1038/sdata.2014.34

Brand LE, Guillard RRL, Murphy LS (1981) A method for the rapid and precise determination of acclimated phytoplankton reproduction rates. J Plankt Res 3:193–201. https://doi.org/10.1093/plankt/3.2.193

Bruyant F, Babin M, Genty B, Prasil O, Behrenfeld MJ, Claustre H, Bricaud A, Garczarek L, Holtzendorff J, Koblizek M, Dousova H, Partensky F (2005) Diel variations in the photosynthetic parameters of *Prochlorococcus* strain PCC 9511: Combined effects of light and cell cycle. Limnol Oceanogr 50:850–863. https://doi.org/10.4319/lo.2005.50.3.0850

Burnap RL, Shen JR, Jursinic PA, Inoue Y, Sherman LA (1992) Oxygen yield and thermoluminescence characteristics of a cyanobacterium lacking the manganese-stabilizing protein of photosystem II. Biochemistry 31:7404–7410. https://doi.org/10.1021/bi00147a027

Campbell L, Vaulot D (1993) Photosynthetic picoplankton community structure in the subtropical North Pacific Ocean near Hawaii (station ALOHA). Deep Sea Res 40:2043–2060. https://doi.org/10.1016/0967-0637(93)90044-4

Campbell L, Nolla HA, Vaulot D (1994) The importance of *Prochlorococcus* to community structure in the central North Pacific Ocean. Limnol Oceanogr 39:954–961. https://doi.org/10.4319/lo.1994.39.4.0954

Chen M, Zhang Y, Blankenship RE (2008) Nomenclature for membrane-bound light-harvesting complexes of cyanobacteria. Photosynth Res 95:147–154. https://doi.org/10.1016/j.bbabio.2013.07.012

De Las Rivas J, Balsera M, Barber J (2004) Evolution of oxygenic photosynthesis: Genome-wide analysis of the OEC extrinsic proteins. Trends Plant Sci 9:18–25. https://doi.org/10.1016/j.plants.2003.11.007

De Las Rivas J, Heredia P, Roman A (2007) Oxygen-evolving extrinsic proteins (PsbO,P,Q,R): Bioinformatic and functional analysis. Biochim Biophys Acta 1767:575–582. https://doi.org/10.1016/j.bbabio.2007.01.018

DeLano WL (2002) The PyMOL Molecular Graphics System San Carlos. CA, USA

Ducruet JM, Vass I (2009) Thermoluminescence: experimental. Photosynth Res 101:195–204. https://doi.org/10.1007/s11120-009-9436-0

Dufresne A, Garczarek L, Partensky F (2005) Accelerated evolution associated with genome reduction in a free-living prokaryote. Genome Biol 6:R14. https://doi.org/10.1186/gb-2005-6-2-r14

Dufresne A, Ostrowski M, Scanlan DJ, Garczarek L, Mazard S, Palenik BP, Paulsen IT, Tandeau de Marsac N, Wincker P, Dossat C, Ferriera S, Johnson J, Post AF, Hess WR, Partensky F (2008) Unraveling the genomic mosaic of a ubiquitous genus of marine cyanobacteria. Genome Biol 9:R90. https://doi.org/10.1186/gb-2008-9-5-r90

Enami I, Yoshihara S, Tohri A, Okumura A, Ohta H, Shen JR (2000) Cross-reconstitution of various extrinsic proteins and photosystem II complexes from cyanobacteria, red alga and higher plant. Plant Cell Physiol 41:1354–1364. https://doi.org/10.1007/s11120-004-7760-y

Enami I, Okumura A, Nagao R, Suzuki T, Iwai M, Shen JR (2008) Structures and functions of the extrinsic proteins of photosystem II from different species. Photosynth res 98:349–363. https://doi.org/10.1007/s11120-008-9343-9

Eswar N, Webb B, Marti-Renom MA, Madhusudhan MS, Eramian D, Shen M-Y, Pieper U, Sali A (2007) Comparative protein structure modeling using MODELLER. Curr Protoc Protein Sci. https://doi.org/10.1002/0471140864.ps0209s50

Fagerlund RD, Eaton-Rye JJ (2011) The lipoproteins of cyanobacterial photosystem II. J Photoch Photobiol 104:191–203. https://doi.org/10.1016/j.jphotobiol.2011.01.022

Falkowski P, Raven J (2007) Aquatic photosynthesis. 2nd edn. Princeton University Press, Princeton

Ferreira KN, Iverson TM, Maghlaoui K, Barber J, Iwata S (2004) Architecture of the photosynthetic oxygen-evolving center. Science 303:1831–1838. https://doi.org/10.1126/science.1093087

Flombaum P, Gallegos JL, Gordillo RA, Rincon J, Zabala LL, Jiao N, Karl DM, Li WK, Lomas MW, Veneziano D, Vera CS, Vrugt JA, Martiny AC (2013) Present and future global distributions of the marine Cyanobacteria Prochlorococcus and Synechococcus. Proc Natl Acad Sci USA 110:9824–9829. https://doi.org/10.1073/pnas.1307701110

Garcia-Robledo E, Padilla CC, Aldunate M, Stewart FJ, Ulloa O, Paulmier A, Gregori G, Revsbech NP (2017) Cryptic oxygen cycling in anoxic marine zones. Proc Natl Acad Sci USA 114:8319–8324

Garczarek L, Dufresne A, Blot N, Cockshutt AM, Peyrat A, Campbell DA, Joubin L, Six C (2008) Function and evolution of the psbA gene family in marine Synechococcus: Synechococcus sp. WH7803 as a case study. ISME J 2:937–953. https://doi.org/10.1038/ismej.2008.46

Geider RJ, Osborne BA (1992) The photosynthesis-light response curve. In: Geider RJ, Osborne BA (eds) Algal Photosynthesis: the measurement of algal gas exchange. Current phycology. Springer, Dordrecht, pp 156–191. https://doi.org/10.1007/978-1-4757-2153-9_7

Glibert PM, Kana TM, Olson RJ, Kirchman DL, Alberte RS (1986) Clonal comparisons of growth and photosynthetic responses to nitrogen availability in marine Synechococcus spp. J Exp Mar Biol Ecol 101:199–208. https://doi.org/10.1016/0022-0981(86)90050-X

Goericke R, Repeta DJ (1992) The pigments of Prochlorococcus marinus: the presence of divinyl chlorophyll a and b in a marine prochlorophyte. Limnol Oceanogr 37:425–433. https://doi.org/10.4319/lo.1992.37.2.0425

Goericke R, Olson RJ, Shalapyonok A (2000) A novel niche for Prochlorococcus sp in low-light suboxic environments in the Arabian Sea and the Eastern Tropical North Pacific. Deep Sea Res Pt I 47:1183–1205. https://doi.org/10.1016/S0967-0637(99)00108-9

Guskov A, Kern J, Gabdulkhakov A, Broser M, Zouni A, Saenger W (2009) Cyanobacterial photosystem II at 2.9-angstrom resolution and the role of quinones, lipids, channels and chloride. Nat Struct Mol Biol 16:334–342. https://doi.org/10.1038/nsmb.1559

Helly JJ, Levin LA (2004) Global distribution of naturally occurring marine hypoxia on continental margins. Deep Sea Res Pt I 51:1159–1168. https://doi.org/10.1016/j.dsr.2004.03.009

Hess WR, Partensky F, Van der Staay GWM, Garcia-Fernandez JM, Boerner T, Vaulot D (1996) Coexistence of phycoerythrin and a chlorophyll a/b antenna in a marine prokaryote. Proc Natl Acad Sci USA 93:11126–11130

Inoue-Kashino N, Kashino Y, Satoh K, Terashima I, Pakrasi HB (2005) PsbU provides a stable architecture for the oxygen-evolving system in cyanobacterial photosystem II. Biochemistry 44:12214–12228. https://doi.org/10.1021/bi047539k

Ishihara S, Takabayashi A, Ido K, Endo T, Ifuku K, Sato F (2007) Distinct functions for the two PsbP-like proteins PPL1 and PPL2 in the chloroplast thylakoid lumen of Arabidopsis. Plant Physiol 145:668–679. https://doi.org/10.1104/pp.107.105866

Kalvelage T, Lavik G, Jensen MM, Revsbech NP, Loscher C, Schunck H, Desai DK, Hauss H, Kiko R, Holtappels M, LaRoche J, Schmitz RA, Graco MI, Kuypers MMM (2015) Aerobic microbial respiration in oceanic oxygen minimum zones. PloS ONE 10:e0133526. https://doi.org/10.1371/journal.pone.0133526

Kana TM, Glibert PM (1987a) Effect of irradiances up to 2000 μE m^{-2} s^{-1} on marine Synechococcus WH7803 - I. Growth, pigmentation, and cell composition. Deep Sea Res 34:479–485. https://doi.org/10.1016/0198-0149(87)90001-X

Kana TM, Glibert PM (1987b) Effect of irradiances up to 2000 μE m^{-2} s^{-1} on marine Synechococcus WH7803 - II. Photosynthetic responses mechanisms. Deep Sea Res 34:497–516. https://doi.org/10.1016/0198-0149(87)90002-1

Kashino Y, Lauber WM, Carroll JA, Wang Q, Whitmarsh J, Satoh K, Pakrasi HB (2002) Proteomic analysis of a highly active photosystem II preparation from the cyanobacterium Synechocystis sp. PCC 6803 reveals the presence of novel polypeptides. Biochemistry 41:8004–8012. https://doi.org/10.1021/bi026012&%23x002B;

Kawakami K, Umena Y, Kamiya N, Shen JR (2011) Structure of the catalytic, inorganic core of oxygen-evolving photosystem II at 1.9 angstrom resolution. J Photochem Photobiol 104:9–18. https://doi.org/10.1016/j.jphotobiol.2011.03.017

Kettler G, Martiny AC, Huang K, Zucker J, Coleman ML, Rodrigue S, Chen F, Lapidus A, Ferriera S, Johnson J, Steglich C, Church G, Richardson P, Chisholm SW (2007) Patterns and implications of gene gain and loss in the evolution of Prochlorococcus. PLoS Genet 3:e231. https://doi.org/10.1371/journal.pgen.0030231

Kimura A, Eaton-Rye JJ, Morita EH, Nishiyama Y, Hayashi H (2002) Protection of the oxygen-evolving machinery by the extrinsic proteins of photosystem II is essential for development of cellular thermotolerance in Synechocystis sp PCC 6803. Plant Cell Physiol 43:932–938. https://doi.org/10.1093/pcp/pcf110

Lavin P, Gonzalez B, Santibanez JF, Scanlan DJ, Ulloa O (2010) Novel lineages of Prochlorococcus thrive within the oxygen minimum zone of the eastern tropical South Pacific. Environ Microbiol Rep 2:728–738. https://doi.org/10.1111/j.1758-2229.2010.00167.x

Li WKW (1994) Primary productivity of prochlorophytes, cyanobacteria, and eucaryotic ultraphytoplankton: measurements from flow cytometric sorting. Limnol Oceanogr 39:169–175. https://doi.org/10.4319/lo.1994.39.1.0169

Li WKW, Dickie PM, Irwin BD, Wood AM (1992) Biomass of bacteria, cyanobacteria, prochlorophytes and photosynthetic eukaryotes in the Sargasso Sea. Deep Sea Res 39:501–519. https://doi.org/10.1016/0198-0149(92)90085-8

Liu HB, Nolla HA, Campbell L (1997) Prochlorococcus growth rate and contribution to primary production in the equatorial and subtropical North Pacific Ocean. Aquat Microb Ecol 12:39–47

Marie D, Partensky F, Vaulot D, Brussaard C (1999) Enumeration of phytoplankton, bacteria, and viruses in marine samples. Current Protocol Cytom 10:11. https://doi.org/10.1002/0471142956.cy111 1s10 11.11–11.11.15.

Michoux F, Boehm M, Bialek W, Takasaka K, Maghlaoui K, Barber J, Murray JW, Nixon PJ (2014) Crystal structure of CyanoQ from the thermophilic cyanobacterium *Thermosynechococcus elongatus* and detection in isolated photosystem II complexes. Photosynth Res 122:57–67. https://doi.org/10.1007/s11120-014-0010-z

Moore LR, Chisholm SW (1999) Photophysiology of the marine cyanobacterium *Prochlorococcus*: Ecotypic differences among cultured isolates. Limnol Oceanogr 44:628–638. https://doi.org/10.4319/lo.1999.44.3.0628

Moore LR, Post AF, Rocap G, Chisholm SW (2002) Utilization of different nitrogen sources by the marine cyanobacteria *Prochlorococcus* and *Synechococcus*. Limnol Oceanogr 47:989–996. https://doi.org/10.4319/lo.2002.47.4.0989

Nishiyama Y, Los DA, Hayashi H, Murata N (1997) Thermal protection of the oxygen-evolving machinery by PsbU, an extrinsic protein of photosystem II, in *Synechococcus* species PCC 7002. Plant Physiol 115:1473–1480. https://doi.org/10.1104/pp.115.4.1473

Nishiyama Y, Los DA, Murata N (1999) PsbU, a protein associated with photosystem II, is required for the acquisition of cellular thermotolerance in *Synechococcus* species PCC 7002. Plant Physiol 120:301–308. https://doi.org/10.1104/pp.120.1.301

Nowaczyk MM, Hebeler R, Schlodder E, Meyer HE, Warscheid B, Rogner M (2006) Psb27, a cyanobacterial lipoprotein, is involved in the repair cycle of photosystem II. Plant Cell 18:3121–3131. https://doi.org/10.1105/tpc.106.042671

Okumura A, Ohta H, Inoue Y, Enami I (2001) Identification of functional domains of the extrinsic 12 kDa protein in red algal PSII by limited proteolysis and directed mutagenesis. Plant Cell Physiol 42:1331–1337

Okumura A, Sano M, Suzuki T, Tanaka H, Nagao R, Nakazato K (2007) Aromatic structure of tyrosine-92 in the extrinsic PsbU protein of red algal photosystem II is important for its functioning. FEBS Lett 581:5255–5258. https://doi.org/10.1016/j.febslet.2007.10.015

Partensky F, Garczarek L (2003) The photosynthetic apparatus of chlorophyll *b*- and *d*-containing Oxychlorobacteria. In: Larkum AWD, Douglas SE, Raven JA (eds) Photosynthesis in Algae. Advances in Photosynthesis Series, vol 14. Kluwer Academic Publishers, Dordrecht, pp 29–62. https://doi.org/10.1007/978-94-007-1038-2_3

Partensky F, Garczarek L (2010) *Prochlorococcus*: Advantages and limits of minimalism. Ann Rev Mar Sci 2:305–331. https://doi.org/10.1146/annurev-marine-120308-081034

Partensky F, Hoepffner N, Li WKW, Ulloa O, Vaulot D (1993) Photoacclimation of *Prochlorococcus* sp. (Prochlorophyta) strains isolated from the North Atlantic and the Mediterranean Sea. Plant Physiol 101(1):285–296. https://doi.org/10.1104/pp.101.1.285

Pittera J, Humily F, Thorel M, Grulois D, Garczarek L, Six C (2014) Connecting thermal physiology and latitudinal niche partitioning in marine *Synechococcus*. ISME J 8:1221–1236. https://doi.org/10.1038/ismej.2013.228

Platt T, Jassby AD (1976) Relationship between photosynthesis and light for natural assemblages of coastal marine-phytoplankton. J Phycol 12:421–430. https://doi.org/10.1111/j.1529-8817.1976.tb02866.x

Porra RJ (2002) The chequered history of the development and use of simultaneous equations for the accurate determination of chlorophylls *a* and *b*. Photosynthesis research 73:149–156. https://doi.org/10.1023/A:1020470224740

Rippka R, Coursin T, Hess W, Lichtlé C, Scanlan DJ, Palinska KA, Iteman I, Partensky F, Houmard J, Herdman M (2000) *Prochlorococcus marinus* Chisholm et al. 1992 *subsp. pastoris subsp.*

nov. strain PCC 9511, the first axenic chlorophyll *a₂/b₂*-containing cyanobacterium (Oxyphotobacteria). Int J Syst Evol Microbiol 50:1833–1847. https://doi.org/10.1099/00207713-50-5-1833

Rocap G, Larimer FW, Lamerdin J, Malfatti S, Chain P, Ahlgren NA, Arellano A, Coleman M, Hauser L, Hess WR, Johnson ZI, Land M, Lindell D, Post AF, Regala W, Shah M, Shaw SL, Steglich C, Sullivan MB, Ting CS, Tolonen A, Webb EA, Zinser ER, Chisholm SW (2003) Genome divergence in two *Prochlorococcus* ecotypes reflects oceanic niche differentiation. Nature 424:1042–1047. https://doi.org/10.1038/nature01947

Roose JL, Pakrasi HB (2008) The Psb27 protein facilitates manganese cluster assembly in photosystem II. J Biol Chem 283:4044–4050. https://doi.org/10.1074/jbc.M708960200

Roose JL, Kashino Y, Pakrasi HB (2007) The PsbQ protein defines cyanobacterial Photosystem II complexes with highest activity and stability. Proc Natl Acad Sci USA 104:2548–2553. https://doi.org/10.1073/pnas.0609337104

Roussel A, Cambillau C (1991) TURBO-FRODO: a tool for building structural models. In: Directory SGGP (ed) Silicon Graphics. Mountain View, CA, p 86

Roy S, Llewellyn CA, Skarstad Egeland E, Johnsen G (2011) Phytoplankton pigments, characterization, chemotaxonomy and applications in oceanography. Cambridge Environmental Chemistry Series. Cambridge University Press, Cambridge

Rutherford AW, Inoue Y (1984) Charge accumulation and photochemistry in leaves studied by thermoluminescence and delayed light emission. Proc Natl Acad Sci USA 81:1107–1111

Sato N (2010) Phylogenomic and structural modeling analyses of the PsbP superfamily reveal multiple small segment additions in the evolution of photosystem II-associated PsbP protein in green plants. Mol Phylogenet Evol 56:176–186. https://doi.org/10.1016/j.ympev.2009.11.021

Scanlan DJ, Ostrowski M, Mazard S, Dufresne A, Garczarek L, Hess WR, Post AF, Hagemann M, Paulsen I, Partensky F (2009) Ecological genomics of marine picocyanobacteria. Microbiol Mol Biol Rev 73:249–299. https://doi.org/10.1128/MMBR.00035-08

Shen JR, Vermaas W, Inoue Y (1995) The role of cytochrome c-550 as studied through reverse genetics and mutant characterization in *Synechocystis* sp. PCC 6803. J Biol Chem 270:6901–6907. https://doi.org/10.1074/jbc.270.12.6901

Shen JR, Ikeuchi M, Inoue Y (1997) Analysis of the *psbU* gene encoding the 12-kDa extrinsic protein of photosystem II and studies on its role by deletion mutagenesis in *Synechocystis* sp. PCC 6803. J Biol Chem 272:17821–17826. https://doi.org/10.1074/jbc.272.28.17821

Shen JR, Qian M, Inoue Y, Burnap RL (1998) Functional characterization of *Synechocysti*s sp. PCC 6803 delta-*psbU* and delta-*psbV* mutants reveals important roles of cytochrome c-550 in cyanobacterial oxygen evolution. Biochemistry 37:1551–1558. https://doi.org/10.1021/bi971676i

Six C, Finkel ZV, Irwin AJ, Campbell DA (2007) Light variability illuminates niche-partitioning among marine picocyanobacteria. PloS One 2:e1341. https://doi.org/10.1371/journal.pone.0001341

Stockner JG (1988) Phototrophic picoplankton: an overview from marine and freshwater ecosystems. Limnol Oceanogr 33:765–775. https://doi.org/10.4319/lo.1988.33.4part2.0765

Thompson JD, Higgins DG, Gibson TJ (1994) Clustal-W - Improving the sensitivity of progressive multiple sequence alignment through sequence weighting, position-specific gap penalties and weight matrix choice. Nucleic Acids Res 22:4673–4680. https://doi.org/10.1007/978-1-4020-6754-9_3188

Thornton LE, Ohkawa H, Roose JL, Kashino Y, Keren N, Pakrasi HB (2004) Homologs of plant PsbP and PsbQ proteins are necessary for regulation of photosystem II activity in the cyanobacterium *Synechocystis* 6803. Plant Cell 16:2164–2175. https://doi.org/10.1105/tpc.104.023515

Ting CS, Hsieh C, Sundararaman S, Mannella C, Marko M (2007) Cryo-electron tomography reveals the comparative three-dimensional architecture of *Prochlorococcus*, a globally important marine cyanobacterium. J Bacteriol 189:4485–4493. https://doi.org/10.1128/JB.01948-06

Ulloa O, Canfield DE, DeLong EF, Letelier RM, Stewart FJ (2012) Microbial oceanography of anoxic oxygen minimum zones. Proc Natl Acad Sci USA 109:15996–16003. https://doi.org/10.1073/pnas.1205009109

Umena Y, Kawakami K, Shen JR, Kamiya N (2011) Crystal structure of oxygen-evolving photosystem II at a resolution of 1.9 A. Nature 473:55–60. https://doi.org/10.1038/nature09913

Veerman J, Bentley FK, Eaton Rye JJ, Mullineaux CW, Vasiliev S, Bruce D (2005) The PsbU subunit of photosystem II stabilizes energy transfer and primary photochemistry in the phycobilisome - Photosystem II assembly of *Synechocystis* sp PCC 6803. Biochemistry 44:16939–16948. https://doi.org/10.1021/bi051137a

Webb B, Sali A (2014) Protein structure modeling with MODELLER. In: Kihara D (ed) Protein structure prediction. Methods in molecular biology, vol 1137. Springer, New York, pp 1–15. https://doi.org/10.1007/978-1-4939-0366-5_1

Wegener KM, Bennewitz S, Oelmuller R, Pakrasi HB (2011) The Psb32 protein aids in repairing photodamaged photosystem II in the cyanobacterium *Synechocystis* 6803. Mol Plant 4:1052–1061. https://doi.org/10.1093/mp/ssr044

Welkie D, Zhang XH, Markillie ML, Taylor R, Orr G, Jacobs J, Bhide K, Thimmapuram J, Gritsenko M, Mitchell H, Smith RD, Sherman LA (2014) Transcriptomic and proteomic dynamics in the metabolism of a diazotrophic cyanobacterium, *Cyanothece* sp. PCC 7822 during a diurnal light-dark cycle. BMC Genom 15:1185. https://doi.org/10.1186/1471-2164-15-1185

Zinser ER, Lindell D, Johnson ZI, Futschik ME, Steglich C, Coleman ML, Wright MA, Rector T, Steen R, McNulty N, Thompson LR, Chisholm SW (2009) Choreography of the transcriptome, photophysiology, and cell cycle of a minimal photoautotroph, *Prochlorococcus*. PloS ONE 4:e5135. https://doi.org/10.1371/journal.pone.0005135

Zouni A, Witt HT, Kern J, Fromme P, Krauss N, Saenger W, Orth P (2001) Crystal structure of photosystem II from *Synechococcus elongatus* at 3.8 angstrom resolution. Nature 409:739–743. https://doi.org/10.1038/35055589

Affiliations

Frédéric Partensky[1,2] · **Daniella Mella-Flores[1,2,3,4]** · **Christophe Six[1,2]** · **Laurence Garczarek[1,2]** · **Mirjam Czjzek[1,5]** · **Dominique Marie[1,2]** · **Eva Kotabová[6]** · **Kristina Felcmanová[6,7]** · **Ondřej Prášil[6,7]**

[1] Sorbonne Université, Station Biologique, CS 90074, 29688 Roscoff cedex, France

[2] CNRS UMR 7144, Station Biologique, CS 90074, 29680 Roscoff, France

[3] Facultad de Ciencias Biológicas, Pontificia Universidad Católica de Chile, Santiago, Chile

[4] Center of Applied Ecology and Sustainability (CAPES-UC), Pontificia Universidad Católica de Chile, Santiago, Chile

[5] CNRS UMR 8227, Marine Glycobiology Group, Station Biologique, CS 90074, 29680 Roscoff, France

[6] Laboratory of Photosynthesis, Institute of Microbiology, MBU AVČR, Opatovický mlýn, 37981 Třeboň, Czech Republic

[7] Faculty of Sciences, University of South Bohemia, Branišovská, 37005 České Budějovice, Czech Republic
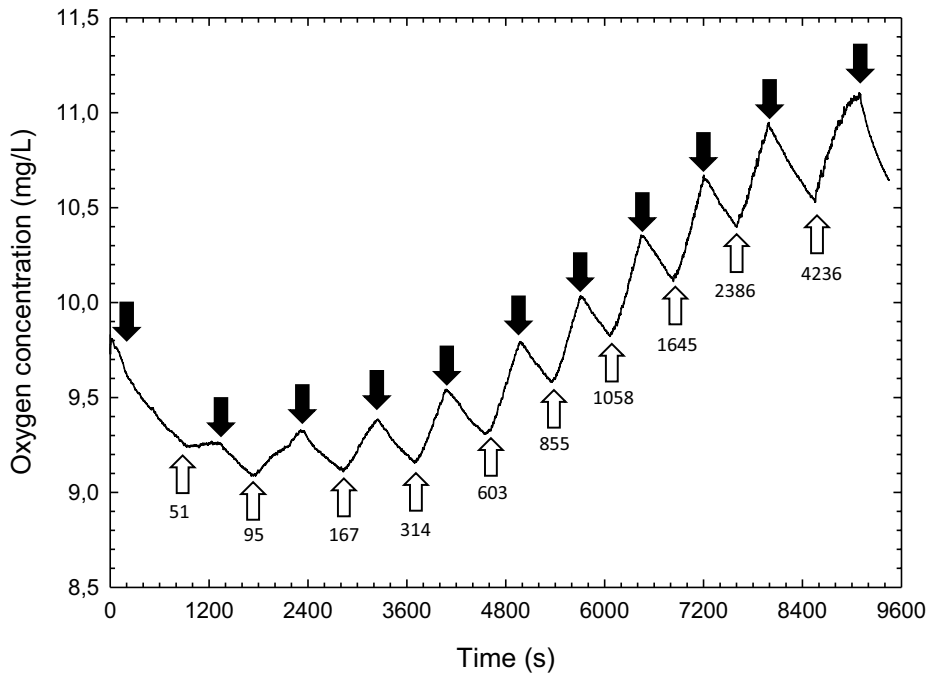
Online resource Fig. S1. An example of oxygen evolution time course. The example shown corresponds to measurements made on a concentrated *Prochlorococcus* sp. MIT9313 culture acclimated to ML. White arrows indicate times at which the light source was switched on, with the corresponding irradiance values in µmol photons m^{-2} s^{-1}, whereas dark arrows correspond to switch off times.
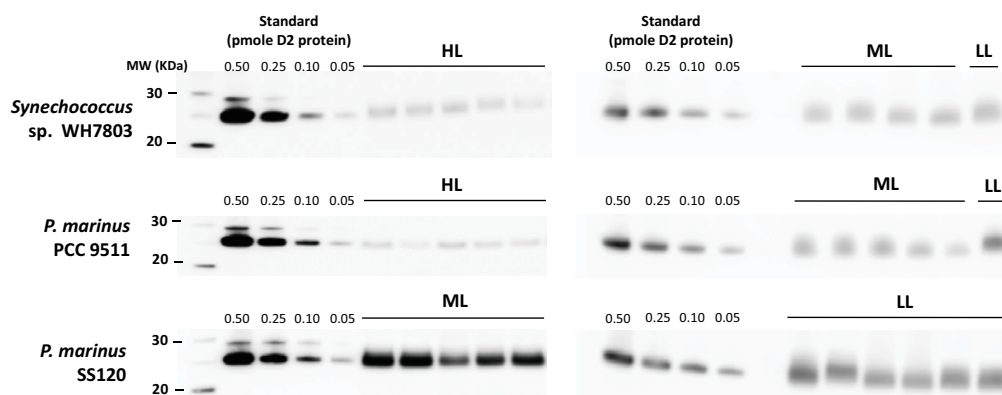
Figure S2: Some examples of quantitative immunoblots against the D2 core protein of PSII for three of the studied marine picocyanobacterial strains, grown at different irradiances (LL, ML and/or HL). The first lane corresponds to the molecular weight (MW) marker. A standard curve of recombinant D2 protein was loaded along with each sample series. Each sample lane was loaded with 2 or 3 µg total protein, as measured using a bovine serum albumin standard. Black lines indicate different replicates of the same strain and light condition (for WH7803 and PCC 9511 at ML, one representative LL sample was loaded as a control).
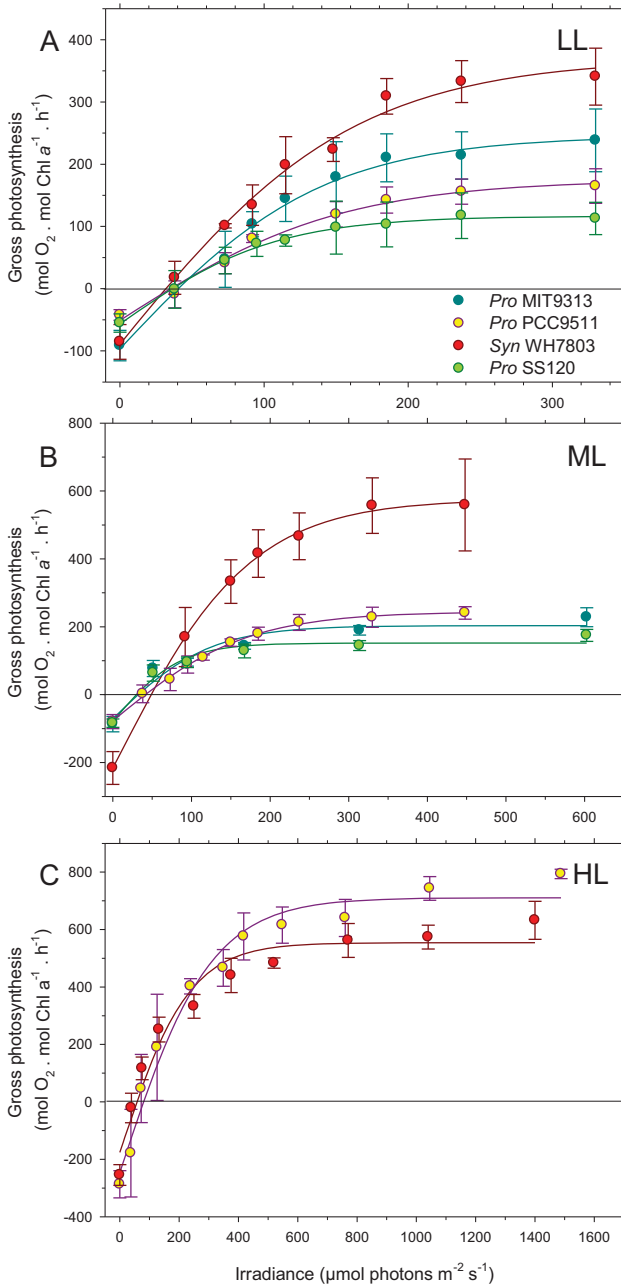
Fig. S3. Light response curves of oxygen evolution for different picocyanobacteria strains normalized per Chl *a* only for *Synechococcus* sp. WH7803 and DV-Chl *a* for *Prochlorococcus* strains MED4, SS120 and MIT9313.
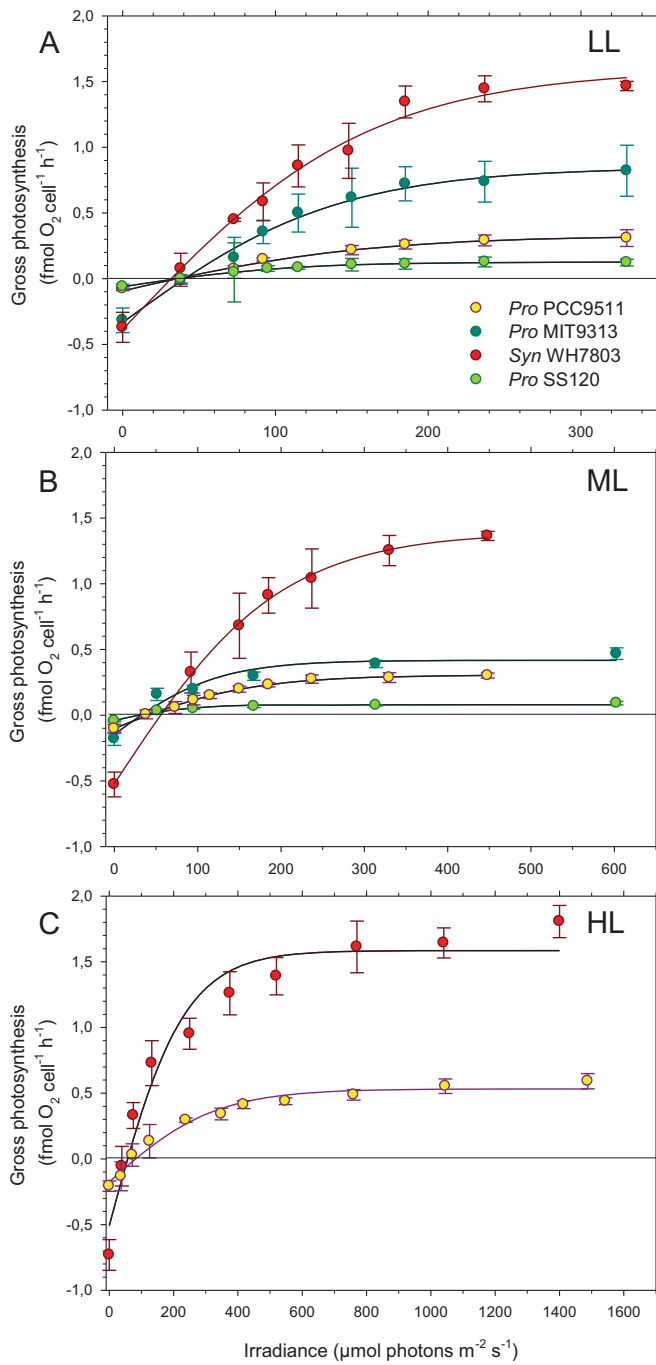
Fig. S4. Same as Fig. S3 but normalized per cell.
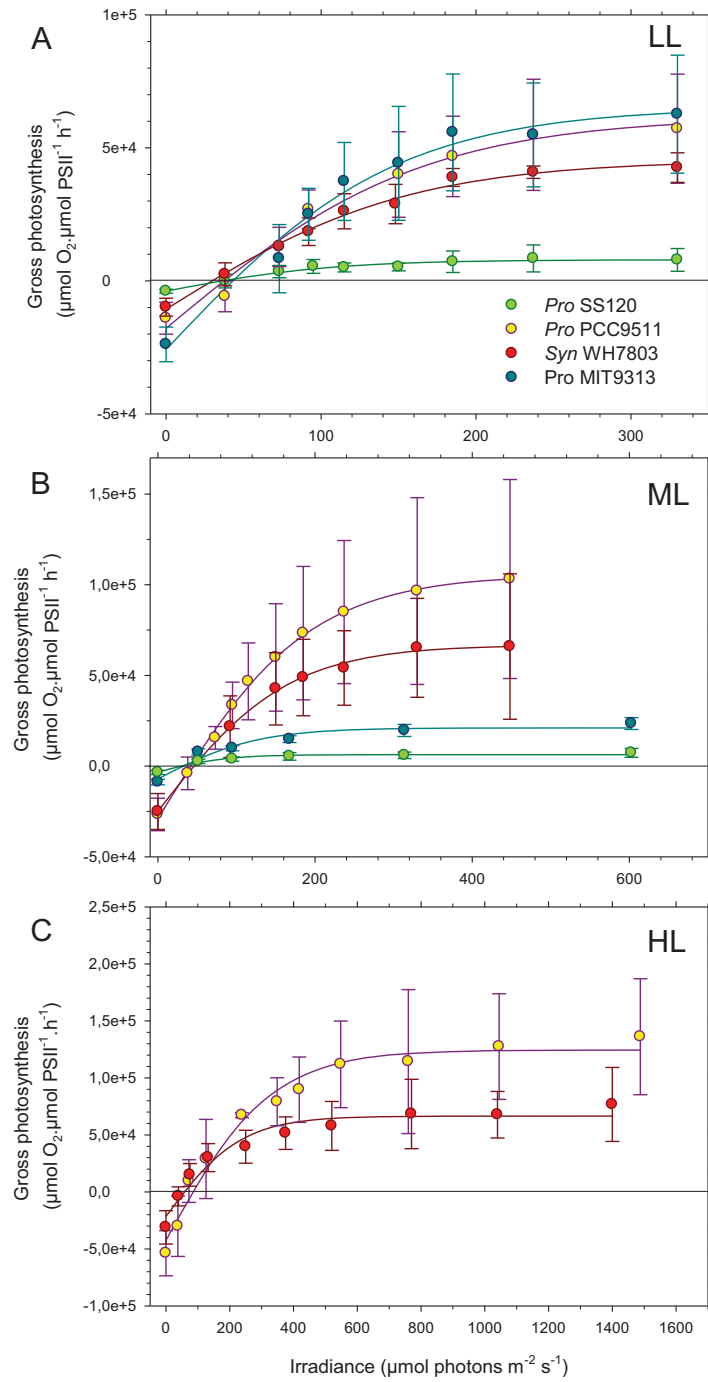
Fig. S5. Same as Fig. S3 but normalized per PSII, as assessed by immunochemical analyses of the D2 protein.
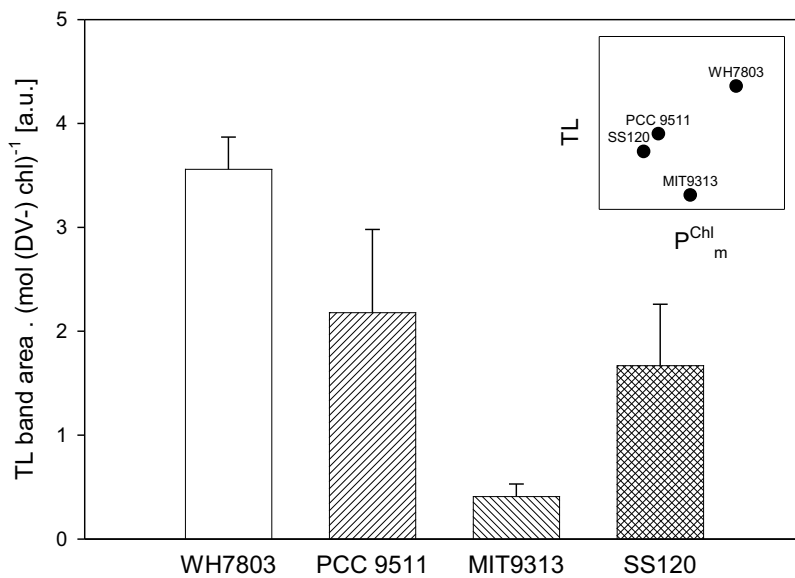
Fig. S6. Intensity of the B-band normalized to (DV-)Chl.
Error bars indicate standard deviation (n>3). Insert graph plots the pigment-normalized TL data against the P^{Chl}_m data from Fig. 1*A*. Scales of the insert axes are: P^{Chl}_m from $0 - 500$ mol O_2 / mol (DV-) Chl *a*; TL from $0 - 5$ arbitrary units (TL area / mol (DV-) Chl *a*).

Fig. S7. Amino acid alignments of the PSII subunit PsbM for a selected set of cyanobacteria.

Genus_Strain_Clade	Sequences
Pro_MED4_HLI	METTNFGFVASLLFVGIPTIFLIGLFISTQDGEKSSFYSDSSKGKLGPKR#--
Pro_MIT9515_HLI	METTNFGFVASLLFVGVPTIFLIGLFISTQDGEKSSFYSDSGKGKLGPKR#--
Pro_AS9601_HLII	METTNFGFVASLLFVGVPTIFLIGLFISTQDGEKSSFYSDSSKGRLGPKR*--
Pro_MIT9107_HLII	METTNFGFLASLLFVGVPTIFLIGLFISTQDGEKSSFYSDSSKGKLGPKG#--
Pro_MIT9123_HLII	METTNFGFLASLLFVGVPTIFLIGLFISTQDGEKSSFYSDSSKGKLGPKG#--
Pro_MIT9201_HLII	METTNFGFVASLLFVGVPTIFLIGLFLSTQEGEKSSFYSDSGKGKLDPKR#--
Pro_MIT9215_HLII	METTNFGFVASLLFVGVPTIFLIGLFLSTQEGEKSSFYSDSGKGKLDPKR#--
Pro_MIT9301_HLII	METTNFGFVASLLFVGVPTIFLIGLFISTQDGEKSSFYSDSSKGRLGPKR#--
Pro_MIT9311_HLII	METTNFGFIASLLFVGVPTIFLIGLFISTQDGEKSSFFSDSSKGKLGPKR#--
Pro_MIT9312_HLII	METTNFGFIASLLFVGVPTIFLIGLFISTQDGEKSSFFSDSSKGKLGPKR#--
Pro_MIT0801_LLI	METTSFGFAASLLFVGVPTIFLIGLFVSTSDGEKSSFYSDTSKGRLSPEPKK#
Pro_NATL1A_LLI	METTSFGFAASLLFVGVPTIFLIGLFVSTSDGEKSSFYSDTSKGRLSPEPKK*
Pro_NATL2A_LLI	METTSFGFAASLLFVGVPTIFLIGLFVSTSDGEKSSFYSDTSKGRLSPEPKK*
Pro_SS120_LLII	METTNFGFIISLLFVGIPTIFLVGLYISTSDGEKSSFFSDSSKGKLGPKS#--
Pro_MIT0602_LLII	METTNFGFIISLLFVGVPTIFLVGLYISTNDGEKSSFFSDSGKGKLGPKN#--
Pro_MIT0603_LLII	METTNFGFIISLLFVGVPTIFLVGLYISTNDGEKSSFFSDSGKGKLGPKN#--
Pro_MIT0601_LLIII	METTNFGFIASLLFVGVPTIFLIGLFISTSDGEKSSFFSDSGKGKLGPK#---
Pro_MIT9211_LLIII	METTNFGFIISFLFVGIPTIFLIGLYISTSDGEKSSFFSDSGKGKLGPK#---
Pro_MIT0701_LLIV	MPVNNFGFLATLLFVAVPMLFLIGLYIQTNSNKS*-------------------
Pro_MIT9303_LLIV	MPVNNFGFLATLLFVAVPMLFLIGLYIQTNSNKS*-------------------
Pro_MIT9313_LLIV	MPVNNFGFLATLLFVAVPMLFLIGLYIQTNSNKS*-------------------
Syn_CC9311_Ia	METNDLGFVASLLFVLVPTVFLIVLFIQTNSREGSS*----------------
Syn_WH8016_Ib	METNDLGFVASLMFVLVPTVFLIVLFIQTNSREGSS*----------------
Syn_WH8109_IIa	METNDLGFVASLLFILVPAIFLIVLYIGTQNNEA*------------------
Syn_CC9605_IIc	METNDLGFVASLMFILVPAIFLIVLYIGTQNNEA*------------------
Syn_WH8102_IIIa	METNDLGFVASLLFILVPAIFLIVLYIGTNRSES*------------------
Syn_CC9902_IVa	METNDLGFVASLMFILVPAIFLIVLYIGTNRSEA*------------------
Syn_BL107_IVa	METNDLGFVASLMFILVPAIFLIVLYIGTNRSEA*------------------
Syn_WH7803_V	METNDLGFVASLLFVLVPTVFLIILYIQTNSKEG*------------------
Syn_WH7805_VIa	METNDLGFVASLLFVLVPTVFLIILFIQTNSREG*------------------
Syn_RS9917_VIII	METNDLGFVASLLFVLVPTVFLIILFIQTNSRQS*------------------
Syn_RS9916_IX	METNDLGFVASLLFVLVPTIFLLILYIQTNSRQG*------------------
Syn_CB0101_5.2A	METNDLGFVASLMFVLVPTVFLLVLYIQTSSRQG*------------------
Syn_CB0205_5.2A	METNDLGFVASLMFVLVPTVFLIVLYIQTSSRQS*------------------
Syn_WH5701_5.2B	METNDLGFVASLMFVLVPAVFLIVLYIQTSSREQG#-----------------
Cya_PCC6307_5.2B	METNDLGFVASLMFVLVPAIFLIILYIQTNSRQGG*-----------------
Cya_PCC7001_5.2B	METNDLGFVASLMFVLVPTVFLLVLYIQTSSRQRG*-----------------
Syn_RCC307_5.3	METNDLGFVATLLFVLVPAIFLIILYIQTNSREG*------------------
ThermoSyn_BP-1	MEVNQLGLIATALFVLVPSVFLIILYVQTESQQKS------------------

Blue case: strain used in the present study
Red case: conserved residue in all marine picocyanobacterial sequences
Orange case: residue with similar properties in all marine picocyanobacterial sequences (hydrophic, polar or small)
Black case: Residue present in only a subset of sequences or having a different property (hydrophic, polar or small) in different sequences

105

Fig. S8. Same as Fig. S7 but for the PSII subunit PsbX

Blue case: strain used in the present study
Red case: conserved residue in all marine picocyanobacterial sequences
Orange case: residue with similar properties in all marine picocyanobacterial sequences (hydrophic, polar or small)
Black case: Residue present in only a subset of sequences or having a different property (hydrophic, polar or small) in different sequences.

Online resource Table S1: Primers used for qPCR analyses.

Forward primer					Reverse primer					Amplicon				
Primer name	Length (nt)	Tm (°C)	%GC	Primer sequence	Primer name	Length (nt)	Tm (°C)	%GC	Primer sequence	Length (nt)	Tm (°C)	%GC	Ta (°C)	Penalty
psbO_MED4_423F	26	59	35	TTCTGCAAAAGATTTAACAGCTGATC	psbOMED4_500R	24	59	50	GGTGTGAATGTAGCACCACTGACT	78	78	46	58	150.0
psbO_MIT9313_55F	19	59	58	TCTGCCCCAAGCAGTTGTGT	psbO_MIT9313_119R	21	59	48	CCAACAACGAAAATCGCTATCG	65	84	60	62	77.0
psbO_SS120_19F	20	58	55	CTAGCCCTGGTGCTTGCTTT	psbO_SS120_95R	21	58	48	TTACCTCTTTCTCCGGATGCA	77	80	51	59	136.0
psbO_WH7803_99F	22	61	50	CACTTAGGAGGACATCCGGAAT	psbO_WH7803_164R	18	60	61	CGAGCCGAATCCGAAAGG	66	82	55	61	84.0
psbU_MIT9313_171F	17	58	59	CGGCATGTTCCCAACCA	psbU_MIT9313_236F	20	59	55	GCATCACTCACGCTGGCATA	66	81	53	60	83.0
psbU_WH7803_127F	18	59	56	CGCGGCGGACAAAGTTGAT	psbU_WH7803_186R	18	60	56	CCCGGGAAATTGCTGGGAA	60	83	57	61	54.0
psbV_MIT9313_381F	20	59	55	CATCAGCAGCAGCGGATGTCT	psbV_MIT9313_445R	20	60	55	CGATTAGGGCGCAGGTCTTCA	65	82	55	60	75.0
psbV_WH7803_144F	20	60	60	AGGCAGTCCCGTCACCTTCT	psbV_WH7803_213R	17	59	65	GCCGCAGCTGGTGTTGA	70	85	61	62	103.0

Online resource Table S2: Comparison of PSII-related genes of the four picocyanobacterial strains used in the present study and list of genes included in the MED4 PSII homology model. X, present; 0, absent; n.a., not applicable.

Cyanorak Cluster Nb	Gene Name	Product	*Synechococcus* sp. WH7803	*Prochlorococcus* sp. MIT9313	*P. marinus* SS120	*P. marinus* MED4	MED4 PSII homology model
CK_00008058	psbA1	PSII protein D1.1	1	2	1	1	X
CK_00000009	psbA2	PSII protein D1.2	3	0	0	0	n.a.
CK_00000570	psbB	PSII chlorophyll-binding protein CP47	1	1	1	1	X
CK_00001031	psbC	PSII CP43 protein	1	1	1	1	X
CK_00000042	psbD	PSII D2 protein	2	1	1	1	X
CK_00000271	psbE	cytochrome b559, alpha subunit	1	1	1	1	X
CK_00001665	psbF1	cytochrome b559, beta subunit	1	1	1	1	X
CK_00033163	psbF2	cytochrome b559, beta subunit homolog	0	0	1	0	n.a.
CK_00000463	psbH	PSII reaction center protein PsbH	1	1	1	1	X
CK_00001317	psbI	PSII reaction center protein PsbI	1	1	1	1	X
CK_00000272	psbJ	PSII reaction center protein PsbJ	1	1	1	1	X
CK_00000252	psbK	PSII reaction center protein PsbK	1	1	1	1	X
CK_00001331	psbL	PSII reaction center protein PsbL	1	1	1	1	X
CK_00002551	psbM	PSII reaction center protein PsbM	1	1	1	1	X
CK_00000480	psbO	PSII manganese-stabilizing protein PsbO	1	1	1	1	X
CK_00000750	cyanoP	PSII protein CyanoP	1	1	1	1	Not in the model
CK_00001550	cyanoQ	PSII protein CyanoQ	1	0	0	0	n.a.
CK_00003852	psbT	PSII reaction center T protein	1	1	1	1	X
CK_00001319	psbU	PSII 12 kDa extrinsic PsbU protein	1	1	0	0	n.a.
CK_00001520	psbV	cytochrome c-550	1	1	0	0	n.a.
CK_00002061	psbX	PSII PsbX protein	1	1	1	1	X
CK_00001996	psbY	PSII PsbY protein	1	1	1	1	X
CK_00001549	psbZ (ycf9)	PSII protein PsbZ	1	1	1	1	X
CK_00000651	psb27	PSII manganese cluster assembly protein Psb27	1	1	1	1	Not in the model
CK_00000907	psb28	PSII reaction centre Psb28 protein	1	1	1	1	Not in the model
CK_00000802	psb29	PSII biogenesis protein Psb29	1	1	1	1	Not in the model
CK_00002206	psb30 (ycf12)	PSII biogenesis protein Psb30	1	1	1	1	X
CK_00001466	psb32	membrane protein involved in the photoprotection of PSII	1	1	0	0	n.a.
CK_00000270	ycf48	PSII stability/assembly factor	1	1	1	1	Not in the model

NB: *psbN* is not listed here since according to Guskov et al. (2009) PsbN is not a PSII protein.

Online resource Table S3. List of proteins from *Prochlorococcus marinus* MED4 that are either specific of *Prochlorococcus* strains with streamlined genomes (i.e. member of clades HL and LLI) or specific of the sole HL-adapted strains (i.e. member of clades HL and HLII).

Specificity	locus tag name	Gene name	Product	Predicted TM helices (Phobius and/or TMHMM)	Predicted signal peptide (SignalP)*	Gene cds in cluster	Protein sequence in cluster representative MED4

PAPER III (Manuscript in preparation)

Carbon metabolism differ in low-light and high-light ecotypes of
Prochlorococcus marinus

Felcmanová K., Lukeš M., Kotabová E., Halsey K. H. and Prášil O.
(2018)

Carbon metabolism differs in low-light and high-light ecotypes of *Prochlorococcus marinus*

Kristina Felcmanová[1,2], Martin Lukeš[1,2], Eva Kotabová[1], Kimberly H. Halsey[3] and Ondřej Prášil[1]

[1] Institute of Microbiology, Czech Academy of Sciences, v. v. i., Novohradská 237, Třeboň 37981, Czech Republic
[2] Department of Experimental Plant Biology, Faculty of Science, University of South Bohemia, Branišovská 31, České Budějovice 37005, Czech Republic
[3] Department of Microbiology, Oregon State University, Nash Hall, Corvallis, OR 97330, USA

ABSTRACT

Prochlorococcus marinus is very important oceanic cyanobacterium living in the oligotrophic regions of oceans contributing up to 50% to the total primary productivity. We investigated photo-physiology and dynamics of newly fixed carbon in steady state cultures of low-light adapted strain *P. marinus* MIT9313 growing under three nitrogen-limited growth rates. We monitored Photosystem II characteristics, including the maximal and effective photochemical efficiency of PSII, the functional absorption cross section and changes in DV-Chl *a* concentrations. To assess gross and net carbon primary production and to follow the carbon utilization within the cell, the carbon assimilation was measured continuously over 24 h.

Increasing nitrogen limitation caused decrease in amount of DV-Chl *a*, reduction of the proportional size of PSII and reduction of the protein pool. However, the maximal and effective photochemical efficiency of PSII as well as Chl-specific net and gross carbon primary production remained unaffected. Approximately, 28% of newly fixed carbon was retained in the biomass across all growth rates.

Our results were compared to those known for physiologically and genetically distinct HL adapted strain PCC 9511. Taken these models together, we observed similar patterns in the adaptation of PSII and in biomass composition with increasing nitrogen limitation. Although the Chl-specific net and gross carbon primary production were not affected by N limitation, the amount of newly fixed carbon by Rubisco as well as amount of carbon retained in biomass were significantly higher in LL adapted strain. Moreover, we found that time-dependent catabolism of newly fixed carbon significantly differ suggesting that cell needs to cover ATP demands.

Generally, from changes in the light-harvesting systems together with well-adapted genome and with possible role of mixotrophy we concluded that LL strain MIT9313 might be more efficient in converting of light energy into biomass.

INTRODUCTION

The marine cyanobacterium *Prochlorococcus marinus* is the most abundant photosynthetic organism in oligotrophic waters in tropical and subtropical regions. The success of *P. marinus* includes its genomic plasticity that has evolved through expansion of its habitat from the surface to 200 m (Partensky and Garczarek 2010). In general, *P. marinus* strains can be divided into two physiologically and genetically distinct groups. Low light (LL) ecotypes are strains inhabiting the deep euphotic zone with relatively high nutrient conditions and where light levels are only 0.1 % of surface irradiance. High light (HL) ecotypes thrive in the higher irradiances of the upper euphotic layer that are also characterized by low nutrient concentrations (Moore et al. 1998, Moore and Chisholm 1999). However, within these two major groups is a high degree of diversity, which has evolved as a consequence of selection pressures resulted in niche-partitioning of *Prochlorococcus* populations in the water-column. According to the phylogenetic studies based on the

sequences of 16S-23S rRNA internal transcribed spacer (ITS), new clades evolved within HL group (six clades HLI-HLVI) and LL group (seven clades LLI-LLVII) (Rocap et al. 2002, Johnson et al. 2006, Huang et al. 2012, Malmstrom et al. 2013, Biller et al. 2015). Most recent studies focused on fundamental differences in diversity and genomic structure of *Prochlorococcus* populations using metagenome and pan-genome approaches (Kent et al. 2016, Kashtan et al. 2017, Delmont and Eren 2018). Characteristics of the *Prochlorococcus* genome revealed distinct differences in chromosome size and number of genes which is a result of gene loss through the evolution. In general, LL strains represented by MIT9313 strain and placed on the base of *Prochlorococcus* radiation, exhibited larger genome and high GC content (50%) in comparison to more recently evolved HL strains represented by MED4 (=PCC 9511) (Rocap et al. 2003, Ting et al. 2009, Biller et al. 2015).

Prochlorococcus marinus strain MIT9313 used in this study is the representative of the LLIV ecotype and it is one of the most early-branching strains among the cultured members of the *Prochlorococcus* genus (Biller et al. 2015). Studies on the three-dimensional architecture revealed that the structure of the intracytoplasmic membranes, where PSII is located, differs significantly from MED4. The bands of internal membranes are tightly appressed to one another in regions along the cell sides (Ting et al. 2007).

Comparative analysis of polypeptides that constitute light-harvesting systems and their genomic analysis revealed significant differences in photosynthetic apparatus (Ting et al. 2009). Integral membrane proteins Pcb that bind photosynthetic pigments, are encoded by two to eight genes in LL strains (two genes *pcbA* and *pcbD* in MIT9313) whereas HL strains (MED4) possess only single *pcbA* gene (highly conserved among strains). Core and extrinsic proteins which form photosystem II reaction center also distinctly varies in number of encoded genes. Core proteins PsbA and PsbD possess two and one copy of gene, respectively. Genes encoding extrinsic proteins associated with oxygen-evolving complex, PsbO and PsbP, were identified in all *Prochlorococcus* strains.

Interestingly, in MIT9313 additional proteins PsbU and PsbV were found. It was shown that these proteins play an important role in PSII stability, in protecting of PSII against photo-damage, against dark inactivation and oxidative stress (Inoue-Kashino et al. 2005, Veerman et al. 2005, Balint et al. 2006, Enami et al. 2008). LL strains inhabit deep euphotic waters with low irradiance levels, thus it was suggested that multiplication of genes involved in light harvesting is a key factor enabling those strains to thrive in these conditions (Garczarek et al. 2000).

According to the comparative analysis in study by Ting et al. 2014, genomic organization securing the mechanism of carbon uptake and the carbon concentration mechanism are relatively similar among *Prochlorococcus* strains. Strain MIT9313 possess RubisCO form IA, however it was found that it has the highest K_{CO_2} value (gas transfer coefficient of CO_2) reported for this RubisCO type so far (Scott et al. 2007). Moreover, genome possess a gene encoding an additional carboxysome shell protein (CsoS1-2). These two important factors might lead to the optimization of carboxysome-associated processes (Ting et al. 2007, 2014).

Deep euphotic waters are rich to various N sources in comparison to upper layers where only ammonium is present and also are rich to higher concentration of nutrients. Thus, MIT9313 possess genes enabling assimilation not only ammonium but also nitrite, urea, amino acids and oligopeptides (Rocap et al. 2003, García-Fernandéz 2004). Moreover, it was previously shown that *Prochlorococcus* can take up the glucose due to the transporter Pro1404 (Gomez-Baena et al. 2008, Muñoz-Marín et al. 2013). It was revealed that gene for this transporter newly known as *glcH* (high affinity glucose transporter) is present in the genome and highly conserved among *Prochlorococcus* strains (Muñoz-Marín et al. 2017). However, Yelton et al. 2016 proved that number and type of transporters for organic compounds differ among strains. Mixotrophy genes are more abundant in LL strains in comparison to HL strains where only one single glucose transporter gene was found. It was proven that cell take up the glucose every time when glucose is present in the environment but this

ability allow to *Prochlorococcus* to survive at very low metabolic rates (Gómez-Baena et al. 2008). It is suggested that glucose uptake mechanism is a primary active transport. Thus, the capability of mixotrophy might be an important feature because the energetic cost of glucose transport is lower than the glucose biosynthesis (Muñoz-Marín et al. 2017).

With cell abundances up to 10^5 cells per ml in oligotrophic areas (Partensky et al. 1999), *P. marinus* is a significant contributor to primary production (Goericke and Welschhmayer 1993, Liu et al. 1997). It is estimated that *P. marinus* can account up to 48 % of total net primary production in the equatorial Pacific Ocean making it crucial participant to the global carbon cycle (Vaulot et al. 1995).

Quantifying aquatic net primary production (NPP) remains challenging. Commonly, chlorophyll-specific rates of oxygen evolution or carbon fixation are used to derive NPP from ocean colour satellite retrievals. These methods rely on fundamental understanding of the processes that influence intracellular chlorophyll, total pigment or light absorption. For example, phytoplankton differentially adjust their pigment concentration depending on whether nutrients or light is the limiting resource, and these behaviours can significantly impact NPP estimates (Siegel et al. 2013).

Gross carbon production is the rate of CO_2 fixed by photoautrophs. Some of this carbon is used to fuel biosynthesis, some is respired back to CO_2, and the remainder is retained in biomass. This final quantity is NPP. In most studies to date, carbon metabolism varies dramatically depending on nutrient or light limited growth rate (Halsey and Jones, 2015; Fisher and Halsey, 2016, Felcmanová et al. 2017). Quantifying the relative partitioning of carbon into these different processes has improved interpretations of data collected in the laboratory and at sea.

To quantify net and gross primary production, Chl-specific ^{14}C-based production measurements are commonly used. However, these measurements vary depending on growth rate and incubation duration (Pei and Laws 2013). This variability is caused by the lifetime of newly fixed carbon which is affected by the organism's growth rate that is

dependent on nutrient or light availability. Such conditions can activate different metabolic pathways for carbon utilization (Halsey et al. 2011).

We have recently described the photosynthetic energy budget of HL adapted *P. marinus* strain PCC 9511 (Felcmanová et al. 2017). Continuous cultures grown in three steady-state N-limited specific growth rates exhibited similar gross and net carbon primary production. Moreover, this strain expressed patterns of photosynthetic energy allocation that were previously determined in eukaryotic algae (Halsey et al. 2013, 2014). However, it was suggested that cyanobacteria under nitrogen-limited growth might be less efficient in converting photosynthetic energy into biomass in comparison to eukaryotic algae (Felcmanová et al. 2017).

To extend our knowledge about utilization of photosynthetic energy and carbon metabolism in two evolutionary distinct *Prochlorococcus* strains, we examined in this study the influence of N-limited growth of LL adapted *P. marinus* strain MIT9313. We tested whether Chl-specific gross and net carbon primary production (GPC[b] and NPC[b], respectively) were affected by nitrogen-limitation in cells with different steady-state growth rates. We used ^{14}C-uptake measurements with varying incubation durations to assess GPC[b], NPC[b], and carbon turnover rates, fluorescence fluorometry to investigate Photosystem II characteristic (F_V/F_M, σ_{PSII}), and Fourier transform infrared spectroscopy to analyze the biochemical composition of *P. marinus* strain MIT9313 cultured in balanced growth at three different nitrogen conditions at saturating constant light. Similarly to *P. marinus* strain PCC 9511, Chl-specific GPC[b] and NPC[b] were independent of nitrogen-limited growth rate. However, the time-dependent catabolism of newly fixed carbon was significantly different between these two strains reflecting its rapid respiration and probable use for ATP regeneration in LL strain. Such different carbon processing could be result of higher demands for energy in the form of ATP which these LL ecotypes might needed. Obtained results provide key insights into the cell characteristics and to the efficiency of carbon conversion to the biomass between LL and HL adapted *Prochlorococcus* ecotypes.

METHODS

Experimental design

Prochlorococcus marinus strain MIT9313 was cultured in chemostat mode in artificial sea water PCR-S11 medium (Rippka et al. 2000) supplemented with $(NH_4)_2SO_4$ concentrations as described in Felcmanová et al. 2017 to achieve specific growth rates (μ) of 0.3, 0.2, and 0.15 d^{-1}, respectively. Cultures were maintained in steady-state by continuous flow of media through cultures for 10 to 15 generations to ensure full acclimation of cells prior to sampling (LaRoche et al. 2010). A 700 ml of each culture with defined specific growth rate was incubated in triplicate in 1-liter Erlenmeyer flasks, aerated and continuously illuminated by fluorescent tube at 20 µmol quanta $m^{-2} s^{-1}$ at 20°C. Culturing of MIT9313 strain at this irradiance at μ lower than 0.15 d^{-1} was not sustainable. This light intensity was set up experimentally, when we tested the optimal growth of culture and possible photoinhibition under different light conditions similarly as described in (Soitamo et al. 2017).

Growth measurements

To monitor growth of culture, daily measurements of intrinsic fluorescence (F_0) or DV-Chl *a* concentration were used. F_0 was measured using a fluorometer FL3000 (Photon System Instrument, Czech Republic) after 10 min of exposure of cells to darkness.

To assess amount of DV-Chl *a*, samples in triplicate were filtered onto 25 mm glass fibre filters with particle retention of 0.4 µm (MN GF 5, Macherey-Nagel, Germany). Filters were extracted in methanol and stored at -20°C for 24 h. The absorption spectra of the extracts were measured spectrophotometrically (spectrophotometer UV 500, ChromSpec, CZ) and DV-Chl *a* was quantified according to the equation for Chl *a* assessment in Porra (2006).

Elemental composition

To determine cellular carbon and nitrogen concentration, samples were filtered in triplicate onto pre-combusted (5 h at 550°C) MN GF 5 filters, wrapped in tin capsules and stored at -70°C until analysis with CN Elemental Analyzer vario MICRO cube (Elementar Analysensysteme GmbH, Germany) as described in Nelson and Sommers (1996).

Photosystem II Chl a fluorescence characteristics

Chl *a* fluorescence was measured using a custom-designed FL3500 fluorimeter (Photon Systems Instruments, Czech Republic). Culture samples were dark adapted for 10 min at 20°C. Then a series of 100 blue (463 nm) flashes of 1 µs duration was applied to induce single turnover of all RCII. Changes in fluorescence were then measured during sequential exposure to 11 different intensities (0-1023 µmol photons m^{-2} s^{-1}) of blue actinic light. The resulting fluorescence light curves were fitted to the model of Kolber et al. (1998) to derive the maximum and minimal fluorescence (F_M and F_0, respectively) and the effective PSII cross-section (σ_{PSII}). The maximum photochemical efficiency of PSII (F_V/F_M) was calculated as (F_M-F_0/F_M). The effective photochemical efficiency of PSII in actinic light (Φ_{PSII}) was determined as Fq'/F_M' where F_M' is the maximum fluorescence in light adapted state, and $Fq' = F_M'$-F' where F' is the steady-state fluorescence in the light (Kromkamp and Forster 2003).

Short-term ^{14}C uptake incubations

Inorganic ^{14}C (NaH^{14}CO$_3$, MP Biomedicals, CA, USA) with activity 5 µCi was added to 45 ml of culture, which was then aliquoted into scintillation vials (1 ml each), and incubated for 20 min at light intensities from 0.5 to 500 µmol quanta m^{-2} s^{-1} in a temperature controlled photosynthetron-type incubator to determine PE curves. After incubation, samples were acidified with 50 µl 1N HCl to remove excess ^{14}C-bicarbonate and degassed for 24h. To assess time zero activity, 3 times 1 ml of ^{14}C culture was kept in the dark for 20 min, then acidified and treated equal to the other samples. After 24 h degassing, EcoLite

scintillation cocktail (MP Biomedicals, CA, USA) was added to each sample to determine their radioactive decay using a Tri-Carb 2810 TR liquid scintillation analyzer (PerkinElmer, MA, USA). For total activity, three 50 µl of inoculated samples were added to vials containing 50 µl ethanolamine, 900 µl culture media and 5 ml of EcoLite scintillation cocktail and capped immediately and counted. PE curves were modeled according to nonlinear least-square regression by Jassby and Platt 1976 as described in Felcmanová et al. 2017. The light saturation point E_k (µmol quanta m^{-2} s^{-1}) was defined as

$$E_k = P^b_{max}/\alpha^b \qquad (1)$$

where P^b_{max} is the maximum Chl-specific C fixation rate [µmol C (mg DV-Chl *a* h)$^{-1}$] and α^b is the light-limited slope of the PE curve [µmol C (mg DV-Chl *a*)$^{-1}$ h^{-1} (µmol quanta m^{-2} s^{-1})$^{-1}$].

Time-dependence of ^{14}C uptake

A 100 ml aliquot of culture was transferred to a small sterile temperature controlled chemostat with same conditions as the stock chemostat, to follow ^{14}C uptake over 24 h. Bovine carbonic anhydrase (Sigma-Aldrich, St. Louis, MO, USA) with activity 5 U ml^{-1} and NaH^{14}CO$_3$ with activity 1 µCi ml^{-1} were added to the culture in 2 min interval. For another 2 minutes, sampling for ^{14}C uptake rate started and has continued regularly over 24h by taking 1.1 ml samples at each time point and transferring the sample to a 2 ml Eppendorf tube. Two 0.5 ml subsamples were transferred to scintillation vials, acidified and degassed. Moreover, two additional 50 µl samples were taken to determine the total remaining activity. After 24 h, 5 ml scintillation cocktail was added to each sample and measured using liquid scintillation counting.

Fourier transform infrared spectroscopy

A 30 ml of the cell suspension was spinned at 8000 x g for 10 minutes at 20°C to determine the cell macromolecular composition. Cells were washed twice with ammonium formate (28 g l^{-1}), re-suspended in 50 µl of

ammonium formate and spread on a Si 384 well plate (Bruker, Billerica, MA, USA). Samples were measured on a spectrometer Nicolet IS10 (Thermo Scientific, Waltham, MA, USA) equipped with a microarray reader and Deuterated Tri Glycine Sulphate detector. Absorbance spectra were collected in the spectral range from 400 cm^{-1} to 4000 cm^{-1} at a spectral resolution of 4 cm^{-1} and 64 scans were co-added and averaged. A Blackman-Harris three-term apodization function was used, with a zero-filling factor of two. Omnic software (Nicolet) was used for measurement and data processing. Spectra were normalized to the maximum of an amide I absorption band at 1645 cm^{-1} and absorption maxima of lipids (1735 cm^{-1}) to protein (amide I) and lipid to carbohydrate (1152 cm^{-1}) were used for comparison (Giordano et al. 2001).

Statistical analysis

Data were statistically analysed by One-way ANOVA analysis [Dunn's Method to detect significant differences ($p<0.05$)] and by nonlinear least-squares regressions using SigmaPlot 11 (Systat Software GmbH, Germany).

RESULTS

Growth and cell properties

Continuous cultures of *P. marinus* strain MIT9313 were grown under constant irradiance conditions (20 µmol quanta m^{-2} s^{-1}) to obtain the balanced growth. Chemostat cultures were maintained at specific growth rates ranging from 0.15 d^{-1} to 0.3 d^{-1}. Cultures with the maximal specific growth rate were considered to be nitrogen non-limited cultures. Interestingly, MIT9313 strain was not able to grow at µ which was lower than 0.15 d^{-1} under conditions described above. Specific growth rates we work with are comparable to growth rates reported in other previous experiments (Zorz et al. 2015, Kulk et al. 2011, Felcmanová et al. 2017) providing us the opportunity to study and to compare the effects of

nitrogen limitation on photosynthetic energy utilization between HL and LL strains of *P. marinus*.

The amount of DV-Chl *a* was comparable between cells growing at $\mu = 0.2$ d^{-1} and 0.15 d^{-1} and was significantly lower in comparison to nitrogen replete cells ($p < 0.05$) (Table 1). DV-Chl*a*:C and DV-Chl*a*:N showed decreasing trends with μ (Table 1). Elemental C/N ratio was significantly lower at $\mu = 0.3$ d^{-1} ($p < 0.05$).

Photosystem II Chl a fluorescence characteristics

Both the maximum and effective quantum yields of PSII photochemistry (F_V/F_M and $\Phi_{PSII} = F_q'/F_M'$, respectively) slightly decreased in the nitrogen limited cultures in comparison to N-replete culture (Table 2). The functional absorption cross sections of PSII (σ_{PSII}) was significantly lower in cultures growing at 0.15 d^{-1} and 0.2 d^{-1} ($p < 0.05$) (Table 2). However, the decrease in both quantum yields as well as in PSII antenna size was not linearly proportional to the nutrient-dependent decline in growth rate.

Short-term ^{14}C uptake incubations

From the fits of PE curves we determined the light-saturated rate of carbon fixation (P^b_{max}) and the light-limited slope (α). We also assess Chl-specific carbon fixation rate at the growth irradiance (P^b_{Eg} at 20 µmol quanta m^{-2} s^{-1}) to obtain information about how nutrient limitation influences carbon metabolism. Interestingly, all three parameters remained similar across all specific growth rates without any distinct trend line pointing out that the rate of photosynthesis in dependence on irradiance was not influenced by nitrogen limitation. Nevertheless, P^b_{Eg} decreased significantly, but not linearly in severely N limited cells ($p < 0.05$) (Table 3).

Time-dependence of ^{14}C uptake

To reveal the dependency of newly fixed carbon usage on nitrogen limitation, cultures inoculated with ^{14}C bicarbonate were monitored

continuously over 24 h. Our results show that carbon production measurements after isotope addition reflecting gross carbon primary production (GPC[b]) were similar across all three specific growth rates with an average 523 ± 36 µmol C (mg DV-Chl a h)$^{-1}$ (Fig. 1). Kinetics of Chl-specific ^{14}C-uptake rate decreased rapidly in time. In both slowly growing cultures, 50% of labeled carbon was catabolized in 4 min in comparison to cultures growing at 0.3 d^{-1}, where it took 10 min. Moreover, Chl-specific ^{14}C-uptake matched Chl-specific net carbon primary production (NPC[b]) in 4 min in cells growing at 0.15 d^{-1}, in 20 min in cells growing at 0.2 d^{-1} and in 60 min in cells growing at 0.3 d^{-1} pointing out that carbon was catabolized more rapidly with increasing N limitation (Fig. 2). However, after 24 h, NPC[b] did not vary with specific growth rate with an average 148 ± 17 µmol C (mg DV-Chl a h)$^{-1}$ suggesting that 72% of newly fixed carbon was catabolized to CO_2 (Fig. 1).

Fourier transform infrared spectroscopy

The semi-quantitative analysis of the macromolecular composition of cells revealed that in N replete cells, carbon was stored mainly in the protein pool (approx. 50% of NPC[b]). As the nitrogen limitation increased, protein pool in cells was significantly reduced ($p < 0.05$) and carbon storage was redirected to carbohydrates concurrently (Fig. 4). Thus, biomass in severely N limited cells contained mainly carbohydrates (approx. 65%). Interestingly, lipid pool changed very slightly ranging from 11% to 17%, but not linearly with N limitation as protein and carbohydrate pools.

DISCUSSION

This study investigated the effect of nitrogen limitation on cell physiology and photosynthetic energy use efficiency in LL adapted strain *P. marinus* MIT9313. Results demonstrated here provide us a novel knowledge about ongoing metabolic processes in cells of this most-early branching strain.

Together with results obtained for HL and recently evolved strain *P. marinus* PCC 9511 (Felcmanová et al. 2017), we can compare the carbon allocation strategy of these two genetically and physiologically distinct strains grown at steady-state and influenced by different nitrogen conditions.

Cells responded to the decreased nitrogen concentration with reducing amount of cellular DV-Chl *a*, photosynthetic pigment rich in nitrogen associated with reaction centers. This reduction was also reflected by decreasing DV-Chl *a*:C and DV-Chl *a*:N ratio (Table 1) (Halsey and Jones 2015). However, only the latter showed linearity with increasing N limitation (r^2 = 0.99). The non-linear relationship of DV-Chl *a*:C ratio was probably reflected by narrow range between N-limited specific growth rates (0.15 d^{-1} and 0.2 d^{-1}). Although the amount of nitrogen in medium of cells grown at 0.15 d^{-1} was half in comparison to cells grown at 0.2 d^{-1}, both cultures accumulated the same concentration of cellular DV-Chl *a* and similar amount of C (data not shown), which resulted in non-linear relationship with specific growth rate. Elemental C/N ratio increased markedly in cultures which were N-limited (Table 1) (Goldman et al. 1979). Besides smaller amount of DV-Chl *a*, nitrogen limitation strongly influenced also the size of protein pool (Fig. 4), which was accompanied by significantly reduced σ_{PSII} in N-limited slowly growing cells (Table 2). These key changes reflect adjustments of photosynthetic apparatus in response to nitrogen limitation in slowly growing acclimated cells as was observed in *P. marinus* strain PCC 9511 (Felcmanová et al. 2017). Although F_V/F_M and Φ_{PSII}, both slightly decreased across the N limitation (Table 2), the decline was very moderate pointing out that cells were in acclimated state (Parkhill et al.2001). Transient nitrogen deprivation usually leads to significant reduction of photochemical quantum yield as reported in Parkhill et al. 2001 and Lindell et al. 2002. Interestingly, basic parameters describing PE curves did not vary with increasing N-limitation (Table 3) which is in contrast to results known for HL strain PCC 9511 (Felcmanová et al. 2017). By comparing of these parameters with those obtained for PCC 9511, we can conclude that all

three cultures MIT9313 exhibited similar photo-physiology and carbon processing in 20 min as those cultures PCC 9511 growing at $\mu = 0.2$ d^{-1}. Newly fixed carbon through the Calvin cycle is considered to be gross carbon primary production. Metabolic pathways processing and influencing fate of carbon from the GPC^b in the cell differ according to the level of nutrient limitation (Jakob et al. 2007, Halsey et al. 2010, 2013, 2014) and among species with different antenna organization (Kunath et al. 2012, Palmucci et al. 2011). Carbon which is not used for catabolism and is stored in the biomass and used for building of structural macromolecules corresponds to net carbon primary production. We found that neither GPC^b nor NPC^b was influenced by N limitation (Fig. 1) which is consistent with previous results obtained in cyanobacterium *P. marinus* strain PCC 9511 (Felcmanová et al. 2017) and in eukaryotic algae (Halsey et al. 2014). NPC^b constituted 28% of GPC^b in MIT9313 which suggested that 72% of newly fixed carbon is used for transient carbon pool. As was shown previously, transient carbon pool is processed depending on the requirement of the cell (Halsey et al. 2013). Either it is used for ATP or NADP synthesis. However, both pathways differ in time course of transient carbon product utilization. Therefore, to reveal the fate of this carbon pool, P$^b_{Eg}$ was measured. Surprisingly, P$^b_{Eg}$ matched NPC^b values after 20 min of incubation in both slowly growing cultures reflecting that 72% of the newly fixed carbon was catabolized to CO_2 (Table 3, Fig. 1). Thus, newly fixed carbon was short-lived and used for ATP synthesis. On the other hand, in N replete culture, the consumption of the transient carbon pool took 60 min suggesting that newly fixed carbon was longer-lived (Fig. 1). However, the decline in kinetics describing the fate of the transient carbon pool was very sharp in N replete culture and was not linear among the N-limited cultures in comparison to results known for *P. marinus* strain PCC 9511 and for eukaryotic algae (Halsey et al. 2011, 2013). Taken the data for both *Prochlorococcus* strains together and related them to relative growth rates, faster respiration of CO_2 in MIT9313 strain is clearly visible (Fig. 2). In HL strain PCC 9511, P$^b_{Eg}$ decreased linearly with N limitation

pointing out that in N replete culture, long-lived transient carbon was used for synthesis of more energetic demanding compounds (i.e. proteins) (Felcmanová et al. 2017). When P^b_{Eg} was related to the relative growth rate for both LL and HL strain, we found that with higher relative growth rates the transient carbon pool is catabolized slower suggesting that if MIT9313 strain could grow faster, the relationship between P^b_{Eg} and specific growth rate might be similar as was observed at HL strain PCC 9511 (Fig. 3).

Cells grown at balanced growth influenced by different nutrient levels alter the carbon flux among major structural macromolecules resulting in changes in biomass composition (Goldman et al. 1979, Giordano et al. 2001). In *P. marinus* strain MIT9313, amount of carbon allocated in the carbohydrates considerably increased in both slower growing cells at the expense of protein pools, which was markedly reduced. Interestingly, lipid pool did not vary among treatments with approximately 15% of the NPC^b (Fig. 4). This pattern of carbon flux was similar to that observed in the strain PCC 9511 (Felcmanová et al. 2017). Generally, LL strain exhibited significantly larger carbohydrate pool in comparison to the HL strain which might be determined by the availability of energy in the form of ATP obtained by rapid utilization of transient carbon pool and also ATP obtained from glucose which was taken up by primary active transport (Gómez-Baena et al. 2008). Possible mixotrophy and reducing power obtained from glucose might also explain significantly higher content of lipids in LL strain in comparison to HL strain. When the protein: carbohydrates ratio was related to the relative growth rates, fairly linear pattern was revealed in the reallocation of carbon from protein to the carbohydrate pool from the lowest relative growth rate to the highest (Fig. 5).

This study reveals the changes in the photo-physiology of cells and basic processing of newly fixed carbon in cells of *P. marinus* strain MIT9313 under N limitation. We found that LL strain MIT9313 responded to N decrease similarly as physiologically and ecologically distinct HL strain PCC 9511; (i) in both strains changes in pigmentation and alteration of

light-harvesting system ensured maximal photosynthetic efficiency (ii) GPC^b and NPC^b did not vary across N limitation. However, GPC^b was distinctly higher in LL strain MIT9313 [523 ± 36 µmol C (DV-Chl a h)$^{-1}$] in comparison to the value for HL strain PCC 9511 [374 ± 21 µmol C (DV-Chl a h)$^{-1}$] (Felcmanová et al. 2017). Moreover, 28% of GPC^b was stored in the biomass compared to 20% in PCC 9511 and only 18% in M. aeruginosa (Kunath et al. 2012). Our data support our hypothesis about lower conversion of photosynthetic energy into biomass in cyanobacteria caused probably by sharing some of membrane components in photosynthetic and respiratory electron transport. Nevertheless, higher GPC^b and NPC^b, respectively, in MIT9313 could be related to the ecological niche, which this LL strain inhabits. Although, it thrives in the deep euphotic zone with low irradiance, the environment is relatively rich to nutrients and to different N sources that can be used for cell growth. Together with the multiplication of genes and number of unique genes which encoded more amount of proteins involved in light-harvesting systems together with special carboxyzome shell, give the LL ecotypes the ability utilize the low irradiance and available carbon very efficiently. Moreover, the capability of glucose uptake might be advantageous feature. It was shown that glucose taken up from environment could be used to obtain two molecules of ATP or twelve molecules of NADPH per glucose metabolized in LL ecotypes (Gómez-Baena et al. 2008). Interestingly, photosynthetic activity remained unchanged during glucose uptake, so it is hypothesized that this capacity for mixotrophy help to save metabolic energy (Muñoz-Marín et al. 2017). Thus, this ability together with changes on the level of light-harvesting and genome could be a key factors which might facilitate to store more carbon in the biomass in LL ecotypes in comparison to HL ecotype.

Table 1. Cell characteristics of steady-state nitrogen-limited cultures of *P. marinus* (n=4, ± standard deviations).

Variables	Growth rate (d^{-1})		
	0.15	**0.2**	**0.3**
DV-Chla (µg/ml)	0.5 (0.1)$^+$	0.5 (0.1)*	0.8 (0.1)$^{*+}$
DV-Chl*a*:C (x 10^{-2}) (µg/µg)	1.1 (0.4)$^+$	1.2 (0.3)*	2.9 (0.6)$^{*+}$
DV-Chl*a*:N (µg/µg)	0.09 (0.03)$^{*+}$	0.11 (0.02)$^+$	0.16 (0.02)*
C:N (µg/µg)	8.1 (0.3)	9.2 (0.4)*	6.7 (1.0)*

Statistically significant changes are indicated with asterisks and daggers (p < 0.05)

Table 2. Photophysiological fluorescence characteristics of steady-state nitrogen-limited *P. marinus* (n=4, ± standard deviations).

Variables	Growth rate (d^{-1})		
	0.15	**0.2**	**0.3**
F_V/F_M	0.63 (0.04)	0.65 (0.02)	0.71 (0.01)
Φ_{PSII} (Fq'/F$_M$')	0.36 (0.02)	0.39 (0.02)	0.44 (0.04)
σ_{PSII} (A^2 PSII^{-1})	254 (24)$^+$	254 (22)*	315 (27)$^{*+}$

Statistically significant changes are indicated with asterisks and daggers (p < 0.05)

Table 3. Variables describing PE curves measured in steady-state nitrogen-limited *P.marinus* (n=3, ± standard deviations).

	Growth rate (d^{-1})		
Variables	**0.15**	**0.2**	**0.3**
$P^b{}_{max}$ [μmol C (mg DV-Chl *a* h)$^{-1}$]	349 (35)	379 (14)	314 (12)
$P^b{}_{Eg}$ [μmol C (mg DV-Chl *a* h)$^{-1}$]	126 (25)	181 (34)	216 (6)
α^b [μmol C (mg DV-Chl *a*)$^{-1}$ h^{-1} (μmol quanta m^{-2} s^{-1})$^{-1}$]	7 (1.4)	11 (0.4)	8 (1.4)
E_k (μmol quanta m^{-2} s^{-1})	48 (0.01)	33 (0.01)	42 (0.01)
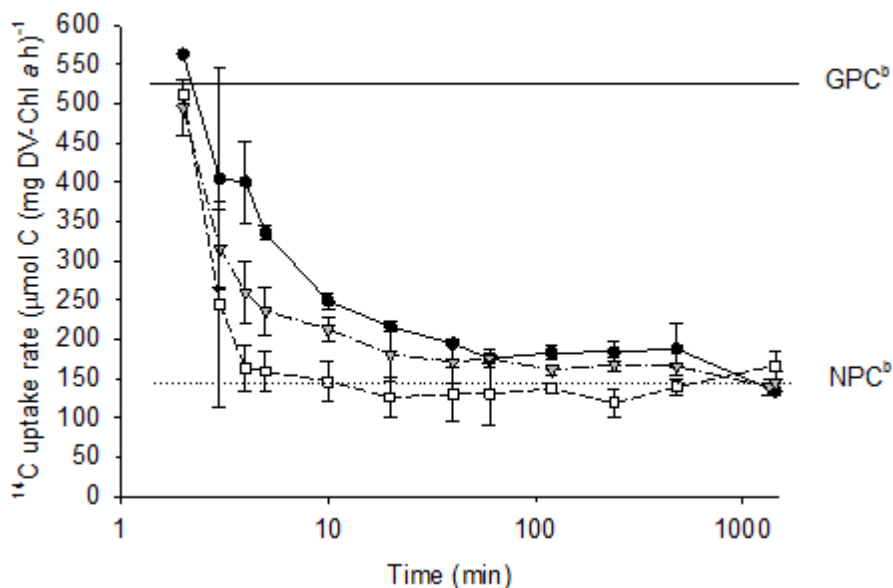
Fig. 1: Kinetics of carbon production based on ^{14}C-uptake measurements for cells growing at 0.3 day^{-1} (*filled circle* and *solid line*), 0.2 day^{-1} (*filled inverted triangle* and *dashed-dotted line*), and 0.1 day^{-1} (*open square* and *dashed line*). The decline in kinetics of ^{14}C-based production show growth-rate dependent utilization of newly fixed carbon. The *solid horizontal line* represents gross carbon primary production and the *dotted horizontal line* represents net carbon primary production. Each data point is the average of three measurements, error bars are standard deviations with n = 3 (where not visible, the error bars are smaller than the size of the symbol).
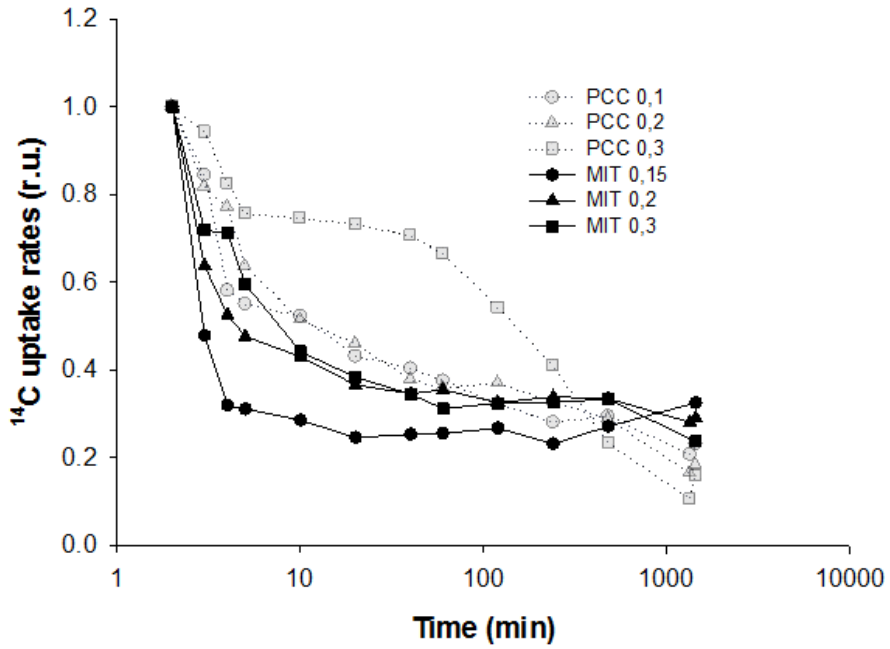
Fig. 2: The comparison of kinetics of ^{14}C-based production showing growth-rate dependent utilization of newly fixed carbon in HL strain PCC 9511 (*grey symbols* and *grey dotted lines*) and LL strain MIT9313 (*filled symbols* and *solid lines*) grown at three N-limited growth rates. Each data point is the average of three measurements, error bars were omitted for more visible data.
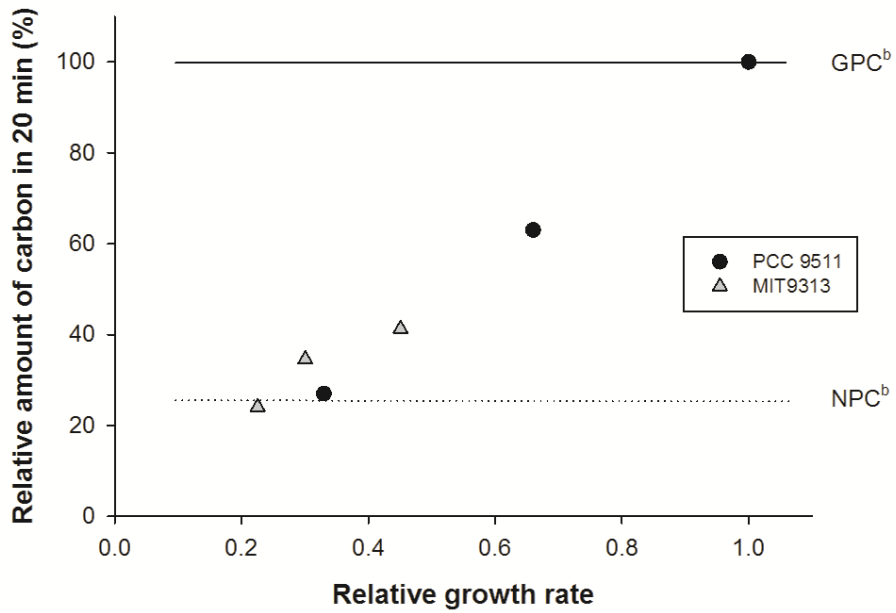
Fig. 3: Relative amount of newly fixed carbon in the form transient carbon pool during 20 min of incubation at the growth irradiance in HL strain PCC 9511 (*black circles*) and LL strain MIT9313 (*grey triangles*) depending on the relative growth rate.
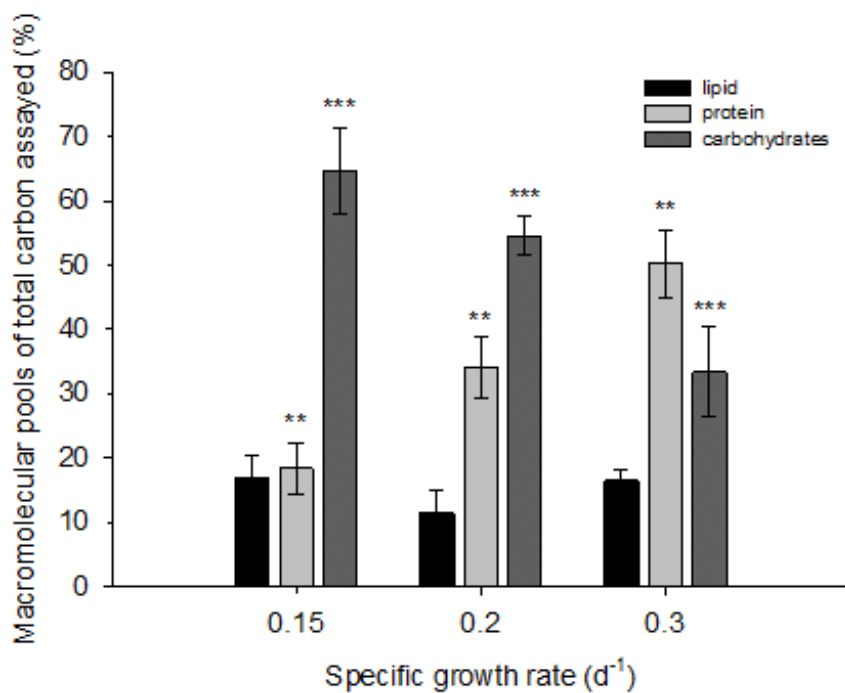
Fig. 4: Relative macromolecular biomass composition of steady-state *P. marinus* cultures determined by FTIR semi-quantitative analysis (n=3, ± standard deviations). Changes in protein (**) and carbohydrates (***) content were statistically significant in all three N-limited cultures (p < 0.05).
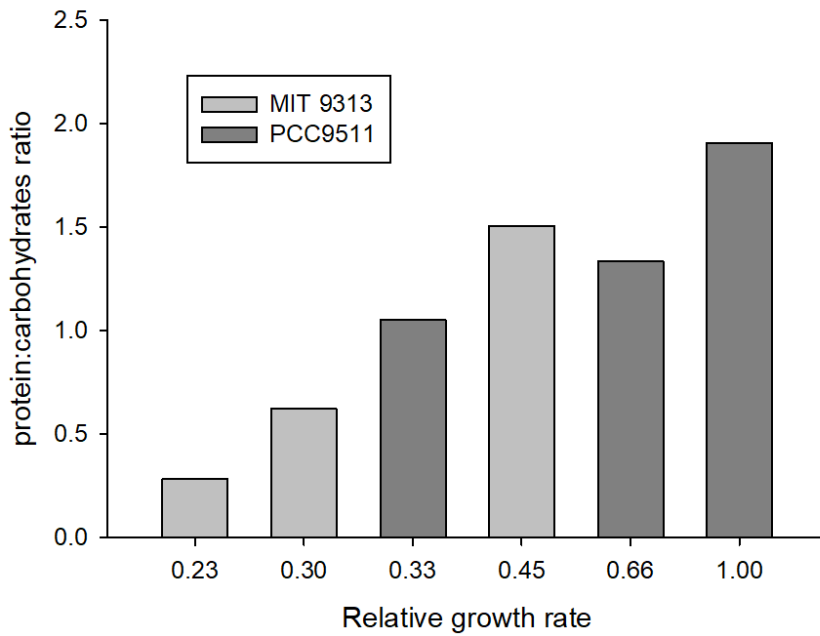
Fig. 5: The comparison of changes in protein: carbohydrates ratio in dependence on relative growth rate of HL strain PCC 9511 and LL strain MIT9313.

References

Balint I, Bhattacharya J, Perelman A, Schatz D, Moskovitz Y *et al*. (2006) Inactivation of the extrinsic subunit of photosystem II, PsbU, in *Synechococcus* PCC 7942 results in elevated resistance to oxidative stress. FEBS Letters 580: 2117-2122.

Biller SJ, Berube PM, Lindell D and Chisholm SW (2015) *Prochlorococcus*: The structure and function of collective diversity. Nature Reviews Microbiology 13: 13-27.

Delmont TO and Eren AM (2018) Linking pangenomes and metagenomes: the *Prochlorococcus* metapangenome. Peer J 6: e4320.

Enami I, Okumura A, Nagao R, Suzuki T, Iwai M *et al*. (2008) Structures and functions of the extrinsic proteins of photosystem II from different species. Photosynthesis Research 98: 349-363.

Felcmanová K, Lukeš M, Kotabová E, Lawrenz E, Halsey KH, Prášil O (2017) Carbon use efficiencies and allocation strategies in *Prochlorococcus marinus* strain PCC 9511 during nitrogen-limited growth. Photosynthesis Research 134: 71-82.

Fisher NL, Halsey KH (2016) Mechanisms that increase the growth efficiency of diatoms in low light. Photosynthesis Research 129: 183-197.

García-Férnandez JM, Tandeau de Marsac N and Diez J (2004) Streamlined regulation and gene loss as adaptive mechanisms in *Prochlorococcus* for optimized nitrogen utilization in oligotrophic environmnets. Microbiology and Molecular Biology Reviews 68: 630-638.

Garczarek L, Hess WR, Holtzendorff, van der Staay GWM and Partensky F (2000) Multiplication of antenna genes as a major adaptation to low light in a marine prokaryote. PNAS 97: 4098-4101.

Giordano M, Kansiz M, Heraud P, Beardall J, Wood B and McNaughton D (2001) Fourier transform infrared spectroscopy as a novel tool to investigate changes in intracellular macromolecular pools in the

marine microalga *Chaetoceros muellerii* (Bacillariophyceae). Journal of Phycology 37: 271-279

Goericke and Welschmeyer (1993) The marine prochlorophyte Prochlorococcus contributes significantly to phytoplankton biomass and primary production in the Sargasso Sea. Deep-Sea Research 40: 2283-2294.

Goldman JC and Peavey DG (1979) Steady-state growth and chemical composition of the marine Chlorophyte *Dunaliella tertiolecta* in nitrogen-limited continuous cultures. Applied and Environmnetal Microbiology 38: 894-901.

Gómez-Baena G, López-Lozano A, Gil-Martínez J, Lucena JM, Díez J *et al*. (2008) Glucose uptake and its effect on gene expression in *Prochlorococcus*. PlosOne 10: e3416.

Halsey KH and Jones B (2015) Phytoplankton strategies for photosynthetic energy allocation. Annual Review of Marine Science 7: 265-97.

Halsey KH, Milligan AJ, Behrenfeld MJ (2010) Physiological optimization underlies growth rate-independent chlorophyll-specific gross and net primary production. Photosynthesis Research 103: 125-137.

Halsey KH, Milligan AJ, Behrenfeld MJ (2011) Linking time-dependent carbon-fixation efficiencies in *Dunaliella tertiolecta* (Chlorophyceae) to underlying metabolic pathways. Journal of Phycology 47: 1-11.

Halsey KH, Milligan AJ, Behrenfeld MJ (2014) Contrasting strategies of photosynthetic energy utilization drive lifestyle strategies in ecologically important picoeukaryotes. Metabolites 4: 260-280.

Halsey KH, O'Malley RT, Graff JR, Milligan AJ and Behrenfeld MJ (2013) A common partitioning strategy for photosynthetic products in evolutionarily distinct phytoplankton species. New Phytologist 198: 1030-1038.

Huang S, Wilhelm SW, Harvey HR, Taylor K, Jiao N and Chen F (2012) Novel lineages of *Prochlorococcus* and *Synechococcus* in the global oceans. The ISME Journal 6, 285–297.

Inoue-Kashino N, Kashino Y, Satoh K, Terashima I and Pakrasi HB (2005) PsbU provides a stable architecture for the oxygen-evolving system in cyanobacterial photosystem II. Biochemistry 44: 12214-1228.

Jakob T, Wagner H, Stehfest K, Wilhelm C (2007) A complete energy balance from photons to new biomass reveals a light- and nutrient-dependent variability in the metabolic costs of carbon assimilation. Journal of Experimental Botany 58: 2101-2112.

Jassby AD and Platt T (1976) Mathematical formulation of the relationship between photosynthesis and light for phytoplankton. Limnology and Oceanography 21: 540-547.

Johnson ZI, Zinser ER, Coe A, McNulty NP, Malcolm E *et al*. (2006) Niche partitioning among Prochlorococcus ecotypes along ocean-scale environmental gradients. Science 311: 1737-1740.

Kashtan N, Roggensack SE, Berta-Thompson JW, Grinberg M, Stepanauhaskas R *et al*. (2017) Fundamental differences in diversity and genomic population structure between Atlantic and Pacific *Prochlorococcus*. The ISME Journal 11: 1997-2011

Kent AG, Dupont CL, Yooseph S and Martiny AC (2016) Global biogeography of *Prochlorococcus* genome diversity in the surface ocean. The ISME Journal 10: 1856-1865.

Kolber ZS, Prášil O, Falkowski PG (1998) Measurements of variable chlorophyll fluorescence using fast repetition rate techniques: defining methodology and experimental protocols. BBA 1367: 88-106.

Kromkamp JC and Forster RM (2003) The use of variable fluorescence measurements in aquatic ecosystems: differences between multiple and single turnover measuring protocols and suggested terminology. European Journal of Phycology 38: 103-112.

Kulk G, van de Poll WH, Visser RJW and Buma AGJ (2011) Distinct differences in photoacclimation potential between prokaryotic and eukaryotic oceanic phytoplankton. Journal of Experimental Marine Biology and Ecology 398: 63-72.

Kunath C, Jakob T, Wilhelm C (2012) Different phycobilin antenna organizations affect the balance between light use and growth rate in the cyanobacterium *Microcystis aeruginosa* and in the cryptophyte *Cryptomonas ovata*. Photosynthesis Research 111: 173-183.

LaRoche J, Rost B, Engel A (2010) Bioassays, batch culture and chemostat experimentation. In Riebesell U (eds) Guide to best practices for ocean acidification research and data reporting. Publication office of the European Union, Luxembourg.

Lindell D, Erdner D, Marie D, Prášil O and Koblížek M *et al.* (2002) Nitrogen stress response of *Prochlorococcus* strain PCC 9511 (Oxyphotobacteria) involves contrasting regulation of *ntcA* and *amt1*. Journal of Phycology 38: 1113-1124.

Liu H, Nolla HA, Campbell L (1997) *Prochlorococcus* growth rate and contribution to primary production in the equatorial and subtropical North Pacific Ocean. Aquatic Microbial Ecology 12: 39-47.

Malmstrom RR, Rodrigue S, Huang KH, Kelly L, Kern SZ *et al*. (2013) Ecology of uncultered *Prochlorococcus* clades revealed through single-cell genomics and biogeographic analysis. The ISME Journal 7: 183-198.

Moore LR and Chisholm SW (1999) Photophysiology of the marine cyanobacterium Prochlorococcus: Ecotypic differences among cultured isolates. Limnology and Oceanography 44: 628-638.

Moore LR, Rocap G, Chisholm SW (1998) Physiology and molecular phylogeny of coexisting *Prochlorococcus* ecotypes. Nature 393: 464-467.

Munoz-Marín MdC, Gómez-Baena G, Díez J, Beynon RJ, González-Ballester D *et al.* (2017) Glucose uptake in *Prochlorococcus*:

Diversity of kinetics and effects on the metabolism. Frontiers in Microbiology 8: 327.

Munoz-Marín MdC, Luque I, Zubkov MV, Hill PG, Díez J *et al.* (2013) *Prochlorococcus* can use the Pro1404 transporter to take up glucose at nanomolar concentrations in the Atlantic Ocean. PNAS 110: 8597-8602.

Nelson DW and Sommers LE (1996) Total carbon, organic carbon, and organic matter. In: Sparks DL (eds) Methods of soil analysis, Part 2: Chemical Methods. SSSA Book Series No. 5.

Palmucci M, Ratti S, Giordano M (2011) Ecological and evolutionary implications of carbon allocation in marine phytoplankton as a function of nitrogen availability: a Fourier transform infrared spectroscopy approach. Journal of Phycology 47: 313-323.

Parkhill JP, Maillet G and Cullen JJ (2001) Fluorescence-based maximal quantum yield for PSII as a diagnostic of nutrient stress. Journal of Phycology 37: 517-529.

Partensky F and Garczarek L (2010) *Prochlorococcus*: advantages and limits of minimalism. Annual Review of Marine Science 2: 305-331.

Partensky F, Hess WR and Vaulot D (1999) *Prochlorococcus*, a marine photosynthetic prokaryote of global significance. Microbiology and Molecular Biology Reviews 63: 106-127.

Pei S and Laws EA (2013) Does the 14C method estimate net photosynthesis? Implications from batch and continuous culture studies of marine phytoplankton. Deep-Sea Research I 82: 1-9.

Porra RJ (2006) Spectrometric assays for plant, algal and bacterial chlorophylls. In Grimm B (ed) Chlorophylls and bacteriochlorophylls biochemistry, biophysics, function and applications. Springer, Berlin, 95-107.

Rippka R, Coursin T, Hess W, Lichtlé C, Scanlan DJ *et al.* (2000) *Prochlorococcus marinus* Chisholm et al. 1992 subs. pastoris subsp. nov. strain PCC 9511, the first axenic chlorophyll a_2/b_2-containing cyanobacterium (Oxyphotobacteria). International

Journal of Systematic and Evolutionary Microbiology 50: 1833-1847.

Rocap G, Distel DL, Waterbury JB and Chisholm SW (2002) Resolution of *Prochlorococcus* and *Synechococcus* ecotypes by using 16S-23S ribosomal DNA internal transcribed spacer sequences. Applied and Environmental Microbiology 68: 1180-1191.

Rocap G, Larimer FW, Lamerdin J, Malfatti S, Chain P *et al.* (2003) Genome divergence in two *Prochlorococcus* ecotypes reflects oceanic niche differentiation. Nature 424: 1042-1047.

Scott KM, Hen-Sax M and Harmer TL, Longo DL, Frame CH *et al.* (2007) Kinetic isotope effect and biochemical characterization of form IA RubisCO from the marine cyanobacterium *Prochlorococcus marinus* MIT9313. Limnology and Oceanography 52: 2199-2204.

Siegel DA, Behrenfeld MJ, Maritorena S, McClain CR, Antoine D *et al.* (2013) Regional to global assessments of phytoplankton dynamics from the SeaWiFS mission. Remote Sens Environ 135: 77-91

Soitamo A, Havurinne V and Tyystjarvi E (2017) Photoinhibition in marine picocyanobacteria. Physiologia Plantarum 161: 97-108.

Ting CS, Dusenbury KH, Pryzant RA, Higgins KW, Pang CJ *et al.* (2014) The *Prochlorococcus* carbon dioxide-concentrating mechanism: evidence of carboxyzome-associated heterogeneity. Photosynthesis Research 123: 45-60.

Ting CS, Hsich C, Sundararaman S, Mannella C and Marko M (2007) Cryo-electron tomography reveals the comparative three-dimensional architecture of *Prochlorococcus*, a globally important marine cyanobacterium. Journal of Bacteriology189: 4485-4493.

Ting CS, Ramsey ME, Wang YL, Frost AM, Jun E, Durham T (2009) Minimal genomes, maximal productivity: comparative genomics of photosystem and light-harvesting complexes in the marine cyanobacterium, *Prochlorococcus*. Photosynthesis Research 101: 1-19.

Vaulot D, Marie D, Olson RJ, Chisholm SW (1995) Growth of *Prochlorococcus* a photosynthetic prokaryote, in the equatorial Pacific Ocean. Science 268: 1480-1482.

Veerman J, Bentley FK, Eaton-Rye JJ, Mullineaux CW, Vasiľev S and Bruce D. (2005) The PsbU subunit of photosystem II stabilizes energy transfer and primary photochemistry in the phycobilisome photosystem II assembly of Synechocystis sp. PCC 6803. Biochemistry 44: 16939-16948.

Yelton AP, Acinas SG, Sunagawa S, Bork P, Pedrós-Alió C *et al*. (2016) Global genetic capacity for mixotrophy in marine picocyanobacteria. The ISME Journal 10: 2946-2957.

Zorz JK, Allanach JR, Murphy CD, Roodvoets MS, Campbell DA and Cockshutt AM (2015) The RUBISCO to photosystem II ratio limits the maximum photosynthetic rate in picocyanobacteria. Life 5: 403-417.

Curriculum vitae

Kristina Felcmanová
(*1985, Náchod)

Academic achievements

2011 – 2015   Ph.D. at Department of Experimental Plant Biology, Faculty of Science, University of South Bohemia in České Budějovice; interrupted in 2015-2017

2009 – 2011   M.Sc. at Department of Experimental Plant Biology, Faculty of Science, University of South Bohemia in České Budějovice

Professional positions

2015 – up to now   Research assistant, Department of Membrane Transport, Institute of Physiology CAS, Prague

Professional experience

2011/2012/2013   Research fellowship, Oregon State University, Department of Microbiology, USA
(hosted by K. H. Halsey)

2011   Short research fellowship, University in Leipzig, Institute of Biology, Department of Plant Physiology, Germany (hosted by H. Wagner)

2009   Short research fellowship, Norwegian University of Science and Technology, Department of Biotechnology, Norway (hosted by L. M. Olsen)

Publications

Partensky F., Mella-Flores D., Six C., Garczarek L., Czjzek M., Marie D., Kotabová E., Felcmanová K. and Prášil O. (2018) Comparison of photosynthetic performances of marine picocyanobacteria with different configurations of the oxygen-evolving complex. Photosynthesis Research, https://doi.org/10.1007/s11120-018-0539-3.

Felcmanová K., Lukeš M., Kotabová E., Lawrenz E., Halsey K. H., Prášil O. (2017) Carbon use efficiencies and allocation strategies in *Prochlorococcus marinus* strain PCC 9511 during nitrogen-limited growth. Photosynthesis Research, 134 (1), 71-82.

Ferimazova, N., Felcmanová, K., Šetlíková, E., Küpper, H., Maldener, I., Hauska, G., Šedivá, B., Prášil, O. (2013) Regulation of photosynthesis during heterocyst differentiation in *Anabaena* sp. strain PCC 7120 investigated in vivo at single-cell level by chlorophyll fluorescence kinetic microscopy. Photosynthesis Research, 116 (1): 79-91.

Komárek, O., Felcmanová, K., Šetlíková, E., Kotabová, E., Trtílek, M., Prášil, O. (2010) Microscopic Measurements of the Chlorophyll *a* Fluorescence Kinetics. In: David, J., Borowitzka, M. A., Prášil, O. Chlorophyll *a* Fluorescence in Aquatic Sciences: Methods and Applications. Springer, pp. 91-101.

Regulation of photosynthesis and primary production of phytoplankton under nutrient and light stress
Ph.D. Thesis Series, 2018, No. 6